ABSTRACT

CEDDIA, RYAN PATRICK. Genomic Characterization of Two Models of Obesity in Mice: Divergent Selection for Epididymal Fat and the Effects of *trans*-10, *cis*-12-Conjugated Linoleic Acid. (Under the direction of Dr. Melissa Schuster Ashwell).

Obesity is rapidly becoming a major problem in the United States and throughout the world. Polygenic models of obesity are most similar to human obesity because few humans are genetically obese due to a mutation in a single gene. Numerous studies have selected mice for body size and growth rate as models for selection of agriculturally important species. One series of selection experiments produced lines of mice having differing epididymal fat (EF) masses but similar body weights. These mice may be used as a model for adipose deposition without confounding the effects of body weight. One method of studying these mice is to examine gene expression. Expression of thousands of genes can be investigated at one time using microarrays. We used microarrays and real-time RT-PCR to compare gene expression between the high epididymal (HE) and low fat (LF) lines of mice, which have dissimilar EF mass but similar body weights. Microarray analysis identified 19 genes with differential expression between the HE and LF lines of mice with 5 of these genes differentially expressed in both liver and EF tissues. We found differential regulation of genes known to play a role in glucose uptake and lipid metabolism. In addition, we identified a differentially expressed gene, *solute carrier family 22 member 4*, located within the confidence interval of a quantitative trait loci associated with EF mass, making it a positional candidate. Furthermore, we identified a linked group of three genes (*Sortilin 1*, *guanine nucleotide binding protein alpha inhibiting 3*, and *selenium-binding protein 2*) on *Mus musculus* chromosome 3 (MMU3), which may represent a genomic "hot spot" for genes associated with EF mass. In this study, differential

expression of several genes not previously associated with obesity or adipose deposition were identified and may represent new targets for further research. Another aspect of obesity currently being investigated is anti-obesity compounds. One such compound is *trans*-10, *cis*-12-conjugated linoleic acid (CLA). CLA has been reported to reduce body weight and adipose mass in many species. Numerous studies have reported an increase in size, cytoplasmic vacuolization, and fatty acid synthesis in liver of CLA fed mice. The livers of CLA fed mice gain mass due to lipid accumulation; however, the precise molecular mechanisms are unknown. To elucidate these mechanisms, we examined the fatty acid composition, histology, and gene expression profile of liver from a polygenic obese line of mice fed CLA. Using a Periodic acid-Schiff stain, histological evidence suggests that glycogen content is unchanged in the liver of the CLA fed mouse implying that hepatic cytoplasmic vacuolization is due to increased lipid content. Microarray analysis identified 1393 genes differentially expressed at a nominal P-value of 0.01. Following Bonferroni correction and excluding lowly expressed transcripts, 198 genes were identified as being differentially expressed with 17 genes having ≥2 fold change. Real-time RT-PCR showed up regulation of *acylglycerol-3-phosphate O-acyltransferase 2* and *diacylglycerol O-acyltransferase 2* in CLA fed mice, both necessary for triglyceride biosynthesis. Expression of *B-cell leukemia/lymphoma 6*, a nuclear transcriptional repressor, and *signal transducer and activator of transcription 5B*, a transcription factor, were shown to be greater in the liver of CLA fed mice. Both genes are associated with immunoregulation. Comparing real-time RT-PCR to microarray data suggest a Bonferroni correction to microarray data is necessary in order to eliminate false positive data. Further verification of microarray results is needed to validate microarray data after a Bonferroni correction.

Genomic Characterization of Two Models of Obesity in Mice: Divergent Selection for Epididymal Fat and the Effects of *trans*-10, *cis*-12-Conjugated Linoleic Acid

by
Ryan Patrick Ceddia

A thesis submitted to the Graduate Faculty of
North Carolina State University
in partial fulfillment of the
requirements for the Degree of
Master of Science

Animal Science

Raleigh, North Carolina

2007

APPROVED BY:

(Dr. Eugene J. Eisen)

(Dr. Jack Odle)

(Dr. Christopher M. Ashwell)

(Dr. Melissa S. Ashwell)
Chair of Advisory Committee

DEDICATION

To my grandparents, Don and Wanda Groh. Thank you for your love and inspiration.

BIOGRAPHY

Ryan Patrick Ceddia was born on August 14, 1982 in Columbus, Ohio, the first child of Joseph Charles Ceddia, Jr. and Susan Lynn Ceddia. Ryan and his brother Keith grew up in central Ohio, residing in Columbus, Dublin, Worthington, and Sunbury. From an early age their parents instilled in them a love of animals. While residing in Dublin, Ryan began to show an interest in equine activities. After moving to a small farm near Sunbury, Ohio in 1994 Ryan joined 4-H and began raising horses, angora goats, chickens, turkeys, and guinea fowl. As a member of Pegasus 4-H Club, Ryan served as reporter, treasurer, vice-president and president. Also during high school, Ryan showed horses in the National Reining Horse Association. After graduating from Worthington Christian High School in 2001, Ryan went on to further his education at The Ohio State University. While attending Ohio State, Ryan was a member of the OSU Equestrian Team for four years and served the team as the Public Relations Chairman for one year. Ryan also completed an undergraduate honors research project entitled Sodium Dependent Vitamin C Transporter in the Sheep Corpus Luteum: Sequence Analysis. Ryan graduated *cum laude*, With Distinction from Ohio State in 2005 with a Bachelor of Science in Agriculture. He majored in Animal Sciences and minored in Life Sciences. Following graduation, Ryan moved to Cary, North Carolina to attended North Carolina State University at Raleigh in order to pursue a Master of Science degree. At NCSU, Ryan majored in Animal Science and minored in Biotechnology. Working in the Domestic Animal Genomics Laboratory, Ryan studied gene expression in mice with emphasis on obesity. Following completion of his degree, Ryan plans to work as a research assistant in the Cutaneous Oncology Program at Case Western Reserve University School of Medicine in Cleveland, Ohio.

ACKNOWLEDGMENTS

I would like to thank all of the people who have made this work possible. Many thanks are extended to Dr. Melissa Ashwell for her guidance and support throughout my Master's project. I would also like to thank all the members of the Ashwell lab, Melissa Ashwell, Chris Ashwell, Shelly Nolin, Audrey O'Nan, Ben Dorshorst, Michael Gonda, Shelly Druyan, and Chagai Rot, who have made me feel at home here in North Carolina. I thank the members of my committee, Dr. Melissa Ashwell, Dr. Chris Ashwell, Dr. Eugene Eisen, and Dr. Jack Odle for their direction throughout my project.

I would like to express my gratitude towards everyone who has provided me technical assistance on the project. I would like to thank Melissa Ashwell and Michael Gonda for their numerous reviews of this manuscript. I acknowledge to Shelly Druyan for teaching me how to use JMP Genomics and for her invaluable contribution to the microarray data analysis. Grateful appreciation for technical assistances foes to Shelly Nolin for all her help with the microarrays and real-time RT-PCR. Also, I would like to thank Shelly Nolin for her assistance in caring for the mice.

Finally, I would like to thank my parents for all of their love and support. Without their support, this would not have been possible.

TABLE OF CONTENTS

PAGE

LIST OF TABLES

PAGE

LIST OF FIGURES

PAGE

LITERATURE REVIEW

Obesity – Why is it a problem?

Obesity is rapidly becoming a major problem for both adults and children in the United States and throughout the world. This condition can be caused by many factors, including genetic, metabolic, behavioral, and environmental influences (149). In fact, obesity has reached epidemic proportions in many countries, including the US. Obesity is defined as having a body mass index (BMI) that is greater than 30 kg/m² and as of 2004, 32.2% of adults in the US were considered obese (119). Between 1950 and 2000, the proportion of overweight men and women rose from 21.8% to 35.2% and from 15.0% to 33.1.9%, respectively (123). Even more striking has been the approximately three fold rise in BMI between 1950 and 2000, with men seeing a change from 5.8% to 14.8% for a BMI of ≥ 30 kg/m², and from 0.2% to 5.4% for a BMI ≥ 35 kg/m² (123). Women also saw a rise in the prevalence of obesity with a change from 3.9% to 14% for a BMI of ≥ 30 kg/m², and 1.7% to 4.4% for a BMI ≥ 35 kg/m² (123). Obesity has been estimated to have caused almost 112,000 excess deaths in 2000 (53) and it has been estimated to cost the US over $117 billion per year (149).

It is well known that obesity causes an increase of diseases such as cardiovascular disease, cancer, and osteoarthritis. Abdominal obesity, which is based upon the amount of adipose tissue in the abdominal region, appears to be a more important risk factor contributing to cardiovascular disease than general obesity (150). Abdominal obesity is difficult to correctly measure, as it requires imaging techniques such as magnetic resonance and computed tomography; hence waist circumference is often used instead. In the four

decades between 1960 and 2000, the proportion of abdominal obesity in men and women rose from 12.7% to 38.3% and 19.4% to 59.9%, respectively (122). This was accompanied by a rise in the mean waist circumference from 89 to 99 cm for men and 77 to 94 cm for women (122). Due to the importance of abdominal obesity, and the difficulty in correctly measuring it, finding genes that are directly involved in regulating it is of utmost importance. Most gene expression studies have focused on overweight or obese individuals. Eisen (37, 41) developed two lines of mice that contain differing amounts of epididymal fat content while maintaining the same body weight. Murine epididymal fat pad depots, the adipose tissue around the epididymis, are best correlated to visceral adipose tissue, the adipose depot around internal organs, in humans. Visceral adipose tissue deposition is closely linked to abdominal obesity (164). Eisen's mice may serve as a genetic model for visceral adipose deposition. This model will hopefully allow researchers to target the underlying causes of abdominal obesity.

Animal Models of Obesity – Genetically Selected Animals

The extreme health and financial costs of obesity make it a serious problem that must be dealt with in modern societies. Understanding the mechanisms of obesity in humans will aid in its prevention and treatment. Because obesity studies often require sacrificing the organism being studied, human studies are usually impractical. There are a variety of animal models that have been developed to meet this need. Due to their low cost, short lifespan, and high availability, mice have become the model organism of choice for many studies. Models of obesity can be grouped into two general categories: diet induced and genetic. Genetic models can be further divided into three categories: single-gene loss-

of-function, transgenic, and polygenic. Single-gene loss-of-function models can arise from either a spontaneous mutation or as an artificial transgenic knock-out. Perhaps the most well known mouse model for obesity is the *ob*/*ob* model which is homozygous for a spontaneous mutation in the leptin gene (73). Transgenic models, other than transgenic knock-out models, have genes that are artificially altered to cause increased expression or restricted expression to specific tissues to make the animal obese. These models often require altering the gene to such an extent that it is unlikely a similar event will occur naturally, unless a known mutation is introduced using a knock-in approach. Polygenic models of obesity arise from animals selected for a number of generations for traits that are related to obesity. This results in animals with many polymorphisms, with each causing a small contribution toward the obese phenotype. These models are most similar to human obesity because there are few humans that are genetically obese due to a mutation in a single gene. Mouse lines have been selected for body mass, body composition, food intake, heat loss, and spontaneous activity, all of which represent important components of obesity (147).

Body Mass

In numerous studies mice have been selected for different sizes and weights. Most studies selecting for large body size also saw an increase in the amount of adipose tissue while studies selecting for a small body size saw a reduction in adipose mass. These studies were the predecessors to more challenging studies which have selected mice for complex traits such as the mass of a single organ. What follows is a summary of results for several

of these line developed by Eisen (41, 37, 156). All lines were replicated to reduce the potential effects of genetic drift on selection response.

M16

The M16 line of mice has been selected for 3 to 6 week post weaning gain using within full-sib family selection, selecting the top 25% from 16 parental pairs (156). These mice were selected from the randombred Institute of Cancer Research (ICR) strain of mice. M16 mice were selected as part of a larger experiment to study the effects of selection intensity and population size on genetic improvement (62). These mice are moderately obese and have increased fat, lean, and ash weights (42, 46). The obesity is caused by both an increased number and size of adipocytes (42, 46). M16 mice are hyperphagic, hyperglycemic, hypercholesterolemic, hyperinsulinemic, and hyperleptinemic (2, 45, 140)

L_6

The L_6 line was selected for decreased body weight at six weeks of age on a within-family basis (168). This line was begun by reciprocally crossing two F_1 stocks (CAF_1, AKD2 F_1). CAF_1 is a cross between a BALB/c female and an A male inbred strain. The L_6 mice have a reduced growth rate and fat content, an unchanged protein and ash content, and an increased water content compared to the control line (90).

Site Specific Fat Deposition

HF vs. LF

Previous studies have estimated the heritabilities of growth and body weight in mice, producing animals with varying amounts of adipose tissue. In order to estimate realized heritabilities of components of fat and lean tissue growth and realized genetic

correlation between the two components, single-trait divergent selection was performed on a cross of M16 and L_6 mice for high and low 12-week epididymal fat depot content (39, 41). This resulted in HF (high fat) and LF (low fat) lines, respectively. The lines were selected for epididymal fat pad weight because the epididymal fat pad is easily dissected and is phenotypically highly correlated with total body fat percentage in adult mice (47). The correlation between epididymal fat pad weight and total body fat in mice is 0.71 (47), similar to the correlation between visceral adipose tissue and total body fat in humans, having a correlation of 0.81 (145).

The HF and LF lines were begun from 15 pairs of F_3 M16/L_6 cross mice. An average of four mating pairs per family, i.e. sixty pairs of mice, was made from the previous generation. Following the mating period, males were sacrificed at 12 weeks of age to obtain carcass measurements. One male was selected from each of the 15 full sib families. There was no selection on the females, as these were mated randomly to the males. Litters from the selected sire were standardized to ten pups at 1 day of age. Within full-sib family selection was practiced for 10 generations (39, 41).

Carcass evaluation revealed that epididymal fat, subcutaneous fat, fat percentage, and body length are increased in the HF line compared to the LF (40). The LF line, compared to HF, has a greater lean index and water percentage (40). The enlarged size of the HF mice cause them to possess a greater amount of lean body mass (44). The lines also differ in their growth patterns. Selection for these lines of mice not only altered the amount of fat in the animal, but also altered its distribution. The HF line saw an increase in gonadal fat pad percentage and a decrease in subcutaneous and mesentery fat with fat around the

kidneys unchanged (134). The LF line, on the other hand, saw a decrease in gonadal and kidney fat, but realized an increase in subcutaneous and mesentery fat (134). In summary, the HF line has an unusual growth pattern of growth spurts which result in an overall larger animal (6, 40). To compensate for this, it consumes more feed (40). It also has an altered fat distribution with gonadal fat composing a greater percentage of the animals' adipose tissue (134). The LF line has a normal growth pattern and normal body weight (6). Despite the lack of change in growth parameters, it also has an altered fat distribution, with gonadal fat composing a lower percentage of the animal's adipose tissue (134).

HE vs. LE

Selection for the HF and LF lines using single-trait divergent selection resulted in two lines of mice with differing amounts of adipose tissue and differing body sizes. These lines focused on a single trait; hence, they do not appropriately characterize real-world challenges. In the "real-world," producers must select livestock for high weight gain, but also select for decreased fat content. In order to better replicate "real-world" situations, restricted index selection was conducted for high and low epididymal fat weight while holding body weight constant at 12 weeks of age resulting in the high epididymal (HE) and low epididymal (LE) lines of mice (37). These mice were selected and maintained under the similar conditions as the HF and LF mice and were derived from the random control mice generated when the HF and LF lines were made to facilitate comparisons between the lines.

Selection for the HE line resulted in mice that have an increased amount of epididymal fat and no change in body weight (37, 43). The degree of change was in good

agreement with theoretical expectations. Subcutaneous fat also increased in the HE line, but the change was not significant (38). Contrary to expectations, the LE line of mice demonstrated a negligible change in epididymal fat content and an increase in body weight (37, 43). The response of this line was opposite to the expectation. It is possible that this aberrant result was caused by a greater sensitivity of the restricted selection index to shifts in genetic parameters and gene frequency caused by the selection (43). Other possibilities include linkage disequilibrium and genetic drift (43). The LE line has an increase in hind carcass weight and a decrease in subcutaneous fat pad weight (38). Both HE and LE lines have an increased feed intake, hence, feed efficiency is decreased in the HE and increased in the LE (38).

HF, LF, HE & LE Compared

Comparing the lines generated in both selection experiments yields unexpected results. The HE and LF lines have no change in body weight but have divergent fat content (36, 43). In contrast, the HF and LE lines have an increased growth rate and divergent fat content (36, 43). As a result, there are two pairs of mouse lines with similar body weights and differing fat content (HE vs. LF and HF vs. LE) with the latter pair having an increased growth rate compared to the former.

Applications to Agriculture

Most of these selection experiments in mice were not designed to create models of human obesity; instead they were intended to be used as models of selection for agriculturally important species such as pigs and chickens. Mice have been important as selection models because they have a shorter life cycle and are less expensive to maintain

than livestock. By using mice for the initial selection experiments, researchers can estimate the heritability and correlations of traits before initiating selection in livestock. This way, valuable time will not be wasted by putting selection pressure in the wrong areas.

Selection of livestock species is used to create animals that produce more, better, and cheaper end products. Livestock used for meat are heavily selected for carcass traits, such as body size and muscle content. Of major concern to livestock producers is the partitioning of nutrients from feed. Because different parts of the animals have different commercial values, it is of interest to maximize the amount of energy that is being used for valuable end products, such as lean meat, and minimize the amount that is utilized for less valuable products, such as adipose (143). Genetic selection has altered livestock's composition of muscle and adipose so that less fat is produced (21). The cellular effects of altered adiposity are often similar between mice and livestock species; for example, adipocyte hypertrophy and hyperplasia are often responsible for greater fat content (21). Furthermore, the genetics of obesity is similar between livestock species and humans. For instance, a study found that several candidate genes for fat deposition in pigs are also genes associated with obesity in humans (85).

It is clear that the genetic causes for fat deposition in animals are similar to that in humans. Understanding the genetic changes related to obesity in rodents and livestock will further the knowledge of genetics in human obesity. One way to further our comprehension is to study gene expression in specific tissues. By examining differences in gene expression, we can begin to understand the underlying genetic basis for selected lines of animals. It is often difficult to directly study changes in gene expression in livestock

species because presently the molecular tools are not as developed as are those for humans and mice. For these reasons, gene expression studies in rodents may serve as an alternative because they will translate to livestock species where similar methods of selection have likely led to similar alterations in gene expression.

Ways to Measure Gene Expression

Microarrays

Perhaps the most efficient way to measure gene expression changes is through microarray analysis. This method allows a researcher to analyze the expression of virtually every gene in an organism's genome from a single experiment, assuming every gene is represented on the microarray. A microarray slide consists of a nucleic acid target that hybridizes to its complementary probe. This interaction is detected by fluorescent dyes to determine if a particular gene is expressed and to what extent. There are two platforms commonly used for microarray experiments: Affymetrix arrays and spotted arrays (Table 1.1). Each platform has advantages and disadvantages which are discussed in greater detail below in regards to printing and experimental design.

Printing and Probe Synthesis

Probes may be synthetically-made oligonucleotides or PCR products. In spotted arrays, probes are synthesized externally and delivered onto the arrays. When printing to a glass surface, reactive amines (such as poly-lysine), aldehyde, or epoxy groups must be added to allow the oligonucleotides to attach. The most popular method of delivering probes to arrays is via robotic spotting. In this method, probes are stored in microplates. A robot prints the arrays by transferring probes from microplates using a print head. The print

head wicks up the probes and transfers them to the array. The probes are then free to flow off the pins and stick to the array by hydrostatic interaction. Longer probes are more sequence specific and are thus less likely to bind to the wrong sequence; however, synthetically made nucleotides are rarely more than seventy nucleotides long due to the decreased fidelity of manufacturing longer probes.

In contrast to spotted arrays, oligonucleotides are synthesized directly on silicone GeneChips in the Affymetrix platform. Affymetrix (Santa Clara, CA) pioneered the technology, hence the name. The oligonucleotides on Affymetrix arrays are made via a process called photolithography. In photolithography, nucleotides can only bind to a surface when it is illuminated by light. Masks are used to regulate where light can and cannot shine. By using four masks, one mask for each different nucleotide, the first nucleotide in the probe can be added. For example, in order to make an array with twenty nucleotide probes, eighty masks must be used. Affymetrix probes are usually 20 nucleotides long due to the cost of masks. Affymetrix chips are more expensive than spotted arrays but are desirable due to the large number of probes and reduced spot variation. The choice between Affymetrix and spotted arrays depends on both the cost of the arrays and the size of the experiment, as both types of arrays have benefits and disadvantages.

Experimental Design

When designing microarray experiments, it is important to take into consideration what types of arrays are to be used. Spotted arrays are commonly hybridized with two different colored dyes, representing two different samples, on the same array. Alternatively,

Affymetrix arrays can only be hybridized with one dye color. By using spotted arrays, twice as many samples can be tested on an array compared to Affymetrix. One drawback to using the two colored arrays is that the dyes are incorporated into cDNA at different levels so it is usually necessary to label the same sample with both dyes (Figure 1.1). Another important consideration when designing experiments is the use of replicates (95). There are two types of replicates: biological and technical. A biological replicate entails using multiple animals. Oftentimes it is not feasible to use a large number of animals in a microarray experiment simply due to the cost of the arrays and materials. One way to circumvent this is to pool samples (3). Pooling samples is beneficial for several reasons. First, it increases sample size without buying more arrays. Second, the amount of RNA needed per biological specimen is reduced. There are also some drawbacks to pooling samples. Pooling interferes with ability to accurately assess individual variation and pools do not necessarily correspond to exact averages of individuals. Technical replicates include hybridizing the same target onto multiple arrays and having replicate spots on the array. Having replicate spots on the microarray is beneficial because it increases the statistical power of the experiment for the genes that are spotted multiple times. This way, a small fold change can be detected without using a large number of arrays.

Methods

All RNA is the product of gene expression so microarrays are used to detect changes in amounts of RNA. RNA is normally reverse transcribed into cDNA, labeled with fluorophores, and hybridized to oligonucleotide probes. There are two methods of labeling cDNA: direct and indirect. Direct methods involve incorporating radioactively labeled

nucleotides or fluorescent dyes during cDNA synthesis. Indirect methods involve incorporating a conjugate during cDNA synthesis, which is in turn used to bind the fluorescent dyes post synthesis. The preference of which labeling method to use largely depends on the user, as both methods have been optimized by various companies, leading to similar efficiencies (55). One method of indirect labeling, used by Pronto!™ Plus Indirect Systems (Promega, Madison, WI), incorporates aminoallyl labeled nucleotides during cDNA synthesis. These can then bind to CyDye™ NHS Ester, thereby labeling the cDNA with a fluorescent dye (Figure 1.2).

Labeling reactions are not inherently all the same; the amount of dye incorporated into the cDNA varies from reaction to reaction. This is measured by frequency of incorporation (FOI). FOI is the number of Cy-labeled nucleotides per 1,000 nucleotides of cDNA, this can be calculated using the following equations:

$$\text{FOI} = \frac{\text{pmol incorporated dye} \times 324.5}{\text{ng cDNA}}$$

pmol dye incorporated: $\text{Cy3} = A_{550} \times \text{volume (µl)} / 0.15$
$\text{Cy5} = A_{650} \times \text{volume (µl)} / 0.25$

In these equations, 324.5 is the average molecular weight of one kb of DNA in g/mol and 0.15 and 0.25 are the extinction coefficients at OD_{550} and OD_{650} for Cy3 and Cy5, respectively. The amount of dye incorporated and cDNA can be calculated based upon their absorbance at their respective wavelengths using a spectrophotometer. The FOI should fall between 12 and 40 dye molecules per 1000 nucleotides with Cy5 being slightly greater than Cy3 because Cy5 is incorporated at a greater frequency. Aberrant FOI results are an

indication of a problem during the labeling process. This could identify problems such as genomic DNA contamination.

The microarray must be prepared prior to hybridizing the labeled cDNA onto the array. Generally, this involves treating it with a blocking agent, such as Cot-1 DNA, polyadenylic acid or salmon sperm DNA, which will bind nonspecifically to the array. This procedure will prevent labeled cDNA from binding nonspecifically and thereby increasing the background. The microarrays are washed to relax the oligonucleotides, making them more accessible to the cDNA. After preparation, the labeled cDNA is placed on the array and protected with a cover slip. In some instances, cover slips with raised Teflon edging are used, which allows for greater flow of the hybridization solution over the array and reduces background. The array is placed in a hybridization chamber in a water bath to ensure an even temperature throughout the array. This step is important because temperature may affect hybridization stringency. At cooler temperatures, the cDNA will be more likely to bind to the oligonucleotide probes, which can result in false positives and higher background levels. At higher temperatures, the cDNA will be less likely to bind to the probes, which will result in reduced hybridization, and possibly false negatives. There are other factors which can affect the stringency of the hybridization such as the amount of labeled cDNA that is deposited onto the array and the nucleotide sequence of the probes. Higher amounts of labeled cDNA will be more likely to bind to the probes and to non-specific places on the array resulting in higher background and possibly false positives, similar to using a lower hybridization temperature. The nucleotide sequence of the probes can have an effect if they have vastly different GC content. Microarray probes can also

bind differently at different temperatures. Hence, it is best that microarray probes be designed to possess similar annealing temperatures to minimize these effects.

Data Analysis

After the microarrays have been hybridized, they are next scanned to obtain an image of the microarray. These images must be loaded into a program which is capable of extracting data from the images. One must first identify the spots on the array by creating a grid over the spots and making sure that the grid correctly identifies each probe on the array. A change in the intensity of the fluorescence of a spot on the array indicates a change in expression of the gene for which the spot corresponds. In spotted arrays, where two colors of dyes are used, the differing colors result from the competition of hybridization between the two samples. For instance, if the transcript of the Cy3 labeled sample is in greater abundance than it is in the Cy5 sample, then the corresponding spot will be green. There are a variety of computer programs available for doing the mathematical calculations to determine if a gene on a microarray is differentially expressed. Statistical Analysis System (SAS) and JMP (SAS Institute, Cary, NC) were some of the first programs used while a new program, JMP Genomics (SAS Institute, Cary, NC), has recently been developed with microarrays in mind. This SAS based program can accommodate larger data sets than JMP and has statistical methods commonly used in microarray analysis built into a convenient menu driven format.

The first step in microarray data analysis is preprocessing of microarray data, which involves normalization and transformation of the data to remove systematic variation (3). For instance, microarray data are commonly transformed to a $\log_2$ scale which accounts for

non-normal distribution of the data. Normalization removes much of the technical variation by adjusting individual spot intensities, which allows comparisons both within and between arrays (5). Early methods of normalization relied upon techniques such as ANOVA, but methods such as locally weighted least squares regression (lowess) have been shown to be more correct (5). This is because microarray data are nonlinear, because most of the genes on the array are not differentially expressed, and ANOVA assumes the data are linear (5). JMP Genomics uses separate functions to normalize within and between arrays and offers the choice between ANOVA, lowess, and other forms of normalization. Figure 1.3 shows a comparison of the distribution of intensities for eight spotted arrays before and after normalization. Before the data were normalized, the distribution of each array was different, but normalization forced the arrays to have a similar distribution pattern so their data could be compared.

Finally, after the data have been collected and manipulated, a conclusion must be made about which genes are differentially expressed. One of the earliest methods of determining if a gene was differentially expressed between two samples was to look at the fold change, a standard of measurement comparing a gene's mRNA expression level between two different experimental conditions (3). This can be mathematically defined as:

$$\text{Fold Change} = \frac{\max(\bar{y}_{g1}, \bar{y}_{g2})}{\min(\bar{y}_{g1}, \bar{y}_{g2})}$$

where $\bar{y}_g$ is the mean of the intensity measurements for the g^{th} gene (86). Using an arbitrary fold change to determine if a gene is differentially expressed is both unreliable and inefficient because it fails to find genes that are differentially expressed when the fold change is low and identifies genes as being differentially expressed even if there is a large

variation in measurements (86). The basis for this argument is because fold change does not account for variance and does not provide an estimate for error rates (3). For these reasons, statistical significance must be determined. There are a variety of statistical tests, which have been used to determine statistical significance such as ANOVA and *t*-tests. Due to the large number of genes being tested in a microarray experiment, certain corrections to the ANOVA or *t*-test must be made (5). Examples of multiple testing corrections include Bonferroni and false discovery rate (FDR) (11). These control the probability that a gene will be shown to be differentially expressed when in reality it is not. The Bonferroni correction is usually too conservative for microarray experiments so FDR, which is less conservative, is often a better choice (3, 5).

There are several ways to view microarray data in graph form. Commonly used forms are heat maps and volcano plots. In heat maps the cells represent relative expression values while the rows represent genes of similar expression values and columns represent different biological samples (Figure 1.4). Another popular way to look at the data is to use volcano plots. Using volcano plots, one can visualize fold change and statistical significance at the same time (Figure 1.5). In volcano plots the log odds of differential expression is on the Y-axis while the Log Cy3 to Cy5 ratio (fold change) is on the X-axis. Finally, once the data have been analyzed, different genes can be selected for validated.

Quantitative Real-Time RT-PCR

Microarray experiments can produce a large amount of false positive results. For this reason the data are often verified using another method to measure gene expression. There have been a variety of attempts to use polymerase chain reactions (PCR) as an

indicator of initial starting material. Early techniques assumed that a greater amount of PCR product produced indicated a greater amount of starting material. Later techniques attempted to determine the initial quantity of a transcript in a PCR based upon the amplification during the exponential phase; however, this is difficult because the reaction must be stopped to take a measurement. Quantitative real-time reverse-transcription polymerase chain reaction (qPCR) is the technique of collecting amplification data throughout the PCR process while it is occurring (170). Measurement of PCR product quantity while the reaction is occurring is achieved using fluorescent dyes which fluoresce in the presence of the PCR product. The level of fluorescence in a qPCR reaction is determined using a camera on the thermocycler. qPCR is superior to other ways of measuring gene expression, such as microarrays, northern blots, and semi-quantitative PCR, because data quality is better, sensitivity is higher, and the dynamic range is higher (89). In addition, more biological and technical repeats can be performed due to the relatively low cost of qPCR experiments (89).

Methods

The first step in qPCR is reverse transcription (RT). RT utilizes the reverse transcriptase enzyme, found in retroviruses, to convert RNA into cDNA. Though the reverse transcriptase of most retroviruses can be used in theory, most commercially available enzymes are derived from the Moloney Murine Leukemia Virus or the Avian Myeloblastosis Virus (89). Essentially, the reverse transcriptase binds to the RNA and makes a cDNA copy. A variety of priming strategies can be used to increase the affinity of reverse transcriptase for RNA: oligo(dT) primers, random sequence primers, and gene

specific primers. Oligo(dT) primers consist entirely of thymidine residues; the theory behind using these primers is that they will bind specifically to the poly adenosine tail of mRNA, which will cause only mRNA to be reverse transcribed. The downside to this is that the 3' end of mRNA will be preferentially transcribed, which will cause sequences located at the 5' end to be artificially scarce. As an alternative, random sequence primers, which have a random sequence, as their name implies, will theoretically bind anywhere on the RNA, resulting in a more even distribution of cDNA sequences. The downside to random primers is they also amplify rRNA and tRNA. The third type of primers, sequence specific primers, is rarely used because they amplify a single sequence; as a result, these would not be beneficial to use when trying to detect multiple targets from the same cDNA pool. The RT process is the procedure where the most variation is introduced into the experiment due to differences in priming strategy efficiencies and RNA concentration; because of this, it is important to use consistent conditions throughout cDNA synthesis (148).

After cDNA has been synthesized, the amplification reaction is performed. In a PCR, primers are necessary to allow the DNA polymerase to extend the product. These are designed to bind to specific sequences on the cDNA so that ideally only one PCR product may be formed. In qPCR the choice of primers is especially important because a poor set of primers can hinder the PCR reaction. There are several general rules for designing qPCR primers; for instance, the amplification region should span an intron/exon boundary so that the presence of genomic DNA amplification can be detected. If genomic DNA is present in a RT-PCR reaction, it may amplify along with the cDNA. In a qPCR reaction this factor is

deleterious because genomic DNA will give the impression that there is extra cDNA. Another way to prevent this is to design primers that lie on an intron/exon boundary, which will not allow amplification of genomic DNA. There are many other general rules for designing optimal qPCR primers, such as optimal length of the primers, length of the product, GC content of the primers, and melting temperature of the primers; hence, many primer design programs have been created, which aid in the development of qPCR primers.

There are a variety of dyes used to detect PCR products in qPCR reactions. One of the most popular dyes is SYBR Green I (Figure 1.6). SYBR Green I is an asymmetric cyanine dye, which binds to the minor groove of DNA (89). When SYBR Green I is unbound it produces no fluorescence because vibrations engage both aromatic systems, which convert excitation energy into heat instead of light (89). When bound to DNA, the rotation around the methane bond is restricted causing the excitation energy to be released as light (89). SYBR Green I is frequently used because no fluorescently labeled primers or probes are needed. Furthermore, the same SYBR Green I can be used in different PCR reactions because it is not sequence specific.

Another prevalent detection system is TaqMan chemistry. This systems uses hydrolysis probes to detect PCR product accumulation. These probes are specific for the sequence that is being amplified during PCR. These probes contain a reporter and quencher, so when the probe is intact there is no fluorescence, as the quencher reduces the reporter's fluorescence intensity (170). The probe binds DNA and is degraded by the 5' nuclease activity of DNA polymerase during the extension step of PCR thereby releasing the reporter from the quencher and, by this means, activating the reporter (170). Though

this method is more expensive, it is widely used because the probe increases the sequence specificity of the fluorescence, as opposed to SYBR Green I which binds to any double stranded DNA. Although TaqMan is sometimes considered better than SYBR Green I, studies have shown that both boast similar precision with SYBR Green I possibly being more precise (169). The major benefit of TaqMan chemistry is that it allows multiplexing and identification of single nucleotide polymorphisms (SNPs), which SYBR Green I does not. Besides TaqMan probes, there are several other strategies which use reporter and quencher dyes such as molecular beacons, scorpions, Sunrise™ primers, and LUX™ fluorogenic primers (169, 170). In addition to these chemistries, hybridization probes use donor and acceptor molecules to create fluorescence instead of using a quencher (170).

Data Analysis

Though SYBR Green I does not discriminate between sequences, the identity of products labeled with SYBR Green I can still be determined using sequencing and melting curve analyses (Figure 1.7). The melting curve is generated by gradually raising the temperature of the qPCR mixture. At a certain temperature, the qPCR products will denature. Because SYBR Green I fluoresces only in the presence of double stranded DNA, the fluorescence will cease when the qPCR product melts. Because different sequences will have different melting temperatures, the presence of multiple PCR products can easily be determined by looking at the melting curve because if there are multiple products, there will be multiple peaks. Also, the melting curve gives some information on amount of product present; the more qPCR product present, the higher the peak (169).

Data from real-time PCR are measured in C_t's, cycle thresholds, or C_p's, crossing points, which are the time at which fluorescence intensity is greater than the background fluorescence (Figure 1.8) (170). When the initial quantity of the target molecule is greater, the amplification, and therefore the fluorescence intensity, will increase faster resulting in a lower C_t value. There are two ways to quantify qPCR data: absolute and relative. Absolute quantification requires the use of a quantification curve, which produces a linear relationship between C_t and a known amount of DNA. Therefore, by plotting the C_t of the sample on the standard curve, the initial copy number of the gene of interest can be determined. In relative quantification, quantification of the gene of interest is based upon a control/housekeeping gene. There are a variety of ways to normalize to a housekeeping gene, but basically, they either subtract or divide the C_t of the housekeeping gene from that of the sample gene's C_t. The housekeeping gene is thought to be consistently expressed between all tissues, time points, and treatments, which is why it is used as a reference to which other genes are normalized. In short, the relative expression of the housekeeping gene is forced to zero while the expression of the other genes is similarly adjusted. These genes are necessary for cell survival; hence they are often referred to as housekeeping genes. Housekeeping genes can either be mRNA, such as glyceraldehyde-3-phosphate dehydrogenase (GAPDH), β-actin, and hypoxanthine-guanine phosphoribosyl transferase (HPRT), or rRNA, such as 18S ribosomal RNA and 28S ribosomal RNA. If an rRNA housekeeping gene is used, random primers must be used during the RT reaction. Much attention has been paid to the choice of a housekeeping gene because if the expression of the control gene changes, it skews all of the results from qPCR. For instance, if the control

gene is up regulated one fold in a treatment group, the expression of all genes in that group will appear to be expressed one fold less than in actuality because the change in expression of the control gene is forced to zero. Despite the importance of the housekeeping gene, no perfect gene has been found. Even before the invention of qPCR, all of the classical housekeeping genes had been found to vary to some extent depending on the treatment; for this reason, many studies have begun to use multiple housekeeping genes (72).

When validating microarray data, an alternative to using classical housekeeping genes exists. Because microarray data are not normalized to a housekeeping gene, its results are not based on one or a few genes. Gene expression as determined by microarray data are based upon the assumption that the majority of genes on the array are not differentially expressed compared to qPCR which is based upon the assumption that the housekeeping gene is not differentially expressed. Hence, genes can be chosen as controls based upon the microarray results providing a way to avoid the bias of classical control genes (170). Because choosing the wrong housekeeping gene can dramatically alter the results of a qPCR experiment, this is one of the most important parts of the experiment.

Besides concern about the choice of housekeeping gene, another concern in qPCR studies is quality of the reaction as a whole, which can be measured by its efficiency. A PCR reaction with a perfect efficiency has a doubling of PCR products every cycle; because most reactions are not perfect, efficiency is measured as a way of indicating how close to perfect the reaction is (89, 170). A variety of factors can influence the efficiency of a reaction, such as the quality of the primers, thermocycling conditions, and the concentration of components in the qPCR mix. When efficiency is not measured, the

efficiency is assumed to be perfect, which is atypical of most reactions. Most qPCR reactions do not exhibit a perfect efficiency; hence, the initial concentration is overestimated. Amplification efficiency is usually calculated based upon a standard curve (Figure 1.9); however, there are alternative methods. For instance, data collected during the exponential phase of amplification can be log transformed and the slope of the regression line can be used as the amplification efficiency (103).

There are a variety of ways to calculate the relative expression ratio between sample and housekeeping genes. Several of these models correct for differing efficiencies of qPCR reactions. One method for relative quantification is the comparative C_t method, also known as the $2^{-\Delta\Delta C_t}$ method. The $2^{-\Delta\Delta C_t}$ method calculates the relative change in gene expression between a housekeeping gene and sample gene. This method can correct for non-ideal amplification efficiencies; however, it cannot account for differences in efficiencies between control and sample genes (170). An alternative method of relative quantification is the Pfaffl model (132). This model combines both quantification and normalization into the same equation while also accounting for differences in efficiencies between sample and housekeeping genes. Besides these, there are a variety of other, less common, models for calculating relative quantification fold changes. In some situations, such as when all qPCR have high efficiencies, the choice of models is not especially important; however, for more complex data it is necessary to choose the most correct model for the data in order to avoid making wrong conclusions.

Summary

Both microarrays and qPCR are valuable tools for measuring gene expression. Microarrays provide a mechanism by which thousands of genes can be analyzed at one time, whereas qPCR provides a highly sensitive method of measurement of a single gene's expression. Animal models that have been created to better understand issues relating to medicine and agriculture are readily available for further research. The use of microarrays and qPCR to examine gene expression in these models has already proven beneficial in the understanding of these models.

Gene Expression and Obesity

Due to the complex nature of obesity, gene expression studies have been readily used to further understanding of this condition. There have been a variety of models used to understand obesity, most of which focus on diet induced obesity while a few have focused on genetically induced obesity. Most genetic models use single-gene loss-of-function and transgenic animals. In these models, gene expression studies serve to elucidate the effects of the genetic alterations. Polygenic models serve as important alternatives to single gene models because they more accurately characterize the nature of genetic obesity in humans. Because the underlying genetic causes of obesity are unknown in polygenic models, genomic techniques such as microarrays and quantitative trait loci (QTL) analyses are the only methods to discover the genetic changes that have occurred. Diet induced obesity models serve an entirely different purpose; studies using these models seek to understand the effects of diet and the obese phenotype on gene expression without the effect of different genetic backgrounds. It can be argued that these models are most typical of obese Americans because many people are obese simply because they consume unhealthy or too

much food. Regardless of which model is best, all models serve a different role in understanding the mechanisms of obesity and provide important information unique to that model.

Polygenic Models

Polygenic models best represent genetic obesity in humans because many small changes lead to the obese phenotype. Gene expression studies using these models serve, not only to characterize the obese phenotype, but also to provide information about the underlying genetic alterations. A microarray study using high fat (Fat, F-line) and low fat (Lean, L-line) lines of mice found differential regulation of many genes involved in cholesterol biosynthesis in the liver of these mice (151). These mice have a QTL, a region of DNA that is associated with the high/low fat phenotype, near the location of several cholesterol biosynthesis genes, including the transcription factor sterol regulatory element binding protein-2 (SREBP-2). This study specifically focused on this QTL because it has an absolute effect of 0.71% on percentage of body fat. The authors concluded that the positional candidate gene for this QTL is squalene epoxidase (Sqle), which happens to be regulated by SREBP-2; however, they did not provide evidence for choosing this gene over several other genes within the confidence interval for the QTL associated with cholesterol biosynthesis. For instance, SREBP-2 also was differentially expressed indicating that it may be responsible for the gene expression differences observed in Sqle (151). Stylianou and coworkers (151) hypothesized that these changes in gene expression, which suggest an increase in cholesterol in the F-line, may boost cholesterol deposition in adipose cells, thereby increasing adiposity. Alternatively, they propose that a rise in cholesterol amplifies

fatty acid synthesis, producing the increase in obesity. Similar results were obtained from the livers of fat and lean chickens divergently selected for high and low abdominal fat content (13). These results showed that SREBP-1, as well as four SREBP-1 target genes involved in fatty acid synthesis, were up regulated in the fat chickens (13). Together, these studies show that differential regulation of SREBPs and their target genes can have a profound impact on an animal's phenotype.

Single Gene Models

There are few polygenic models of obesity due to the fact that creating inbred strains of animals is both time consuming and expensive. As an alternative, many researchers focus on models that result from a single mutation, a knockout, or a transgene. These models are obese due the altered expression or function of a single gene. This is beneficial because it allows the researchers to understand the effect of a single gene. This is also disadvantageous because in real-life, few people are genetically obese because of a single mutation.

One of the best characterized models of obesity is the *ob*/*ob* mouse model. The *ob*/*ob* mouse is homozygous for a mutation in the leptin gene, which causes the *ob*/*ob* mouse to be extremely obese. The *ob* mutation, a spontaneous mutation, was first discovered in mice at the Roscoe B. Jackson Memorial Laboratory in 1949 and has continued to be an important model for obesity (73). In order to characterize the effects of leptin on obesity, one study used microarrays to characterize the differences in gene expression in white adipose tissue between wild-type, *ob*/*ob*, and transgenic mice expressing a constitutively low level of leptin (146). This study demonstrated that genes

associated with metabolism, such as SREBP-1, and SREBP-1 target genes, such as Fatty Acid Synthase (FAS) and Squalene Synthase (SQS), were down regulated in *ob*/*ob* mice. This is unexpected because SREBP-1 is commonly up regulated in obese models. Furthermore, genes associated with inflammation were up regulated. This is not surprising because inflammation is a common component of obesity (115). Transgenic mice expressing low levels of leptin showed some correction of gene expression abnormalities seen in *ob*/*ob* mice. Genes involved in inflammation had the greatest degree of correction while genes associated with metabolism displayed the least.

Genetically lean models are also useful in understanding obesity. Using an estrogen-related receptor α (ERRα) knockout model, Luo and colleagues (106) used microarrays to look at gene expression changes. ERRα$^{-/-}$ mice lack an orphan nuclear receptor transcription factor. These mice had less adipose tissue, which appeared to be due to a reduced adipocyte size. Reduced expression of genes involved in lipid metabolism, including SREBP-1 and SREBP-2 target genes FAS and stearoyl-coenzyme A desaturase (SCD) 2, was found in ERRα$^{-/-}$ mice. Another study found similar results using perilipin (plin) knockout mice, which are also lean (22). Plin is a protein that protects lipid droplets from lipolysis; therefore, plin$^{-/-}$ mice maintain constitutive lipolysis and reduced adipose depots. These mice also showed a reduced expression of transcripts associated with fatty acid metabolism in white adipose tissue such as SCD-1, SCD-2, and long-chain fatty-acyl elongase, which are SREBP-1 target genes.

Besides these, studies which demonstrate that SREBPs and SREBP target genes are some of the most likely genes to be regulated in genetic models of obesity, another study

used microarrays to study the effects of over expression of SREBPs or removal of SREBPs in murine liver (68). To do this they used a mouse model that over expresses trancriptionally active forms of SREBP-1 and SREBP-2 as well as knockout mice for SREBP cleavage-activating protein (SCAP). As the name implies, SCAP is necessary for both SREBP-1 and SREBP-2 activation; hence, knocking it out effectively inhibits all SREBP activity. As expected, mice over expressing SREBP-1 developed fatty livers as a result of the increased fatty acid synthesis (68). The rates of fatty acid and cholesterol synthesis were reduced 70-80% in $SCAP^{-/-}$ mice (68). As expected, most SREBP target genes were up regulated in mice expressing active SREBPs and down regulated in $SCAP^{-/-}$ mice (68). Together these studies show that genes associated with fatty acid metabolism are some of the genes that are most likely to be differentially regulated in genetic models of obesity.

Diet Induced Models

Although genetics plays a major role in obesity, many individuals are obese simply because of their diet. Many studies try to examine the effects of diet induced obesity on gene expression changes. These studies are more abundant than genetic studies due to the fact that genetically altered subjects are not needed.

A study using white adipose tissue from C57BL/6J mice examined the effects of feeding a high fat diet for 7 weeks on gene expression using microarrays (112). This study found that several genes associated with lipid metabolism, such as FAS and SQS, were down regulated in the obese animals. Despite the fact that these genes are transcriptionally regulated by SREBP-1, no change in SREBP-1 expression was observed. This study also

found an up regulation of pro-inflammatory genes. A similar study using Wistar rats fed a cafeteria diet (a fat-rich hypercaloric diet containing pate, chips, chocolate, bacon, biscuits, and chow) for 9 weeks found very different results (104). This study found that SQS and SCD were up regulated in the obese rats. Furthermore, leptin and genes associated with adipocyte differentiation, such as CAAT/enhancer binding protein-α (C/EBP-α) and peroxisome proliferator-activated receptor-γ (PPARγ), were also up regulated. Another similar study using a cDNA subtraction screen, another method of analyzing differential gene expression between two samples, on Sprague-Dawley rats that had been fed a high fat diet for one week found results with similarities to both of the previous studies (101). For instance, this study found that SCD was up regulated even though no other genes associated with lipogenesis were found to be differentially expressed. Also, semiquantitive RT-PCR, a precursor to qPCR, which visually determines relative transcript numbers by agarose gel electrophoresis, showed that SREBP-1 was down regulated. It is likely that this study was not able to observe many of the gene expression changes associated with a high fat diet due to the fact that the rats were only fed the diet for one week and because less sensitive tests were used.

Because there is no special line or transgenic animal needed for diet induced studies, humans may be used in these experiments. One study used non-diabetic Pima Indians (a tribe which has one of the highest prevalence rates of obesity) to study the effects of obesity on gene expression (97). Similar to studies using rats and mice, this study found up regulation of many genes involved in inflammation and immune response in

obese subjects. Interestingly, this study found no clear change in lipid metabolism as five genes were found to be up regulated and seven were down regulated in obese subjects.

Summary

These studies demonstrate that the obese phenotype causes a differential regulation of gene expression. The genes differentially regulated vary between models. In general, genes involved with inflammation tend to be up regulated in obese subjects. The role these genes play in obesity is still an enigma as it is not clear whether inflammation is a cause of obesity or is simply an effect (115). Most of these studies show a differential regulation of genes associated with lipid metabolism and cholesterol biosynthesis, of which the SREBP target genes were a conspicuous group in many studies. Though many studies have demonstrated differential regulation of these genes, they are not in agreement about the direction of change. These genes are obviously important regulators of obesity because they regulate the production of lipid. It is likely that the different types of obesity models in these studies cause the differing results. For instance, adipose mass can be increased by either hypertrophy or hyperplasia. In the latter, an increase in lipid synthesis would not be necessary for the obese phenotype because the increase in adipose mass would result from an increase in cell numbers. Another possibility for these discrepancies is the cause of obesity. For instance, the animal may become obese due to an increase in food consumption or a decrease in energy expenditure. Because these studies survey different aspects of obesity, it is not surprising that they found different results. These studies highlight the need to consider a variety of models when studying obesity.

Conjugated Linoleic Acid

Another aspect of obesity research currently being investigated is the study of anti-obesity compounds. In the modernized society which much of the world now lives, food is readily available and the need for physical activity is reduced. As a result, many people become overweight. Because being overweight is aesthetically unpleasant and is detrimental to ones health, there is a need to loose weight. There are a variety of compounds which have been found to augment weight loss. One such compound is conjugated linoleic acid (CLA) which has been shown to possess anti-lipogenic effects in mice, rats, chickens, pigs, and humans (8, 71, 76). These compounds deserve to be studied so their efficacy and safety can be determined. Also, by investigating them, different aspects of obesity may be elucidated.

Chemistry

CLA is a term that refers to positional and geometrical isomers of linoleic acid (LA) (144). LA has 18 carbons and two *cis* double bonds at the 9 and 12 positions (Figure 1.10). Like LA, CLA also has 18 carbons and two double bonds, but the double bonds do not need to be *cis* or at the 9 and 12 positions; the two double bonds in CLA can be at the positions 8 and 10, 9 and 11, 10 and 12 or 11 and 13 (141). Most naturally occurring fatty acids are *cis* fatty acids while most *trans* fatty acids, which we hear about regularly in the news due to their health risks, are produced synthetically during partial dehydrogenation. Though most *trans* fatty acids in the American diet are produced synthetically, some are produced naturally. For example, CLA is produced in the rumen as an intermediate during biohydrogenation of unsaturated fatty acids (54, 141). The first step in hydrogenation of

unsaturated fatty acids is catalyzed by *Butyrivibrio fibriosovens*, which produces *cis*-9, *trans*-11 CLA (49, 54, 141). Because this is the first step in the hydrogenation process, the majority of natural CLA isomers are *cis*-9, *trans*-11. Not surprisingly, the main source of natural CLA in the diet comes from ruminant products such as milk, cheese, beef, and lamb (51, 144). Until recently, it has been very difficult to purify specific isomers of CLA; hence, most studies have focused on feeding a mixture of CLA isomers. However, more recent studies using pure CLA isomers show that the *cis*-9, *trans*-11 and *trans*-10, *cis*-12 isomers are the biologically active isomers and have slightly different effects (Figure 1.11) (125). For instance, it is primarily the *trans*-10, *cis*-12 isomer which has delipidative effects (49, 63, 125, 130) while the *cis*-9, *trans*-11 isomer is mostly responsible for the anti-carcinogenic effects of CLA (125).

CLA and Health

CLA has been repeatedly shown to possess many beneficial effects on health, such as cancer, arthrosclerosis, and diabetes (1, 8, 9, 29, 76, 81, 82, 88, 94, 107, 109, 141, 157). These effects of CLA have been demonstrated in numerous cell types and animal models.

The first evidence that CLA influenced cancer came in 1979 when Pariza and colleagues (124) found that a component of cooked ground beef had anti-carcinogenic properties. The chemical responsible for the anti-carcinogenic properties was later demonstrated to be CLA (59). More extensive studies later confirmed that CLA inhibited cancer in almost all tissue types (82, 94). Furthermore, CLA inhibits cancer at almost all stages including initiation, promotion, progression, and metastasis (9, 94). It appears that CLA modulates these effects mainly through inhibiting cellular proliferation and promoting

apoptosis (9, 34, 52, 82, 94, 157). Evidence for this comes from the fact that many studies illustrate that CLA increases apoptosis and inhibits DNA synthesis (23, 48, 64, 74, 75, 83, 84, 96, 110, 111, 120, 126, 127, 159). Furthermore, gene expression studies have demonstrated that CLA down regulates cell cycle promoting genes and up regulates pro-apoptotic genes (70, 92).

Numerous studies have provided evidence that CLA has a beneficial role in atherosclerosis, the hardening of blood vessels due to plaque buildup. CLA exerts its beneficial effects mainly through reducing low-density lipoprotein-cholesterol and triacylglycerol levels, leading to a reduction in the amount of cholesterol deposited in arteries (141). CLA produces such a severe effect on cholesterol and triacylglycerol levels that it can even cause a reduction in the amount of established atherosclerosis (141). It appears that CLA begets these effects by improving plasma lipoprotein metabolism, which ameliorates the lipoprotein profile (141). Indeed, several studies have demonstrated that CLA causes an increase in the expression of lipogenic enzymes in the liver (131, 136, 158).

The effects of CLA on diabetes are more controversial as there are conflicting reports on its effects on insulin sensitivity. It appears that CLA causes beneficial effects through the reduction of pro-inflammatory cytokines, which play an important role in energy homeostasis (163). Numerous studies have confirmed that CLA increases cytokine production in various tissues, especially adipose tissue (70, 92, 133). Microarray results suggest that CLA regulates insulin activity in the livers of CLA fed mice, in which expression of the insulin receptor was down regulated (136). Furthermore, insulin is well-known to exert many of its effects through the phosphatidylinositol 3-kinase (PI3K)

pathway, which is generally down regulated by CLA (154). Besides these pathways, insulin also can induce adipose differentiation (Figure 1.12).

In conclusion, numerous studies have established that CLA has many benefits on health. CLA has generally beneficial effects against cancer by increasing apoptosis. It also possesses beneficial effects against atherosclerosis by altering lipid and cholesterol metabolism. While CLA has been clearly shown to affect diabetes, it is unclear if the effect is positive or negative. Taken together, CLA appears to be a compound which has many beneficial effects, ranging from weight loss to cancer prevention.

CLA and Body Composition

CLA causes beneficial effects against obesity by modulating body composition. While CLA possesses anti-lipogenic effects in many species, perhaps the effects are most pronounced in the mouse where CLA can reduce body-fat mass by 50 to 70% (8, 71, 76). The exact mechanisms of the actions of CLA are unknown; studies have suggested CLA causes an increase in energy expenditure and decrease in feed consumption, but these results are controversial.

A summary of results from various mouse studies on the effects of CLA on body mass are given in Table 1.2. CLA, in most cases, causes a reduction or no change in body mass. Feeding more of the *trans*-10, *cis*-12 isomer may increase the probability of observing a significant change in body weight. This can be accomplished by feeding a diet with more CLA, using a CLA isomer mix that consists of a greater percentage of *trans*-10, *cis*-12 CLA, and/or feeding the CLA diet for a longer period of time. Despite this generality, there were still several studies finding no change in body mass despite feeding

high amounts of *trans*-10, *cis*-12 CLA and others that fed low amounts of *trans*-10, *cis*-12 CLA and found statistically significant results. Opposing results have been reported in only one study, where Miner and coworkers (111) saw an increase in body mass when CLA was fed to M16 mice. Disputing this study using this same line of mice, another group found a decrease in body mass when fed CLA (70). There are several possible explanations for the many discrepancies. For instance, Hayek and coworkers (65) found a decrease in body weight for 4 month old C57BL/6NCrlBR mice, but not for 22 month old mice, suggesting age may play an important role in the efficacy of CLA. Similar to the results by Hayek and colleagues (65) it was the older M16 mice used by Miner and coworkers (111) which had an increased body mass when fed CLA, while the younger M16 mice used by House and colleagues (70) had reduced body weight. Another study demonstrated that the dry weight, the weight of the body without water, was reduced when fed CLA but the live weight was not (162), raising the possibility that the increased weight may be from water. Also, there was a large difference in the purity of the CLA isomers, so while both studies fed 1% CLA diets, the diet associated with increased body weight fed half as much *trans*-10, *cis*-12 CLA as the other study (70, 111). In general, CLA tends to reduce body mass in mice; however, this effect is not universal.

Because CLA reduces body mass in several studies, one might expect CLA to affect feed intake. Similar to previous results, discrepancies abound in the feed intake arena. Results from these studies are summarized in Table 1.2. Given the fact there are many mixed results for the effect of CLA on both body mass and feed intake, one might expect studies reporting a reduction in body mass would report a reduction in feed intake, but this

is not the case. Many of the studies displaying a reduction in body mass showed no change in feed intake and vice versa. Based upon these results, we can only conclude that if CLA affects feed intake, it leads to a reduction in feed intake.

Because CLA has no clear effect on feed intake, increases in energy expenditure may explain the observed effects on body mass. A summary of four studies looking at energy expenditure are given in Table 1.2. All but one mouse line indicated that CLA increased energy expenditure. Only the MH line, genetically selected for high heat loss, exhibited a decrease in energy expenditure and may be the result of a genetic interaction (111). The genetic selection for high heat loss in the MH line created a mouse that expends a great deal of heat in the absence of CLA. It is possible that addition of CLA to the diet attenuated this effect by interfering with a pathway that had already been altered by genetic selection. Based upon these results, it seems that CLA has a positive effect on energy expenditure.

Because many studies observed a decrease in body mass of mice fed CLA, physiological adjustments must accompany these changes. All studies reported reduction in adipose tissue mass in mice fed CLA (Table 1.2). Many of these studies illustrated a dose dependent reduction in adipose tissue mass; in other words, the more *trans*-10, *cis*-12 CLA isomer fed and the more days it was fed, the more adipose tissue lost (31, 158).

Many studies did not show a decrease in body weight, but still exhibited a decrease in the amount of adipose tissue in their mice; so, where did this extra mass go? Many studies displayed an increase in organ, especially liver and spleen, weight in CLA fed mice. Most of the studies reported an increase in liver weight; however, others reported no

change (Table 1.2). The lack of change reported by Poirier and colleagues (133) is likely because these mice were gavage fed 0.1g CLA daily for one week, which was a shorter time and possibly a lower dose than most other studies. A significant novel genetic interaction may explain why the M16, MH, and ML selected lines do not illicit an increase in liver weight. Furthermore, the study which did not show an effect for CLA using the MH, ML, and a randombred control line of mice only fed 26.93% pure *trans*-10, *cis*-12 CLA at 0.5% of the diet for 2 weeks, which is less than most other studies. Yamasaki and coworkers (174) did not see a change in liver weight but the CLA isomer mix contained a very low percentage of *trans*-10, *cis*-12 CLA, which may not have been adequate to alter liver weight.

In conclusion, CLA has no clear effect on total body weight or feed intake. CLA most likely increases energy expenditure and liver weight, despite the fact there are a few reports which did not report a change. It is clear that CLA causes a decrease in adipose tissue mass. It is likely that the increase in liver weight, and possibly other organs, generally accounts for the numerous studies that have not found a decrease in body weight of mice fed CLA. Hence, a difference in body weight was probably only observed when the increase in organ weight was not enough to compensate for the decrease in adipose weight or when the mice were not fed a high enough concentration of *trans*-10, *cis*-12 CLA for an adequate length of time.

Cellular Responses

When one considers that CLA reduces the amount of adipose tissue and more than likely increases the weight of the liver, one wonders where this extra/loss of mass comes

from. The reduction of adipose tissue during CLA supplementation has been attributed to inhibition of proliferation, differentiation and increasing apoptosis in preadipocytes (71, 157). By inducing apoptosis in adipose tissue, CLA effectively reduces the number of cells, thereby causing a decrease in tissue weight. Numerous studies have established that CLA induces apoptosis in a dose dependent manner *in vitro* (48, 74, 75, 83, 96, 110, 120) and *in vivo* (23, 64, 84, 111, 126, 127, 159). Furthermore, histological analyses of adipose tissue from CLA treated mice show a reduction in size and number of adipocytes (14, 92, 159, 172). Another mechanism by which CLA may reduce cell numbers is through obstruction of the cell cycle, through inhibition of DNA synthesis (75, 83). CLA is known to impede progression through the S phase because there is an increase in the proportion of S phase cells and a reduced proportion of G1/G0 phase cells after 72 hours of CLA treatment (48, 110). CLA also exerts its adipose reducing effects by causing delipidation. In adipocytes *trans*-10, *cis*-12 CLA causes an observable decrease in lipid content *in vitro* (16-19, 26, 48, 50, 57, 77). By inhibiting DNA synthesis, inducing apoptosis, and instigating delipidation, CLA causes a significant reduction in adipose tissue weight.

Adipocyte Development and Lipid Metabolism

Adipose mass may be decreased by decreasing cell numbers and/or cell size. As has been previously discussed, CLA causes a decrease in the lipid content in adipocytes, thereby reducing the size of the adipocytes. It also has been shown that CLA reduces the number of adipocytes by inhibiting preadipocyte differentiation *in vitro* (15). Adipogenesis has been best studied through the effects of several adipogenic transcription factors. Predictably, CLA has an effect on many of these transcription factors.

Peroxisome Proliferator-Activated Receptors (PPAR)

CCAAT/enhancer binding proteins (C/EBPs) and peroxisome proliferator-activated receptor (PPAR) γ transcription factors are among the best characterized adipogenic factors. C/EBP-β and C/EBP-δ are among the first genes to be induced during adipose development, which then induce the expression of C/EBP-α and PPARγ (Figure 1.12) (108). PPARs are nuclear hormone receptors and, like other nuclear hormone receptors, their ligands are lipids. Unlike most nuclear receptors which have a single ligand, PPARs possess many natural ligands, including CLA (33, 98). Numerous studies have demonstrated that CLA causes a decrease in PPARγ expression (15-17, 70, 77). Contrary to this, cell culture experiments illustrate that CLA can weakly induce expression of PPARγ (8, 17, 57). Cells that have been stimulated with a PPARγ agonist show a significant reduction in PPARγ expression and lipid content when treated with CLA (17, 57, 77). These results indicate that CLA exerts an antagonistic effect on PPARγ.

Another PPAR isotype, PPARα, also plays a role in metabolism, but its role is very different than PPARγ. PPARα plays a major role in lipid utilization while PPARγ is mostly associated with lipid storage (33). Their expression profiles agree with this as PPARα is highly expressed in liver while PPARγ is mainly expressed in white adipose tissue (33). Consistent with its role in increasing lipid metabolism, CLA is a potent ligand and activator of PPARα (113). Through this mechanism, CLA induces many genes associated with lipid metabolism.

The actions of CLA on PPARs cause a two pronged approach to decreasing body weight. First, CLA antagonizes the actions of PPARγ thereby inhibiting adipose

development and lipid accumulation. Second, CLA activates PPARα to increase the transcription of genes involved in lipid metabolism and β-oxidation. Together, these two transcription factors can explain much of the anti-lipogenic effects of CLA.

Sterol Regulatory Element Binding Protein (SREBP)

Another group of transcription factors, SREBPs, also play a major role in metabolism. Different SREBP isoforms regulate different aspects of metabolism; SREBP-1 is involved in fatty acid synthesis while SREBP-2 is involved with intracellular cholesterol metabolism (20, 35, 66, 67, 137). Studies show that CLA regulates SREBP-1 expression differently in adipose and liver tissue. SREBP-1 is reduced (58, 175) or unchanged (138, 139, 142) by CLA in adipose tissue, while, in liver, its expression is increased (138, 152, 158). SREBP-1 increases fatty acid synthesis, so it is logical that it is reduced in adipose tissue and increased in liver because, in the presence of CLA, adipose loses while liver gains lipid mass.

SCD (stearoyl-coenzyme A desaturase), also known as Δ^9 desaturase, is an enzyme transcriptionally regulated by SREBP-1. SCD represents the rate-limiting step in the conversion of saturated fatty acids to monounsaturated fatty acids (116). Repression of SCD limits the availability of oleic acid, which, in turn, limits the amount of cholesterol transported out of the liver. It is well known that dietary polyunsaturated fatty acids, such as LA and CLA, reduce SCD activity (116). Previous studies have demonstrated a reduced (93), unaffected (102, 136, 162), and increased (131, 158) level of SCD-1 in murine liver in the presence of CLA. By regulating PPAR and SREBP activity, CLA can cause many changes to fatty acid and cholesterol synthesis and metabolism.

Signaling Pathways

Several experiments have studied gene expression in an attempt to clarify the mechanisms by which CLA exerts its anti-lipogenic effects. CLA causes many genes to be differentially regulated, as demonstrated by two microarray experiments, which show thousands of genes differentially expressed in white adipose tissue (70, 92) and hundreds of genes differentially expressed in liver (136) of mice fed CLA. One would hope that these gene expression studies would settle some of the discrepancies of CLA action, but instead, they are full of their own inconsistencies. These data show CLA regulates genes that are involved with apoptosis, energy expenditure, fatty acid oxidation, lipolysis, inflammation, lipogenesis, as well as differentiation.

Cytokines

Genes that encode cytokines are commonly differentially expressed by CLA feeding (16, 27, 70, 92, 133). Cytokines are soluble proteins, which are excreted by cells and function in much the same way as hormones. Many cytokines, such as interleukins, interferons, tumor necrosis factor α (TNF-α) and leptin, have been demonstrated to be differentially regulated by CLA (70, 92, 135, 174). Cytokines are well known to act through the Janus kinase (Jak)/signal transducer and activator of transcription (Stat) pathway (Figure 1.13) (60, 87, 99, 117). The Jak/Stat pathway is essential for several cellular processes, including immune response, cellular proliferation, cell movement, and apoptosis (4, 69).

TNF-α can promote apoptosis, which it does by stimulation of various caspases (161). In adipose tissue TNF-α is known to stimulate lipolysis (91). This is effected through

three different pathways; inhibition of insulin signaling, increased degradation of G protein alpha inhibitor ($G\alpha_i$), which inhibits the antilipolytic effects of adenosine, and decreased expression and phosphorylation of perilipins, which protect lipid droplets from hydrolysis (91). Due to its role in promotion of apoptosis and lipolysis, it is not surprising that most studies exhibit an up regulation of TNF-α by CLA (70, 71). There is an opposing view which states that CLA attenuates the effects of TNF-α (94). These authors argue that TNF-α is a key mediator of cancer, atherosclerosis, and obesity, and suggest that CLA protects cells from the negative effects of TNF-α in these diseases.

Interleukins and interferons are, like TNF-α, pro-inflammatory cytokines, which are well known for their role in inflammation and immunity (78). Inflammation is recognized as an important component of obesity, though it is not clear if it is a cause or effect (115). Given this, it is not surprising that in many studies, CLA has shown a generally beneficial effect on inflammatory responses (107, 118, 141).

Leptin is another cytokine best known for its weight reducing effects, which makes it a likely candidate for regulation by CLA (61). Leptin acts mainly on the central nervous system to regulate food intake and energy expenditure (7). Because CLA does not have a clear effect on food intake or energy expenditure, it is not surprising that CLA does not have a clear effect on leptin expression (71). Most studies show that leptin is down regulated by CLA (92, 114, 153, 165) while one study demonstrated that CLA up regulated the expression of leptin in human adipocytes *in vitro* (17).

Intracellular Signaling Pathways

In addition to the Jak/Stat pathway, there are a variety of other intracellular pathways that are modulated by CLA. There is much crosstalk between these various pathways. An example of a pathway altered by CLA is the nuclear factor-κB pathway, which, like the Jak/Stat pathway, is best known for its role in inflammation and innate immunity, and is an important activator of anti-apoptotic gene expression (78). The effects of CLA on this pathway are unclear as different studies using different isomers and cell types have shown that CLA activates (27) and inactivates (24, 100, 105) this pathway. Another pathway which is affected by CLA is the PI3K/AKT pathway. (AKT is a serine/threonine kinase activated by PI3K). Most studies suggest that CLA down regulates this pathway (25, 70, 84, 96). The PI3K/AKT pathway is known to regulate processes such as proliferation, growth, and apoptosis, most of which are affected by CLA.

Summary

These pathways represent a few of the pathways regulated by CLA. Microarray data provide clear evidence that CLA regulates the expression of many genes (70, 92, 136). The precise molecular mechanisms of CLA's actions remain unclear as there are many studies that have presented conflicting results. This is not surprising given the fact that there is vast disagreement on the effects of CLA on body composition in mice. This is further confounded by the use of multiple species, tissue types, and isomers, all of which seem to have a different effect. It is clear, however, that the *trans*-10, *cis*-12 isomer exerts anti-adipogenic effects. These anti-adipogenic effects are caused by a reduction in adipocyte size and number. There is also much evidence which suggests that lipid metabolism is

increased. In conclusion, CLA has potential as an anti-obesity compound but more research is needed to determine its precise physiological role.

Conclusion

Obesity is a major problem in the United States and around the world. Using gene expression techniques, such as microarrays and qPCR, many of the genomic causes of obesity have been brought to light. There are many animal models which serve to elucidate the underlying causes of obesity. Single gene, polygenic, and nutritional models have all been used to shed light onto gene expression changes associated with obesity. Potential anti-obesity compounds, such as *trans*-10, *cis*-12 CLA, have been identified. CLA causes a rapid reduction in adipose tissue, and by doing so, alters many genes' expression. CLA has potential as a natural anti-obesity compound but more research is needed to determine its precise physiological role. Obesity is a complex disease and studying gene expression in model organisms aids in understanding.

Table 1.1 Comparison of Affymetrix and Spotted Microarrays.

	Affymetrix	Spotted
Cost	High	Usually lower
Synthesis of Probes	On array - Photolithography	External synthesis
Delivery of Probes	Synthesized on array	Delivered to array - robot spotting, inkjet, etc.
Length of Probe	Short ~ 20 nucleotides	Long - 70 nucleotides and cDNA are common
Number of Probes	High	40,000 is near the upper limit
Type of Platform	Silicone	Usually glass
Number of Colors	1	2 - more than two is uncommon

There are two types of microarrays, Affymetrix and spotted. These are compared in order to highlight the pro's and con's of the different types of arrays. There are several differences between these arrays which can affect data and experimental design.

Table 1.2 Effects of CLA on Mice

Strain	Age[1]	Isomer[2]	Amount[3]	Duration[4]	Body Mass Change	Energy Intake Change	Energy Expenditure Change	Adipose Weight Change	Liver Weight Change	Reference
C57BL/6N	5	6.5% triglyceride	14.0%	3	NC			↓	↑	(174)
C57BL/6N	5	5.9% free fatty acid	12.5%	3	NC			↓	↑	(174)
C57BL/6J	6	33.7%	2.0%	3	↓	↓		↓		(153)
ICR	6	33.7%	2.0%	3	↓	NC		↓		(153)
C57BL/6J	6	34%	1.5%	3	↓	NC		↓	↑	(152)
ICR	6	34%	1.5%	3	↓	NC		↓	↑	(152)
Balb/c	6	30.1%	1.5%	5	↓	NC	↑	↓	↑	(155)
C57BL/6N	5	0.7% triglyceride	1.4%	3	NC			↓	NC	(174)
C57BL/6N	5	0.6% free fatty acid	1.3%	3	NC			↓	NC	(174)
Balb/c A	8 – 10	4.3%	1.2%	3	NC					(56)
SENCAR		45%	1.0% & 1.5%	6	↓					(10)
AKR/J	6	40.7%	1.0–1.2%	6	↓	↓		↓	↑	(167)
ICR	9	92%	1.0%	2	↓			↓	↑	(70)
M16	9	92%	1.0%	2	↓			↓	↑	(70)
C57BL/6J	6	6.2% or 12.5%	1.0%	3	NC	NC		↓	↑	(173)
C57BL/6NCrlBR	16	45%	1.0%	3 & 4	↓					(65)
C57BL/6NCrlBR	88	45%	1.0%	3	↓					(65)
C57BL/6J	10	44%	1.0%	2	NC	↓	↑	↓	↑	(111)
MH	12	44%	1.0%	2	NC	↓	↓	↓	↑	(111)
ML	12	44%	1.0%	2	NC	↓	↑	↓	↑	(111)
M16	26 – 30	44%	1.0%	2	↑			↓	NC	(111)
AKR/J	6	40.7%	1.0%	5	↓	NC		↓		(31)
AKR/J	4	40.7%	1.0%	5	NC	NC	↑	↓		(166)
AKR/J	6	40.7%	1.0%	5					↑	(33)
AKR/J	5	40.7%	1.0%	6	↓	NC	↑	↓	↑	(32)
C57BL/6J	8	36%	1.0%	20	NC	NC		↓	↑	(159)
Std-ddy	5	35.1%	1.0%	4 & 8	↓	NC		↓	NS (↑)	(121)
C57BL/6J	8	34.8%	1.0%	20	↓	NC		↓	↑	(158)
C57BL/6j	8		1.0%	4	↓			↓	↑	(30)
ICR	weanling	13%	0.9% or 0.5%	4	↓	↓		↓		(130)

Table 1.2 Effects of CLA on Mice

Strain	Age[1]	Isomer[2]	Amount[3]	Duration[4]	Body Mass Change	Energy Intake Change	Energy Expenditure Change	Adipose Weight Change	Liver Weight Change	Reference
Balb/c	8	38.8%	0.9%	1 – 6	NS (↓)	NC				(171)
AKR/J	6	40.7%	0.75%	5	↓	NC		↓		(31)
C57BL/6N	9	88.1%	0.5%	8	↓			↓	↑	(165)
C57BL/6N	9	88.1%	0.5%	8	↓				↑	(136)
C57BL/6N	9	88.1%	0.5%	8					↑	(80)
C57BL/6N	8	85 – 88%	0.5%	8				↓	↑	(79)
ICR	weanling	44%	0.5%	4	NS (↓)	↓		↓		(130)
CD-1	8 or 24	44%	0.5%		NS (↓)					(160)
ICR		43.5 – 44.9%	0.5%	7	↓	↓		↓		(129)
ICR		42.4%	0.5%	4	NC			↓		(77)
AKR/J	6	40.7%	0.5%	5	NC	NC		↓		(31)
ICR	weanling	3%	0.5%	4	NC	↓		↓		(130)
MH		26.93%	0.5%	2	↓	NC		↓	NC	(64)
ML		26.93%	0.5%	2	↓	NC		↓	NC	(64)
random bred control line	8	26.93%	0.5%	2	↓	↓		↓	NC	(64)
ICR	3 or 6		0.5%	4	NC	↓		↓		(128)
C57BL/6J	9		0.5%	2	NC	NC		↓		(92)
CD-1	4 – 5	>95%	0.15% or 0.3%	6	NC	NC		↓	↑	(162)
C57BL/6J		96.2%	0.4%	4	NC	↓		↓	↑	(28)
Balb/c	8	37.4%	0.4%	14	↓	NC		↓		(12)
ICR	weanling	79%	0.3%	4	↓	↓		↓		(130)
Balb/c	8	38.8%	0.3%	1 – 6	NS (↓)	NC				(171)
Balb/c	8	38.8%	0.1%	1 – 6	NS (↓)	NC				(171)
C57BL/6J	10	79%	0.1 g daily gavage	1	↓			↓	NC	(133)

1. Age of mice in weeks when CLA feeding trial began.
2. Percent *trans*-10, *cis*-12 CLA isomer in CLA mix.
3. CLA additive as a percent of feed.
4. Length of CLA feeding trial in weeks.

NS = not significant, parenthesis indicates direction of change
NC = no change

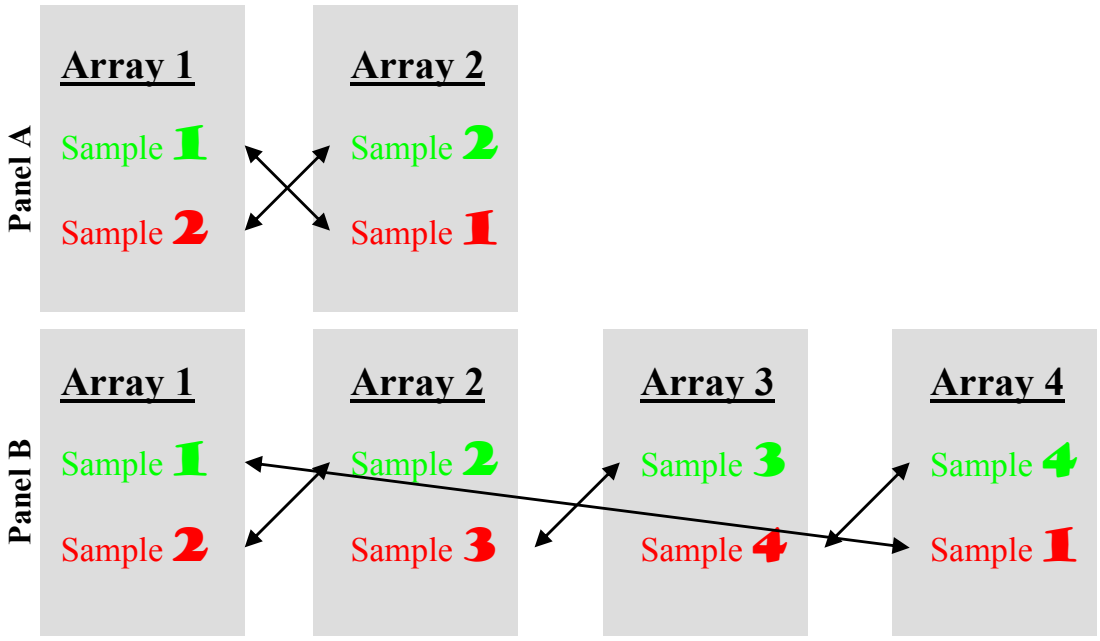

Figure 1.1 Examples of Dye Swap Strategies
Each sample is labeled with both Cy3 (green) and Cy5 (red). Panel A represents a simple dye swap strategy where the same samples are hybridized together. Panel B represents a loop design where the same samples are never hybridized together.

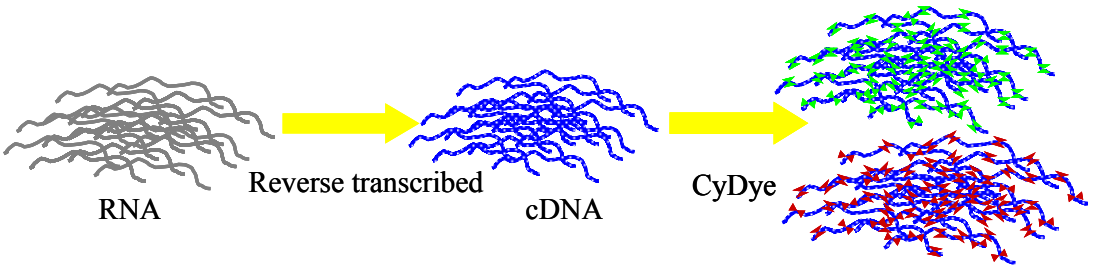

Figure 1.2 Steps in Indirect Labeling.
RNA is reverse transcribed into cDNA using tagged nucleotides represented by the spots on the cDNA. Dyes which can bind to the tag are mixed with the cDNA. The cDNA is thereby labeled by the dye binding to the tag.

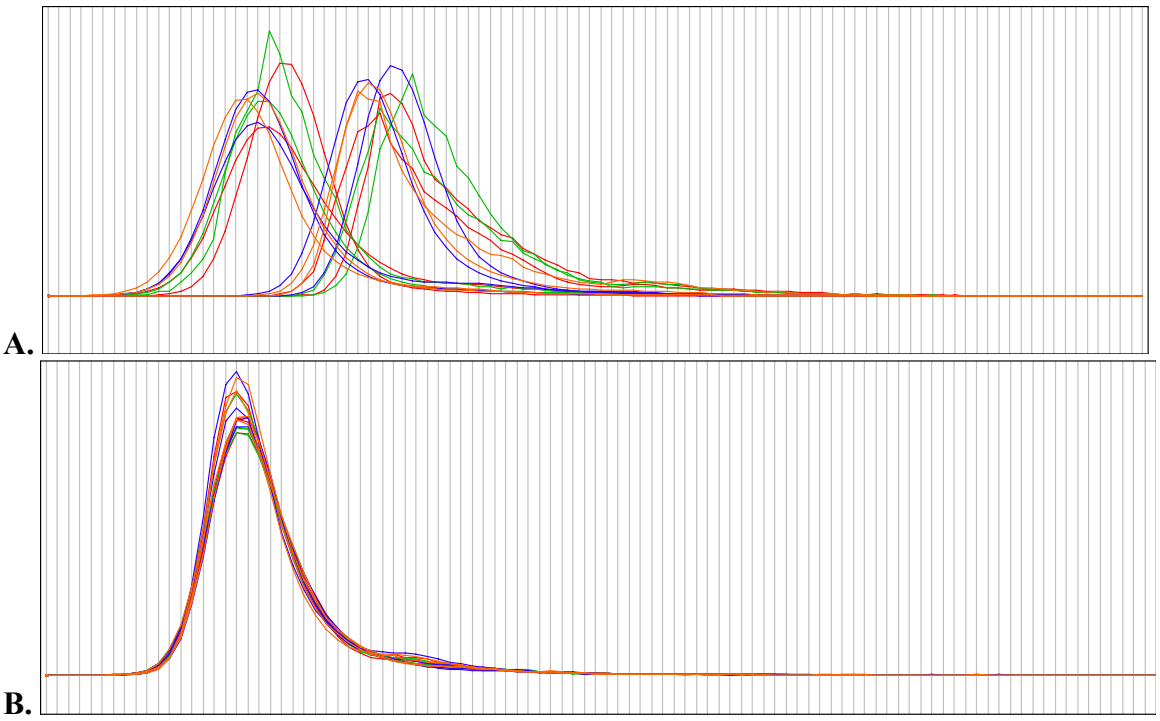

A.

B.

Figure 1.3 Comparison of Distribution of Microarray Data Before and After Normalization

A. Distribution of slides before normalization. Note that first set of peaks corresponds to data from Cy3 dyes while the second set corresponds to Cy5 dyes. **B.** Normalized distribution analysis. Within array normalization was performed using ratio analysis and between array normalization was performed using lowess normalization. Before the data were normalized, the distribution of each array was different. Normalization forced the arrays to have a similar distribution pattern so their data could be compared.

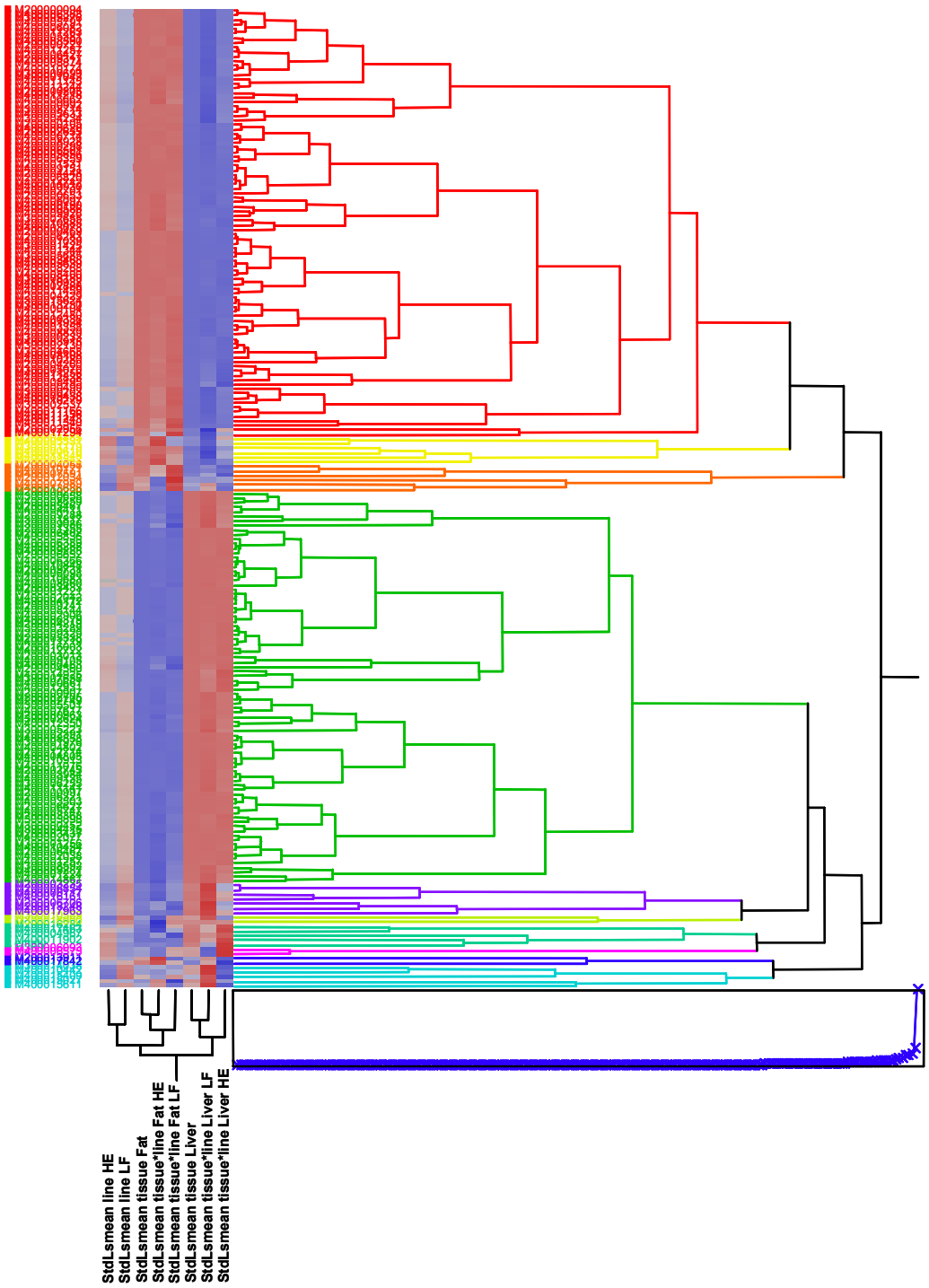

Figure 1.4 Heat Map.

A heat map is a graphical representation of microarray gene expression data. Treatment groups are listed on the X-axis while genes are listed on the Y-axis. The expression of a gene is represented by colors, with brighter colors indicating a greater change. In this case, red represents higher expression and blue represents negative expression.

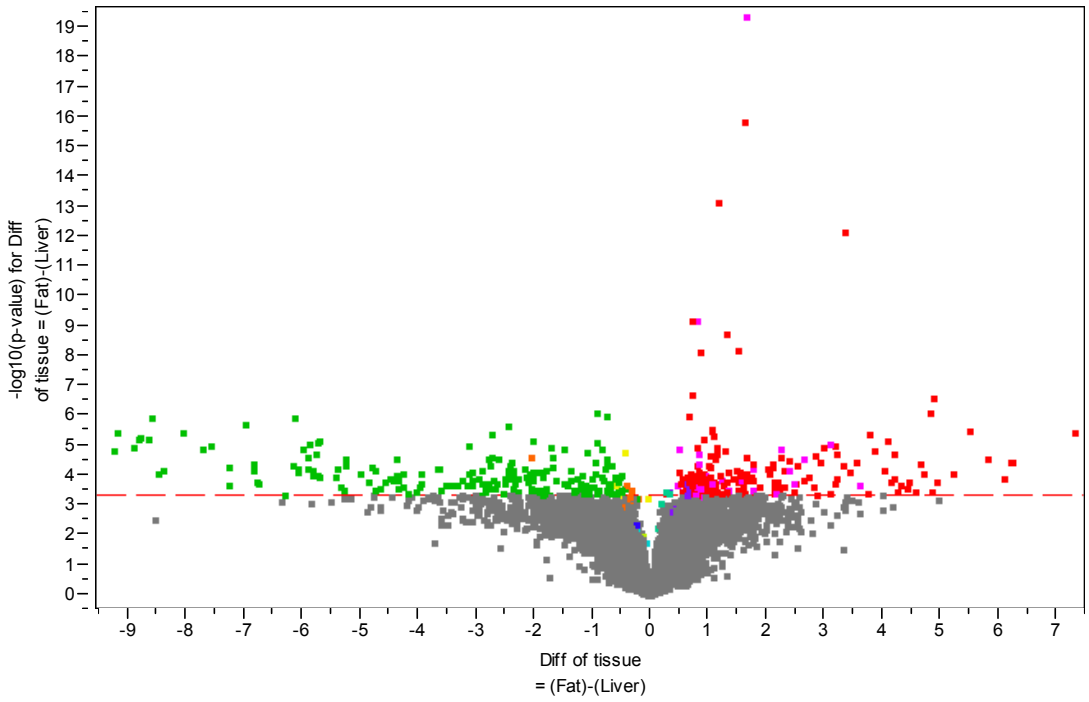

Figure 1.5 Volcano Plot.
In a volcano plot, fold changes are plotted on the X-axis while p-values are plotted on the Y-axis. By visualizing microarray data in this manner, p-values and fold changes may be viewed simultaneously.

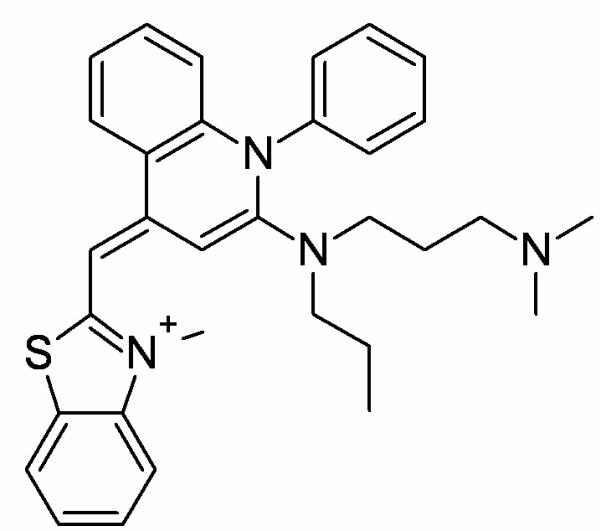

Figure 1.6 Molecular structure of SYBR Green I.
SYBR Green I is a dye which fluoresces in the presence of double stranded DNA.
http://upload.wikimedia.org/wikipedia/commons/2/29/SYBR_green_I_%28topological_formula%29.png

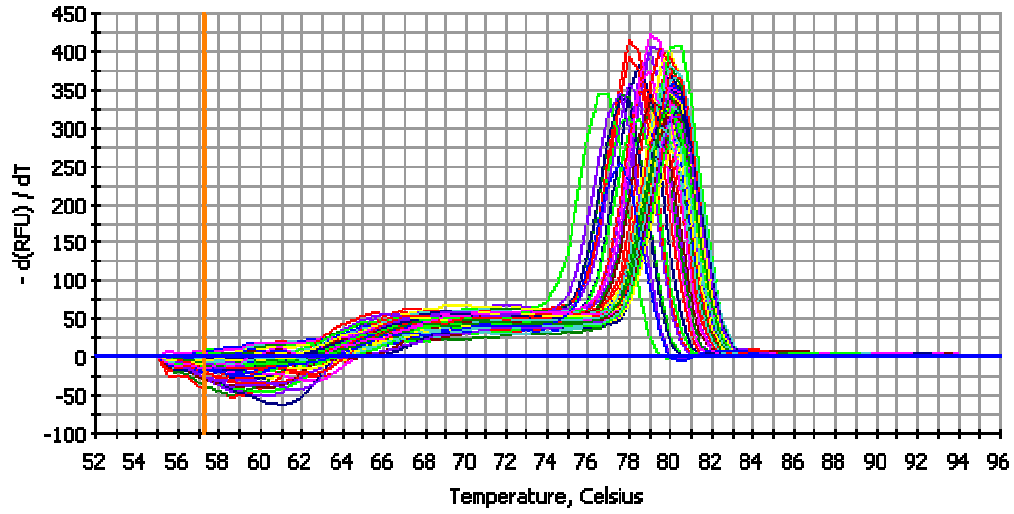

Figure 1.7 Sample Melting Curve.
The melting curve is a plot of the negative derivative of relative fluorescence units with respect to temperature versus temperature in °C which is used to calculate the T_m of the sample.

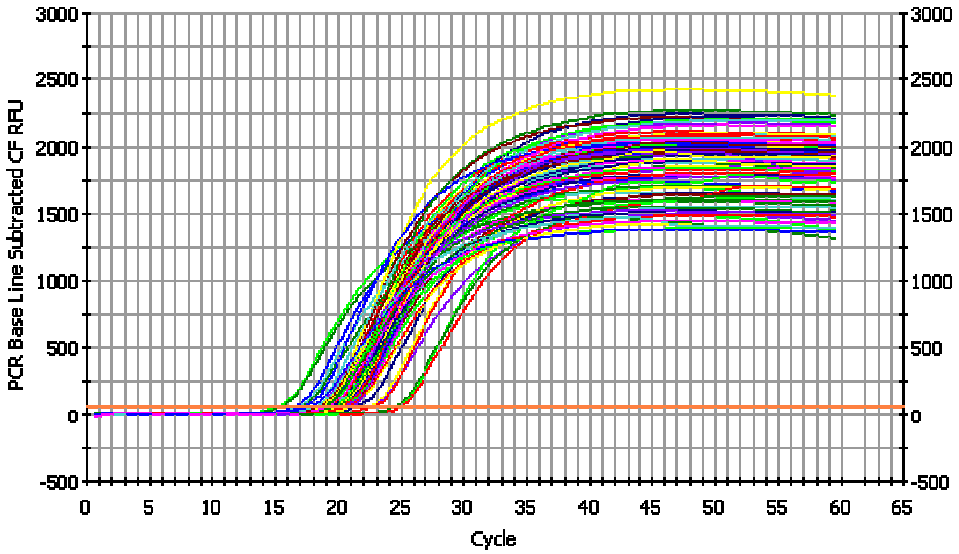

Figure 1.8 Sample qPCR Data.
The orange line represents the threshold at which C_t's are calculated.

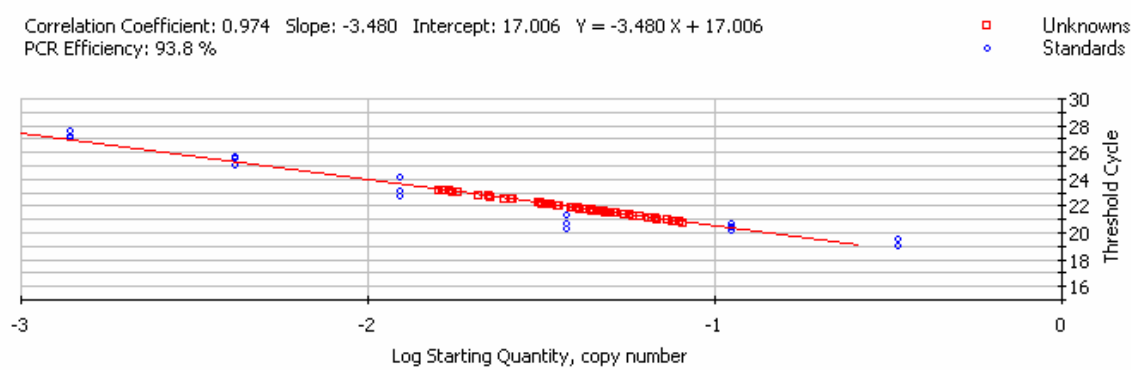

Figure 1.9 Sample Standard Curve.
Efficiency is calculated using the following formula: PCR Efficiency = $[10^{(-1/slope)}]-1$

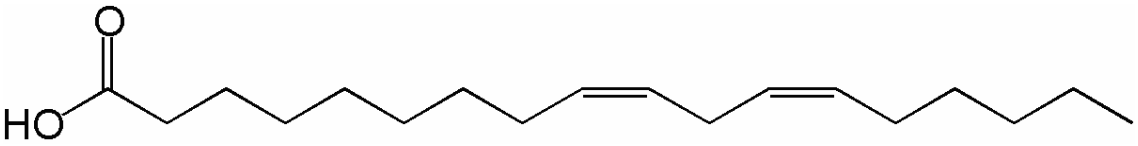

Figure 1.10 Linoleic Acid.
Structure of linoleic acid. Linoleic acid is an 18 carbon fatty acid. Note the two *cis* double bonds at the 9 and 12 positions.
http://upload.wikimedia.org/wikipedia/en/7/70/LAnumbering.png

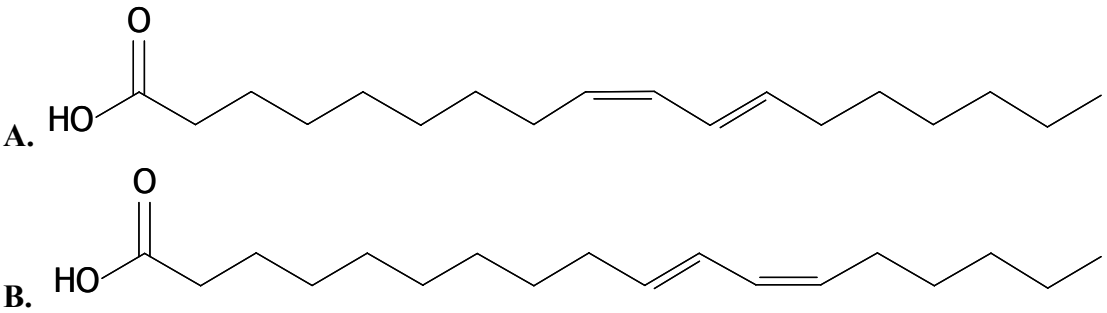

Figure 1.11 Biologically Active Isomers of Conjugated Linoleic Acid (CLA).
CLAs are 18 carbon fatty acids which are positional and geometrical isomers of linoleic acid. The *cis*-9, *trans*-11 CLA (**A.**) and *trans*-10, *cis*-12 (**B.**) are the only known biologically active isomers. *cis*-9, *trans*-11 CLA is the main isomer responsible for the anticarcinogenic effects of CLA while *trans*-10, *cis*-12 CLA is the main isomer responsible for the delipidative effects of CLA.

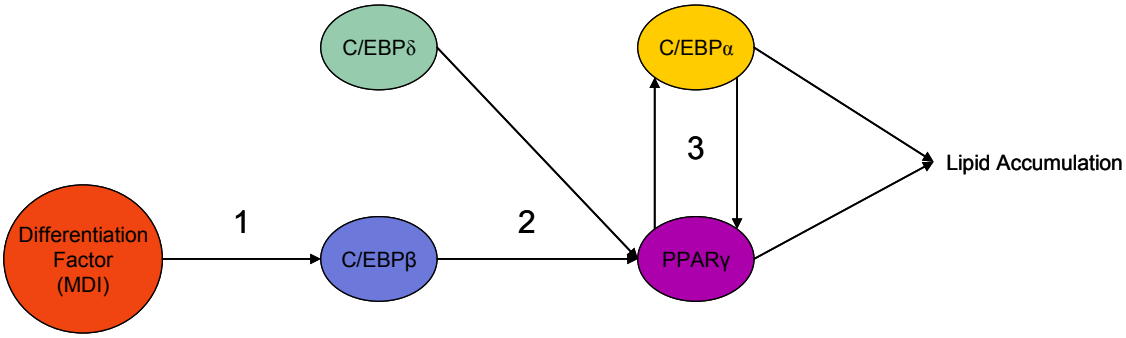

Figure 1.12 Factors Involved in Adipose Differentiation.
Methylisobutylxanthine, dexamethasone, and insulin (MDI) are the most common molecules used to induce differentiation in 3T3-L1 pre-adipocytes *in vitro*. Differentiation is characterized by lipid accumulation. Treatment of cells with differentiation factors ultimately leads to the expression of peroxisome proliferator-activated receptor-γ (PPARγ) and CCAAT-enhancer-binding protein (C/EBP) α. These transcription factors induce genes which compose the adipocyte phenotypeNumbers indicate the steps in *in vitro* induction of adipose differentiation.

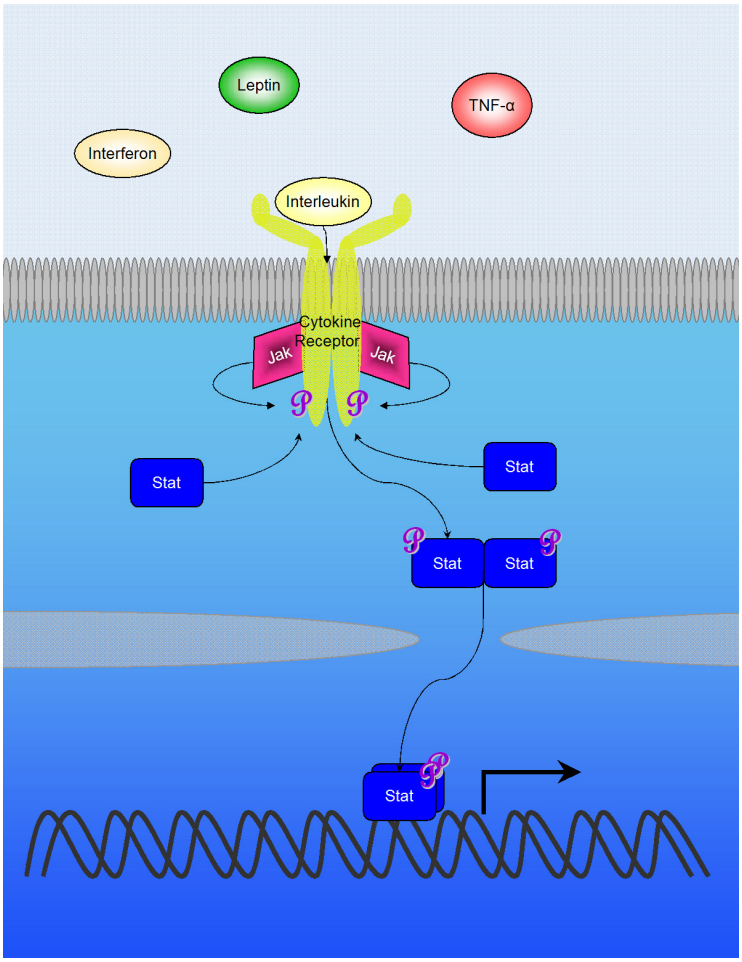

Figure 1.13 Cytokine signaling through the Jak/Stat pathway.
The Jak/Stat pathway is initiated when a cytokine binds to its receptor, causing a conformational change that recruits a Janus kinase (Jak). The recruitment of a Jak allows for phosphorylation of the receptor, allowing signal transducer and activator of transcription (Stat)s to be recruited. The Stats are then phosphorylated, which causes them to dimerize and move into the nucleus where they activate transcription.

References:

1. **Akalln AS, and Tokusoglu Ö**. A potential anticarcinogenic agent: conjugated linoleic acid (CLA). *Pakistan Journal of Nutrition* 2: 109-110, 2003.

2. **Allan MF, Eisen EJ, and Pomp D**. The M16 mouse: An outbred animal model of early onset polygenic obesity and diabesity. *Obesity Research* 12: 1397-1407, 2004.

3. **Allison DB, Cui XQ, Page GP, and Sabripour M**. Microarray data analysis: From disarray to consolidation and consensus. *Nature Reviews Genetics* 7: 55-65, 2006.

4. **Arbouzova NI, and Zeidler MP**. JAK/STAT signalling in *Drosophila*: Insights into conserved regulatory and cellular functions. *Development* 133: 2605-2616, 2006.

5. **Armstrong NJ, and van de Wiel MA**. Microarray data analysis: From hypotheses to conclusions using gene expression data. *Cellular Oncology* 26: 279-290, 2004.

6. **Atchley WR, Cowley DE, Eisen EJ, Prasetyo H, and Hawkins-Brown D**. Correlated response in the developmental choreographies of the mouse mandible to selection for body-composition. *Evolution* 44: 669-688, 1990.

7. **Bastard J-P, Maachi M, Lagathu C, Kim MJ, Caron M, Vidal H, Capeau J, and Feve B**. Recent advances in the relationship between obesity, inflammation, and insulin resistance. *European Cytokine Network* 17: 4-12, 2006.

8. **Belury MA**. Dietary conjugated linoleic acid in health: Physiological effects and mechanisms of action. *Annual Review of Nutrition* 22: 505-531, 2002.

9. **Belury MA**. Inhibition of carcinogenesis by conjugated linoleic acid: Potential mechanisms of action. *Journal of Nutrition* 132: 2995-2998, 2002.

10. **Belury MA, and Kempa-Steczko A**. Conjugated linoleic acid modulates hepatic lipid composition in mice. *Lipids* 32: 199-204, 1997.

11. **Benjamini Y, and Hochberg Y**. Controlling the false discovery rate - a practical and powerful approach to multiple testing. *Journal of the Royal Statistical Society Series B-Methodological* 57: 289-300, 1995.

12. **Bhattacharya A, Rahman MM, Sun DX, Lawrence R, Mejia W, McCarter R, O'Shea M, and Fernandes G**. The combination of dietary conjugated linoleic acid and treadmill exercise lowers gain in body fat mass and enhances lean body mass in high fat-fed male Balb/C mice. *Journal of Nutrition* 135: 1124-1130, 2005.

13. **Bourneuf E, Hérault F, Chicault C, Carré W, Assaf S, Monnier A, Mottier S, Lagarrigue S, Douaire M, Mosser J, and Diot C**. Microarray analysis of differential gene expression in the liver of lean and fat chickens. *Gene* 372: 162-170, 2006.

14. **Bouthegourd JC, Martin JC, Gripois D, Roseau S, Blouquit MF, Even PC, Tome D, and Quignard-Boulange A**. Efficacy of dietary CLA and CLA plus Guarana (ADI pill) on body adiposity, and adipocytes cell number and size. *The FASEB Journal* 16: A370-A370, 2002.

15. **Brodie AE, Manning VA, Ferguson KR, Jewell DE, and Hu CY**. Conjugated linoleic acid inhibits differentiation of pre- and post-confluent 3T3-L1 preadipocytes but inhibits cell proliferation only in preconfluent cells. *Journal of Nutrition* 129: 602-606, 1999.

16. **Brown JM, Boysen MS, Chung S, Fabiyi O, Morrison RF, Mandrup S, and McIntosh MK**. Conjugated linoleic acid induces human adipocyte delipidation: Autocrine/paracrine regulation of MEK/ERK signaling by adipocytokines. *Journal of Biological Chemistry* 279: 26735-26747, 2004.

17. **Brown JM, Boysen MS, Jensen SS, Morrison RF, Storkson J, Lea-Currie R, Pariza M, Mandrup S, and McIntosh MK**. Isomer-specific regulation of metabolism and PPARγ signaling by CLA in human preadipocytes. *Journal of Lipid Research* 44: 1287-1300, 2003.

18. **Brown JM, Halvorsen YD, Lea-Currie YR, Geigerman C, and McIntosh M**. *Trans*-10, *cis*-12, but not *cis*-9, *trans*-11, conjugated linoleic acid attenuates lipogenesis in primary cultures of stromal vascular cells from human adipose tissue. *Journal of Nutrition* 131: 2316-2321, 2001.

19. **Brown M, Evans M, and McIntosh M**. Linoleic acid partially restores the triglyceride content of conjugated linoleic acid-treated cultures of 3T3-L1 preadipocytes. *Journal of Nutritional Biochemistry* 12: 381-387, 2001.

20. **Brown MS, and Goldstein JL**. The SREBP pathway: Regulation of cholesterol metabolism by proteolysis of a membrane-bound transcription factor. *Cell* 89: 331-340, 1997.

21. **Cartwright AL**. Adipose cellularity in *Gallus domesticus*: Investigations to control body-composition in growing chickens. *Journal of Nutrition* 121: 1486-1497, 1991.

22. **Castro-Chavez F, Yechoor VK, Saha PK, Martinez-Botas J, Wooten EC, Sharma S, O'Connell P, Taegtmeyer H, and Chan L**. Coordinated upregulation of oxidative pathways and downregulation of lipid biosynthesis underlie obesity resistance in

perilipin knockout mice - A microarray gene expression profile. *Diabetes* 52: 2666-2674, 2003.

23. **Chen B-Q, Xue Y-B, Liu J-R, Yang Y-M, Zheng Y-M, Wang X-L, and Liu R-H**. Inhibition of conjugated linoleic acid on mouse forestomach neoplasia induced by benzo (a) pyrene and chemopreventive mechanisms. *World Journal of Gastroenterology* 9: 44-49, 2003.

24. **Cheng W-L, Lii C-K, Chen H-W, Lin T-H, and Liu K-L**. Contribution of conjugated linoleic acid to the suppression of inflammatory responses through the regulation of the NF-κB pathway. *Journal of Agricultural and Food Chemistry* 52: 71-78, 2004.

25. **Cho HJ, Kim WK, Kim EJ, Jung KC, Park S, Lee HS, Tyner AL, and Park JHY**. Conjugated linoleic acid inhibits cell proliferation and ErbB3 signaling in HT-29 human colon cell line. *American Journal of Physiology - Gastrointestinal and Liver Physiology* 284: G996-G1005, 2003.

26. **Choi Y, Kim Y-C, Han Y-B, Park Y, Pariza MW, and Ntambi JM**. The *trans*-10,*cis*-12 isomer of conjugated linoleic acid downregulates stearoyl-CoA desaturase 1 gene expression in 3T3-L1 adipocytes. *Journal of Nutrition* 130: 1920-1924, 2000.

27. **Chung SK, Brown JM, Provo JN, Hopkins R, and McIntosh MK**. Conjugated linoleic acid promotes human adipocyte insulin resistance through NFκB-dependent cytokine production. *Journal of Biological Chemistry* 280: 38445-38456, 2005.

28. **Clément L, Poirier H, Niot I, Bocher V, Guerre-Millo M, Krief S, Staels B, and Besnard P**. Dietary *trans*-10,*cis*-12 conjugated linoleic acid induces hyperinsulinemia and fatty liver in the mouse. *Journal of Lipid Research* 43: 1400-1409, 2002.

29. **Cook ME, and Pariza M**. The role of conjugated linoleic acid (CLA) in health. *International Dairy Journal* 8: 459-462, 1998.

30. **Degrace P, Demizieux L, Gresti J, Chardigny J-M, Sébédio J-L, and Clouet P**. Association of liver steatosis with lipid oversecretion and hypotriglyceridaemia in C57BL/6j mice fed *trans*-10,*cis*-12-linoleic acid. *FEBS Letters* 546: 335-339, 2003.

31. **DeLany JP, Blohm F, Truett AA, Scimeca JA, and West DB**. Conjugated linoleic acid rapidly reduces body fat content in mice without affecting energy intake. *American Journal of Physiology - Regulatory Integrative and Comparative Physiology* 276: R1172-R1179, 1999.

32. **DeLany JP, and West DB**. Changes in body composition with conjugated linoleic acid. *Journal of the American College of Nutrition* 19: 487S-493S, 2000.

33. **Desvergne B, and Wahli W**. Peroxisome proliferator-activated receptors: Nuclear control of metabolism. *Endocrine Reviews* 20: 649-688, 1999.

34. **Domeneghini C, Di Giancamillo A, and Corino C**. Conjugated linoleic acids (CLAs) and white adipose tissue: how both in vitro and in vivo studies tell the story of a relationship. *Histology and Histopathology* 21: 663-672, 2006.

35. **Eberlé D, Hegarty B, Bossard P, Ferré P, and Foufelle F**. SREBP transcription factors: Master regulators of lipid homeostasis. *Biochimie* 86: 839-848, 2004.

36. **Eisen EJ**. Genetics of body composition in mice. In: *Forty-Third Annual National Breeders Roundtable Proceedings*. St. Louis, MO: 1994, p. 67-89.

37. **Eisen EJ**. Restricted index selection in mice designed to change body fat without changing body weight: direct responses. *Theoretical and Applied Genetics* 83: 973-980, 1992.

38. **Eisen EJ**. Restricted selection index in mice designed to change body fat without changing body weight: correlated responses. *Theoretical and Applied Genetics* 84: 307-312, 1992.

39. **Eisen EJ**. Selection for components of body composition in mice. In: *Proceedings of the 3rd World Congress on Genetics Applied to Livestock Production*. Lincoln, NE: 1986, p. 389-394.

40. **Eisen EJ**. Selection for components related to body-composition in mice: correlated responses. *Theoretical and Applied Genetics* 75: 177-188, 1987.

41. **Eisen EJ**. Selection for components related to body-composition in mice: direct responses. *Theoretical and Applied Genetics* 74: 793-801, 1987.

42. **Eisen EJ, Bakker H, and Nagai J**. Body-composition and energetic efficiency in two lines of mice selected for rapid growth-rate and their F_1 crosses. *Theoretical and Applied Genetics* 49: 21-34, 1977.

43. **Eisen EJ, Benyon LS, and Douglas JA**. Long-term restricted index selection in mice designed to change fat-content without changing body-size. *Theoretical and Applied Genetics* 91: 340-345, 1995.

44. **Eisen EJ, and Coffey MT**. Correlated responses in body-composition based on selection for different indicator traits in mice. *Journal of Animal Science* 68: 3557-3562, 1990.

45. **Eisen EJ, and Leatherwood JM**. Adipose cellularity and body-composition in polygenic obese mice as influenced by preweaning nutrition. *Journal of Nutrition* 108: 1652-1662, 1978.

46. **Eisen EJ, and Leatherwood JM**. Effect of post-weaning feed restriction on adipose cellularity and body-composition in polygenic obese mice. *Journal of Nutrition* 108: 1663-1672, 1978.

47. **Eisen EJ, and Leatherwood JM**. Predicting percent fat in mice. *Growth* 45: 100-107, 1981.

48. **Evans M, Geigerman C, Cook J, Curtis L, Kuebler B, and McIntosh M**. Conjugated linoleic acid suppresses triglyceride accumulation and induces apoptosis in 3T3-L1 preadipocytes. *Lipids* 35: 899-910, 2000.

49. **Evans M, Lin X, Odle J, and McIntosh M**. *Trans*-10, *cis*-12 conjugated linoleic acid increases fatty acid oxidation in 3T3-L1 preadipocytes. *Journal of Nutrition* 132: 450-455, 2002.

50. **Evans M, Park Y, Pariza M, Curtis L, Kuebler B, and McIntosh M**. *Trans*-10,*cis*-12 conjugated linoleic acid reduces triglyceride content while differentially affecting peroxisome proliferator activated receptor γ2 and aP2 expression in 3T3-L1 preadipocytes. *Lipids* 36: 1223-1232, 2001.

51. **Evans ME, Brown JM, and McIntosh MK**. Isomer-specific effects of conjugated linoleic acid (CLA) on adiposity and lipid metabolism. *Journal of Nutritional Biochemistry* 13: 508-516, 2002.

52. **Field CJ, and Schley PD**. Evidence for potential mechanisms for the effect of conjugated linoleic acid on tumor metabolism and immune function: lessons from n-3 fatty acids. *American Journal of Clinical Nutrition* 79: 1190S-1198S, 2004.

53. **Flegal KA, Graubard BI, Williamson DF, and Gail MHH**. Excess deaths associated with underweight, overweight, and obesity. *Journal of the American Medical Association* 293: 1861-1867, 2005.

54. **Fritsche J, and Steinhart H**. Analysis, occurrence, and physiological properties of trans fatty acids (TFA) with particular emphasis on conjugated linoleic acid isomers (CLA) - a review. *Fett/Lipid* 100: 190-210, 1998.

55. **Goley EM, Anderson SJ, Ménard C, Chuang E, Lü X, Tofilon PJ, and Camphausen K**. Microarray analysis in clinical oncology: Pre-clinical optimization using needle core biopsies from xenograft tumors. *BMC Cancer* 4: 20, 2004.

56. **Göttsche JR, and Straarup EM**. Fatty acid profiles in tissues of mice fed conjugated linoleic acid. *European Journal of Lipid Science and Technology* 108: 468-478, 2006.

57. **Granlund L, Juvet LK, Pedersen JI, and Nebb HI**. *Trans*10, *cis*12-conjugated linoleic acid prevents triacylglycerol accumulation in adipocytes by acting as a PPARγ modulator. *Journal of Lipid Research* 44: 1441-1452, 2003.

58. **Granlund L, Pedersen JI, and Nebb HI**. Impaired lipid accumulation by *trans* 10, *cis* 12 CLA during adipocyte differentiation is dependent on timing and length of treatment. *Biochimica et Biophysica Acta - Molecular and Cell Biology of Lipids* 1687: 11-22, 2005.

59. **Ha YL, Grimm NK, and Pariza MW**. Anticarcinogens from fried ground beef: heat-altered derivatives of linoleic acid. *Carcinogenesis* 8: 1881-1887, 1987.

60. **Haan C, Kreis S, Margue C, and Behrmann I**. Jaks and cytokine receptors - An intimate relationship. *Biochemical Pharmacology* 72: 1538-1546, 2006.

61. **Halaas JL, Gajiwala KS, Maffei M, Cohen SL, Chait BT, Rabinowitz D, Lallone RL, Burley SK, and Friedman JM**. Weight-reducing effects of the plasma protein encoded by the obese gene. *Science* 269: 543-546, 1995.

62. **Hanrahan JP, Eisen EJ, and Legates JE**. Effects of population size and selection intensity of short-term response to selection for postweaning gain in mice. *Genetics* 73: 513-530, 1973.

63. **Hargrave KM, Li CL, Meyer BJ, Kachman SD, Hartzell DL, Della-Fera MA, Miner JL, and Baile CA**. Adipose depletion and apoptosis induced by *trans*-10, *cis*-12 conjugated linoleic acid in mice. *Obesity Research* 10: 1284-1290, 2002.

64. **Hargrave KM, Meyer BJ, Li CL, Azain MJ, Baile CA, and Miner JL**. Influence of dietary conjugated linoleic acid and fat source on body fat and apoptosis in mice. *Obesity Research* 12: 1435-1444, 2004.

65. **Hayek MG, Han SN, Wu DY, Watkins BA, Meydani M, Dorsey JL, Smith DE, and Meydani SN**. Dietary conjugated linoleic acid influences the immune response of young and old C57BL/6NCrlBR mice. *Journal of Nutrition* 129: 32-38, 1999.

66. **Heemers HV, Verhoeven G, and Swinnen JV**. Androgen activation of the sterol regulatory element-binding protein pathway: current insights. *Molecular Endocrinology* 20: 2265-2277, 2006.

67. **Horton JD, Goldstein JL, and Brown MS**. SREBPs: Activators of the complete program of cholesterol and fatty acid synthesis in the liver. *Journal of Clinical Investigation* 109: 1125-1131, 2002.

68. **Horton JD, Shah NA, Warrington JA, Anderson NN, Park SW, Brown MS, and Goldstein JL**. Combined analysis of oligonucleotide microarray data from transgenic and knockout mice identifies direct SREBP target genes. *Proceedings of the National Academy of Sciences of the United States of America* 100: 12027-12032, 2003.

69. **Hou SX, Zheng ZY, Chen X, and Perrimon N**. The JAK/STAT pathway in model organisms: Emerging roles in cell movement. *Developmental Cell* 3: 765-778, 2002.

70. **House RL, Cassady JP, Eisen EJ, Eling TE, Collins JB, Grissom SF, and Odle J**. Functional genomic characterization of delipidation elicited by *trans*-10, *cis*-12-conjugated linoleic acid (t10c12-CLA) in a polygenic obese line of mice. *Physiological Genomics* 21: 351-361, 2005.

71. **House RL, Cassady JP, Eisen EJ, McIntosh MK, and Odle J**. Conjugated linoleic acid evokes de-lipidation through the regulation of genes controlling lipid metabolism in adipose and liver tissue. *Obesity Reviews* 6: 247-258, 2005.

72. **Huggett J, Dheda K, Bustin S, and Zumla A**. Real-time RT-PCR normalisation; strategies and considerations. *Genes and Immunity* 6: 279-284, 2005.

73. **Ingalls AM, Dickie MM, and Snell GD**. Obese, a new mutation in the house mouse. *Journal of Heredity* 41: 317-318, 1950.

74. **Ip C, Ip MM, Loftus T, Shoemaker S, and Shea-Eaton W**. Induction of apoptosis by conjugated linoleic acid in cultured mammary tumor cells and premalignant lesions of the rat mammary gland. *Cancer Epidemiology Biomarkers & Prevention* 9: 689-696, 2000.

75. **Ip MM, Masso-Welch PA, Shoemaker SF, Shea-Eaton WK, and Ip C**. Conjugated linoleic acid inhibits proliferation and induces apoptosis of normal rat mammary epithelial cells in primary culture. *Experimental Cell Research* 250: 22-34, 1999.

76. **Jahreis G, Kraft J, Tischendorf F, Schöne F, and von Loeffelholz C**. Conjugated linoleic acids: Physiological effects in animal and man with special regard to body composition. *European Journal of Lipid Science and Technology* 102: 695-703, 2000.

77. **Kang KH, Liu W, Albright KJ, Park Y, and Pariza MW**. *trans*-10,*cis*-12 CLA inhibits differentiation of 3T3-L1 adipocytes and decreases PPARγ expression. *Biochemical and Biophysical Research Communications* 303: 795-799, 2003.

78. **Karin M**. Nuclear factor-κB in cancer development and progression. *Nature* 441: 431-436, 2006.

79. **Kelley DS, Bartolini GL, Newman JW, Vemuri M, and Mackey BE**. Fatty acid composition of liver, adipose tissue, spleen, and heart of mice fed diets containing *t*10, *c*12-, and *c*9, *t*11-conjugated linoleic acid. *Prostaglandins Leukotrienes and Essential Fatty Acids* 74: 331-338, 2006.

80. **Kelley DS, Bartolini GL, Warren JM, Simon VA, Mackey BE, and Erickson KL**. Contrasting effects of *t*10,*c*12-and *c*9,*t*11-conjugated linoleic acid isomers on the fatty acid profiles of mouse liver lipids. *Lipids* 39: 135-141, 2004.

81. **Kelly GS**. Conjugated linoleic acid: a review. *Alternative Medicine Review* 6: 367-382, 2001.

82. **Khanal RC**. Potential health benefits of conjugated linoleic acid (CLA): a review. *Asian-Australasian Journal of Animal Sciences* 17: 1315-1328, 2004.

83. **Kim EJ, Holthuizen PE, Park HS, Ha YL, Jung KC, and Park JHY**. *Trans*-10,*cis*-12-conjugated linoleic acid inhibits Caco-2 colon cancer cell growth. *American Journal of Physiology - Gastrointestinal and Liver Physiology* 283: G357-G367, 2002.

84. **Kim EJ, Kang I-J, Cho HJ, Kim WK, Ha Y-L, and Park JHY**. Conjugated linoleic acid downregulates insulin-like growth factor-I receptor levels in HT-29 human colon cancer cells. *Journal of Nutrition* 133: 2675-2681, 2003.

85. **Kim K-S, Thomsen H, Bastiaansen J, Nguyen NT, Dekkers JCM, Plastow GS, and Rothschild MF**. Investigation of obesity candidate genes on porcine fat deposition quantitative trait loci regions. *Obesity Research* 12: 1981-1994, 2004.

86. **Kim SY, Lee JW, and Sohn IS**. Comparison of various statistical methods for identifying differential gene expression in replicated microarray data. *Statistical Methods in Medical Research* 15: 3-20, 2006.

87. **Kisseleva T, Bhattacharya S, Braunstein J, and Schindler CW**. Signaling through the JAK/STAT pathway, recent advances and future challenges. *Gene* 285: 1-24, 2002.

88. **Kritchevsky D**. Antimutagenic and some other effects of conjugated linoleic acid. *British Journal of Nutrition* 83: 459-465, 2000.

89. **Kubista M, Andrade JM, Bengtsson M, Forootan A, Jonák J, Lind K, Sindelka R, Sjöback R, Sjögreen B, Strömbom L, Ståhlberg A, and Zoric N**. The real-time polymerase chain reaction. *Molecular Aspects of Medicine* 27: 95-125, 2006.

90. **Lang BJ, and Legates JE**. Rate, composition and efficiency of growth in mice selected for large and small body weight. *Theoretical and Applied Genetics* 39: 306-314, 1969.

91. **Langin D, and Arner P**. Importance of TNFα and neutral lipases in human adipose tissue lipolysis. *TRENDS in Endocrinology and Metabolism* 17: 314-320, 2006.

92. **LaRosa PC, Miner J, Xia YN, Zhou Y, Kachman S, and Fromm ME**. *Trans*-10, *cis*-12 conjugated linoleic acid causes inflammation and delipidation of white adipose tissue in mice: a microarray and histological analysis. *Physiological Genomics* 27: 282-294, 2006.

93. **Lee KN, Pariza MW, and Ntambi JM**. Conjugated linoleic acid decreases hepatic stearoyl-CoA desaturase mRNA expression. *Biochemical and Biophysical Research Communications* 248: 817-821, 1998.

94. **Lee KW, Lee HJ, Cho HY, and Kim YJ**. Role of the conjugated linoleic acid in the prevention of cancer. *Critical Reviews in Food Science and Nutrition* 45: 135-144, 2005.

95. **Lee MLT, Kuo FC, Whitmore GA, and Sklar J**. Importance of replication in microarray gene expression studies: Statistical methods and evidence from repetitive cDNA hybridizations. *Proceedings of the National Academy of Sciences of the United States of America* 97: 9834-9839, 2000.

96. **Lee S-H, Yamaguchi K, Kim J-S, Eling TE, Safe S, Park Y, and Baek SJ**. Conjugated linoleic acid stimulates an anti-tumorigenic protein NAG-1 in an isomer specific manner. *Carcinogenesis* 27: 972-981, 2006.

97. **Lee YH, Nair S, Rousseau E, Allison DB, Page GP, Tataranni PA, Bogardus C, and Permana PA**. Microarray profiling of isolated abdominal subcutaneous adipocytes from obese vs non-obese Pima Indians: Increased expression of inflammation-related genes. *Diabetologia* 48: 1776-1783, 2005.

98. **Lehrke M, and Lazar MA**. The many faces of PPARγ. *Cell* 123: 993-999, 2005.

99. **Levy DE, and Darnell JE**. STATs: Transcriptional control and biological impact. *Nature Reviews Molecular Cell Biology* 3: 651-662, 2002.

100. **Li GM, Dong BY, Butz DE, Park Y, Pariza MW, and Cook ME**. NF-κB independent inhibition of lipopolysaccharide-induced cyclooxygenase by a conjugated linoleic acid cognate, conjugated nonadecadienoic acid. *Biochimica et Biophysica Acta - Molecular and Cell Biology of Lipids* 1761: 969-972, 2006.

101. **Li JP, Yu XX, Pan WT, and Unger RH**. Gene expression profile of rat adipose tissue at the onset of high-fat-diet obesity. *American Journal of Physiology - Endocrinology and Metabolism* 282: E1334-E1341, 2002.

102. **Lin XB, Loor JJ, and Herbein JH**. *Trans*10,*cis*12-18:2 is a more potent inhibitor of de novo fatty acid synthesis and desaturation than *cis*9,*trans*11-18:2 in the mammary gland of lactating mice. *Journal of Nutrition* 134: 1362-1368, 2004.

103. **Liu WH, and Saint DA**. A new quantitative method of real time reverse transcription polymerase chain reaction assay based on simulation of polymerase chain reaction kinetics. *Analytical Biochemistry* 302: 52-59, 2002.

104. **López IP, Marti A, Milagro FI, Zulet MDA, Moreno-Aliaga MJ, Martinez JA, and De Miguel C**. DNA microarray analysis of genes differentially expressed in diet-induced (cafeteria) obese rats. *Obesity Research* 11: 188-194, 2003.

105. **Loscher CE, Draper E, Leavy O, Kelleher D, Mills KHG, and Roche HM**. Conjugated linoleic acid suppresses NF-κB activation and IL-12 production in dendritic cells through ERK-mediated IL-10 induction. *Journal of Immunology* 175: 4990-4998, 2005.

106. **Luo J, Sladek R, Carrier J, Bader J-A, Richard D, and Giguère V**. Reduced fat mass in mice lacking orphan nuclear receptor estrogen-related receptor α. *Molecular and Cellular Biology* 23: 7947-7956, 2003.

107. **MacDonald HB**. Conjugated linoleic acid and disease prevention: A review of current knowledge. *Journal of the American College of Nutrition* 19: 111S-118S, 2000.

108. **MacDougald OA, and Mandrup S**. Adipogenesis: Forces that tip the scales. *TRENDS in Endocrinology and Metabolism* 13: 5-11, 2002.

109. **McLeod RS, LeBlanc AM, Langille MA, Mitchell PL, and Currie DL**. Conjugated linoleic acids, atherosclerosis, and hepatic very-low-density lipoprotein metabolism. *American Journal of Clinical Nutrition* 79: 1169S-1174S, 2004.

110. **Miglietta A, Bozzo F, Bocca C, Gabriel L, Trombetta A, Belotti S, and Canuto RA**. Conjugated linoleic acid induces apoptosis in MDA-MB-231 breast cancer cells through ERK/MAPK signalling and mitochondrial pathway. *Cancer Letters* 234: 149-157, 2006.

111. **Miner JL, Cederberg CA, Nielsen MK, Chen XL, and Baile CA**. Conjugated linoleic acid (CLA), body fat, and apoptosis. *Obesity Research* 9: 129-134, 2001.

112. **Moraes RC, Blondet A, Birkenkamp-Demtroeder K, Tirard J, Orntoft TF, Gertler A, Durand P, Naville D, and Bégeot M**. Study of the alteration of gene expression in adipose tissue of diet-induced obese mice by microarray and reverse transcription-polymerase chain reaction analyses. *Endocrinology* 144: 4773-4782, 2003.

113. **Moya-Camarena SY, Vanden Heuvel JP, Blanchard SG, Leesnitzer LA, and Belury MA**. Conjugated linoleic acid is a potent naturally occurring ligand and activator of PPAR alpha. *Journal of Lipid Research* 40: 1426-1433, 1999.

114. **Nagao K, Inoue N, Wang Y-M, Hirata J, Shimada Y, Nagao T, Matsui T, and Yanagita T**. The 10*trans*,12*cis* isomer of conjugated linoleic acid suppresses the development of hypertension in Otsuka Long-Evans Tokushima fatty rats. *Biochemical and Biophysical Research Communications* 306: 134-138, 2003.

115. **Nawrocki AR, and Scherer PE**. Keynote review: The adipocyte as a drug discovery target. *Drug Discovery Today* 10: 1219-1230, 2005.

116. **Ntambi JM**. Regulation of stearoyl-CoA desaturase by polyunsaturated fatty acids and cholesterol. *Journal of Lipid Research* 40: 1549-1558, 1999.

117. **O'Shea JJ, Gadina M, and Schreiber RD**. Cytokine signaling in 2002: New surprises in the Jak/Stat pathway. *Cell* 109: S121-S131, 2002.

118. **O'Shea M, Bassaganya-Riera J, and Mohede ICM**. Immunomodulatory properties of conjugated linoleic acid. *American Journal of Clinical Nutrition* 79: 1199S-1206S, 2004.

119. **Ogden CL, Carroll MD, Curtin LR, McDowell MA, Tabak CJ, and Flegal KM**. Prevalence of overweight and obesity in the United States, 1999-2004. *Journal of the American Medical Association* 295: 1549-1555, 2006.

120. **Oh YS, Lee HS, Cho HJ, Lee SG, Jung KC, and Park JHY**. Conjugated linoleic acid inhibits DNA synthesis and induces apoptosis in TSU-Pr1 human bladder cancer cells. *Anticancer Research* 23: 4765-4772, 2003.

121. **Ohnuki K, Haramizu S, Ishihara K, and Fushiki T**. Increased energy metabolism and suppressed body fat accumulation in mice by a low concentration of conjugated linoleic acid. *Bioscience Biotechnology and Biochemistry* 65: 2200-2204, 2001.

122. **Okosun IS, Chandra KMD, Boev A, Boltri JM, Choi ST, Parish DC, and Dever GEA**. Abdominal adiposity in US adults: prevalence and trends, 1960-2000. *Preventive Medicine* 39: 197-206, 2004.

123. **Parikh NI, Pencina MJ, Wang TJ, Lanier KJ, Fox CS, D'Agostino RB, and Vasan RS**. Increasing trends in incidence of overweight and obesity over 5 decades. *American Journal of Medicine* 120: 242-250, 2007.

124. **Pariza MW, Ashoor SH, Chu FS, and Lund DB**. Effects of Temperature and Time on Mutagen Formation in Pan-Fried Hamburger. *Cancer Letters* 7: 63-69, 1979.

125. **Pariza MW, Park Y, and Cook ME**. The biologically active isomers of conjugated linoleic acid. *Progress in Lipid Research* 40: 283-298, 2001.

126. **Park HS, Chun CS, Kim S, Ha YL, and Park JHY**. Dietary *trans*-10,*cis*-12 and *cis*-9,*trans*-11 conjugated linoleic acids induce apoptosis in the colonic mucosa of rats treated with 1,2-dimethylhydrazine. *Journal of Medicinal Food* 9: 22-27, 2006.

127. **Park HS, Ryu JH, Ha YL, and Park JHY**. Dietary conjugated linoleic acid (CLA) induces apoptosis of colonic mucosa in 1,2-dimethylhydrazine-treated rats: A possible mechanism of the anticarcinogenic effect by CLA. *British Journal of Nutrition* 86: 549-555, 2001.

128. **Park Y, Albright KJ, Liu W, Storkson JM, Cook ME, and Pariza MW**. Effect of conjugated linoleic acid on body composition in mice. *Lipids* 32: 853-858, 1997.

129. **Park Y, Albright KJ, Storkson JM, Liu W, Cook ME, and Pariza MW**. Changes in body composition in mice during feeding and withdrawal of conjugated linoleic acid. *Lipids* 34: 243-248, 1999.

130. **Park Y, Storkson JM, Albright KJ, Liu W, and Pariza MW**. Evidence that the *trans*-10,*cis*-12 isomer of conjugated linoleic acid induces body composition changes in mice. *Lipids* 34: 235-241, 1999.

131. **Peters JM, Park Y, Gonzalez FJ, and Pariza MW**. Influence of conjugated linoleic acid on body composition and target gene expression in peroxisome proliferator-activated receptor α-null mice. *Biochimica et Biophysica Acta - Molecular and Cell Biology of Lipids* 1533: 233-242, 2001.

132. **Pfaffl MW**. A new mathematical model for relative quantification in real-time RT-PCR. *Nucleic Acids Research* 29: 2001.

133. **Poirier H, Shapiro JS, Kim RJ, and Lazar MA**. Nutritional supplementation with *trans*-10, *cis*-12-conjugated linoleic acid induces inflammation of white adipose tissue. *Diabetes* 55: 1634-1641, 2006.

134. **Prasetyo H, and Eisen EJ**. Correlated responses in development and distribution of fat depots in mice selected for body composition traits. *Theoretical and Applied Genetics* 78: 217-223, 1989.

135. **Ramakers JD, Plat J, Sébédio J-L, and Mensink RP**. Effects of the individual isomers *cis*-9, *trans*-11 vs. *trans*-10,*cis*-12 of conjugated linoleic acid (CLA) on inflammation parameters in moderately overweight subjects with LDL-phenotype B. *Lipids* 40: 909-918, 2005.

136. **Rasooly R, Kelley DS, Greg J, and Mackey BE**. Dietary *trans* 10, *cis* 12-conjugated linoleic acid reduces the expression of fatty acid oxidation and drug detoxification enzymes in mouse liver. *British Journal of Nutrition* 97: 58-66, 2007.

137. **Rawson RB**. The SREBP pathway - Insights from insigs and insects. *Nature Reviews Molecular Cell Biology* 4: 631-640, 2003.

138. **Ringseis R, König B, Leuner B, Schubert S, Nass N, Stangl G, and Eder K**. LDL receptor gene transcription is selectively induced by t10c12-CLA but not by c9t11-CLA in the human hepatoma cell line HepG2. *Biochimica et Biophysica Acta - Molecular and Cell Biology of Lipids* 1761: 1235-1243, 2006.

139. **Ringseis R, Muschick A, and Eder K**. Dietary oxidized fat prevents ethanol-induced triacylglycerol accumulation and increases expression of PPAR alpha target genes in rat liver. *Journal of Nutrition* 137: 77-83, 2007.

140. **Robeson BL, Eisen EJ, and Leatherwood JM**. Adipose cellularity, serum glucose, insulin and cholesterol in polygenic obese mice fed high-fat or high-carbohydrate diets. *Growth* 45: 198-215, 1981.

141. **Roche HM, Noone E, Nugent A, and Gibney MJ**. Conjugated linoleic acid: A novel therapeutic nutrient? *Nutrition Research Reviews* 14: 173-187, 2001.

142. **Roche HM, Noone E, Sewter C, Mc Bennett S, Savage D, Gibney MJ, O'Rahilly S, and Vidal-Puig AJ**. Isomer-dependent metabolic effects of conjugated linoleic acid - Insights from molecular markers sterol regulatory element-binding protein-1c and LXRα. *Diabetes* 51: 2037-2044, 2002.

143. **Schinckel AP, and deLange CFM**. Characterization of growth parameters needed as inputs for pig growth models. *Journal of Animal Science* 74: 2021-2036, 1996.

144. **Sébédio J-L, Gnaedig S, and Chardigny J-M**. Recent advances in conjugated linoleic acid research. *Current Opinion in Clinical Nutrition and Metabolic Care* 2: 499-506, 1999.

145. **Smith SR, Lovejoy JC, Greenway F, Ryan D, deJonge L, de la Bretonne J, Volafova J, and Bray GA**. Contributions of total body fat, abdominal subcutaneous adipose tissue compartments, and visceral adipose tissue to the metabolic complications of obesity. *Metabolism* 50: 425-435, 2001.

146. **Soukas A, Cohen P, Socci ND, and Friedman JM**. Leptin-specific patterns of gene expression in white adipose tissue. *Genes & Development* 14: 963-980, 2000.

147. **Speakman J, Hambly C, Mitchell S, and Król E**. Animal models of obesity. *Obesity Reviews* 8: 55-61, 2007.

148. **Ståhlberg A, Håkansson J, Xian X, Semb H, and Kubista M**. Properties of the reverse transcription reaction in mRNA quantification. *Clinical Chemistry* 50: 509-515, 2004.

149. **Stein CJ, and Colditz GA**. The epidemic of obesity. *Journal of Clinical Endocrinology and Metabolism* 89: 2522-2525, 2004.

150. **Stevens J**. Obesity, fat patterning and cardiovascular risk. In: *Nutrition and biotechnology in heart disease and cancer* edited by Longenecker JB, Kritchevsky D, and Drezner MK. New York, NY: Plenum Publishing Corporation, 1995, p. 21-27.

151. **Stylianou IM, Clinton M, Keightley PD, Pritchard C, Tymowska-Lalanne Z, Bünger L, and Horvat S**. Microarray gene expression analysis of the Fob3b obesity QTL identifies positional candidate gene Sqle and perturbed cholesterol and glycolysis. *Physiological Genomics* 20: 224-232, 2005.

152. **Takahashi Y, Kushiro M, Shinohara K, and Ide T**. Activity and mRNA levels of enzymes involved in hepatic fatty acid synthesis and oxidation in mice fed conjugated linoleic acid. *Biochimica et Biophysica Acta - Molecular and Cell Biology of Lipids* 1631: 265-273, 2003.

153. **Takahashi Y, Kushiro M, Shinohara K, and Ide T**. Dietary conjugated linoleic acid reduces body fat mass and affects gene expression of proteins regulating energy metabolism in mice. *Comparative Biochemistry and Physiology Part B: Biochemistry and Molecular Biology* 133: 395-404, 2002.

154. **Taniguchi CM, Emanuelli B, and Kahn CR**. Critical nodes in signalling pathways: Insights into insulin action. *Nature Reviews Molecular Cell Biology* 7: 85-96, 2006.

155. **Terpstra AHM, Beynen AC, Everts H, Kocsis S, Katan MB, and Zock PL**. The decrease in body fat in mice fed conjugated linoleic acid is due to increases in energy expenditure and energy loss in the excreta. *Journal of Nutrition* 132: 940-945, 2002.

156. **Timon VM, and Eisen EJ**. Comparisons of ad libitum and restricted feeding of mice selected and unselected for postweaning gain. 1. Growth, feed consumption and feed efficiency. *Genetics* 64: 41-57, 1970.

157. **Troegeler-Meynadier A, and Enjalbert F**. Les acides linoléiques conjugués : Intérêts biologiques en nutrition. *Revue de Médecine Vétérinaire* 156: 207-216, 2005.

158. **Tsuboyama-Kasaoka N, Miyazaki H, Kasaoka S, and Ezaki O**. Increasing the amount of fat in a conjugated linoleic acid-supplemented diet reduces lipodystrophy in mice. *Journal of Nutrition* 133: 1793-1799, 2003.

159. **Tsuboyama-Kasaoka N, Takahashi M, Tanemura K, Kim H-J, Tange T, Okuyama H, Kasai M, Ikemoto S, and Ezaki O**. Conjugated linoleic acid supplementation reduces adipose tissue by apoptosis and develops lipodystrophy in mice. *Diabetes* 49: 1534-1542, 2000.

160. **Turnock L, Cook M, Steinberg H, and Czuprynski C**. Dietary supplementation with conjugated linoleic acid does not alter the resistance of mice to Listeria monocytogenes infection. *Lipids* 36: 135-138, 2001.

161. **Varfolomeev EE, and Ashkenazi A**. Tumor necrosis factor: An apoptosis JuNKie? *Cell* 116: 491-497, 2004.

162. **Viswanadha S, McGilliard ML, and Herbein JH**. Desaturation indices in liver, muscle, and bone of growing male and female mice fed *trans*-10,*cis*-12 conjugated linoleic acid. *Lipids* 41: 763-770, 2006.

163. **Wahle KWJ, Heys SD, and Rotondo D**. Conjugated linoleic acids: Are they beneficial or detrimental to health? *Progress in Lipid Research* 43: 553-587, 2004.

164. **Wajchenberg BL**. Subcutaneous and visceral adipose tissue: their relation to the metabolic syndrome. *Endocrine Reviews* 21: 697-738, 2000.

165. **Warren JM, Simon VA, Bartolini G, Erickson KL, Mackey BE, and Kelley DS**. *Trans*-10,*cis*-12 CLA increases liver and decreases adipose tissue lipids in mice: Possible roles of specific lipid metabolism genes. *Lipids* 38: 497-504, 2003.

166. **West DB, Blohm FY, Truettt AA, and DeLany JP**. Conjugated linoleic acid persistently increases total energy expenditure in AKR/J mice without increasing uncoupling protein gene expression. *Journal of Nutrition* 130: 2471-2477, 2000.

167. **West DB, Delany JP, Camet PM, Blohm F, Truett AA, and Scimeca J**. Effects of conjugated linoleic acid on body fat and energy metabolism in the mouse. *American*

Journal of Physiology - Regulatory Integrative and Comparative Physiology 44: R667-R672, 1998.

168. **White JM, Legates JE, and Eisen EJ**. Maternal effects among lines of mice selected for body weight. *Genetics* 60: 395-408, 1968.

169. **Wilhelm J, and Pingoud A**. Real-time polymerase chain reaction. *ChemBioChem* 4: 1120-1128, 2003.

170. **Wong ML, and Medrano JF**. Real-time PCR for mRNA quantitation. *BioTechniques* 39: 75-85, 2005.

171. **Wong MW, Chew BP, Wong TS, Hosick HL, Boylston TD, and Shultz TD**. Effects of dietary conjugated linoleic acid on lymphocyte function and growth of mammary tumors in mice. *Anticancer Research* 17: 987-993, 1997.

172. **Xu XF, and Pariza MW**. Dietary conjugated linoleic acid reduces mouse adipocyte size and number. *The FASEB Journal* 16: A370-A370, 2002.

173. **Yamasaki M, Chujo H, Hirao A, Koyanagi N, Okamoto T, Tojo N, Oishi A, Iwata T, Yamauchi-Sato Y, Yamamoto T, Tsutsumi K, Tachibana H, and Yamada K**. Immunoglobulin and cytokine production from spleen lymphocytes is modulated in C57BL/6J mice by dietary *cis*-9, *trans*-11 and *trans*-10, *cis*-12 conjugated linoleic acid. *Journal of Nutrition* 133: 784-788, 2003.

174. **Yamasaki M, Kitagawa T, Chujo H, Koyanagi N, Nishida E, Nakaya M, Yoshimi K, Maeda H, Nou S, Iwata T, Ogita K, Tachibana H, and Yamada K**. Physiological difference between free and triglyceride-type conjugated linoleic acid on the immune function of C57BL/6N mice. *Journal of Agricultural and Food Chemistry* 52: 3644-3648, 2004.

175. **Zabala A, Churruca I, Fernández-Quintela A, Rodríguez VM, Macarulla MT, Martínez JA, and Portillo MP**. *trans*-10,*cis*-12 conjugated linoleic acid inhibits lipoprotein lipase but increases the activity of lipogenic enzymes in adipose tissue from hamsters fed an atherogenic diet. *British Journal of Nutrition* 95: 1112-1119, 2006.

Microarray Analysis of Two Mouse Lines Divergently Selected for Epididymal Fat Content

Ryan P. Ceddia[1], Shelly Druyan[2], Eugene J. Eisen[1], and Melissa S. Ashwell[1]

[1]Department of Animal Science, North Carolina State University

Raleigh, NC 27695

[2]Department of Poultry Science, North Carolina State University

Raleigh, NC 27695

Corresponding author: Dr. Melissa S. Ashwell, Department of Animal Science, Raleigh, NC 27695, USA

melissa_ashwell@ncsu.edu; 919-513-7488; 919-515-6884 (fax)

Number of Tables: 5

Number of Figures: 3

Keywords: gene expression, genetic selection, mice, epididymal fat, liver, body weight, obesity

Acknowledgements: The authors gratefully acknowledge Shelly Nolin and Audrey O'Nan for technical assistance and Dr. Michael G. Gonda for his critical review of the manuscript.

Abstract

Most studies on adipose gene expression focus on subjects with excessive weight gain. We report microarray data from adipose and liver tissue from two lines of mice selected for high and low epididymal fat pad (EF) weights. The low fat (LF) line was selected for low EF weight as a percentage of body weight (BW); the high epididymal (HE) line was selected for high EF weight as a percentage of BW with BW held constant. Both lines were derived from a cross between a moderately obese line, M16, and a decreased body weight line, L_6. Analysis of microarray data identified 19 genes with differential expression between the HE and LF lines of mice with 5 of these genes differentially expressed in both liver and EF tissues. We found differential regulation of genes known to play a role in glucose uptake and lipid metabolism. In addition, we identified a differentially expressed gene, *solute carrier family 22 member 4* (*SLC22A4*), located within the confidence interval of a quantitative trait loci (QTL) associated with EF in a cross between M16 and L_6 mice, making it a positional candidate for the *Epfq4* QTL. Furthermore, we have identified a linked group of three genes (*Sortilin 1*, *guanine nucleotide binding protein alpha inhibiting 3*, and *selenium-binding protein 2*) on *Mus musculus* chromosome 3 which may represent a genomic "hot spot" for genes associated with EF mass. In this study, differential expression of several genes not previously associated with obesity or adipose deposition were identified and may represent new targets for further research.

Abbreviations

Body weight (BW), epididymal fat pad (EF), false discovery rate (FDR), glucose storage vesicles (GSV), glucose transporter isoform 4 (Glut4), Graves' Disease Carrier (GDC), guanine nucleotide binding protein, alpha inhibiting 3 ($G\alpha_{i3}$), high epididymal (HE), low fat (LF), *mus musculus* chromosome 3 (MMU3), peroxisome proliferator-activated receptor (PPAR), quantitative trait loci (QTL), ribosomal protein S18 (S18), selenium-binding protein 2 (SBP2), solute carrier family 22 member 4 (SLC22A4), Solute carrier family 25 member 16 (SLC25A16), ubiquitin specific protease 19 (usp19), unc-13 homolog B (unc13b).

Introduction

Obesity, which is defined as having a body mass index (BMI) that is greater than 30 kg/m^2, has reached epidemic proportions in many countries and, as of 2004, 32.2% of adults in the US were considered obese (33). Obesity was estimated to cause 112,000 excess deaths in 2000 (19) and to cost the US over $117 billion per year (47). It also is associated with an increase in cardiovascular disease, cancer, and osteoarthritis. Abdominal obesity is based upon the amount of adipose tissue in the abdominal region and appears to be a more important risk factor contributing to cardiovascular disease than general obesity (48). Abdominal obesity is difficult to accurately measure, requiring expensive techniques such as magnetic resonance and computed tomography. As a less expensive alternative, waist circumference is often used. In the four decades between 1960 and 2000, the proportion of abdominal obesity in men and women rose from 12.7% to 38.3% and 19.4% to 59.9%, respectively (34). This rise was accompanied by an increase in the mean waist circumference from 89 to 99 cm for men and 77 to 94 cm for women (34). Due to the

importance of abdominal obesity and difficulty in accurate measurement, identifying genes directly involved in regulating it is of utmost importance.

Obesity can be caused by many factors, including genetic, metabolic, behavioral, and environmental factors (47). In order to better understand these causes, gene expression studies have been performed, most of which have focused on overweight or obese individuals. For example, Baranova and colleagues (1) used microarrays to compare gene expression in visceral adipose tissue between morbidly obese and non-obese patients. Because obesity studies require the use of invasive techniques, animals are often used as models of obesity. Using high fat and low fat lines of mice, Stylianou and coworkers (50) used microarrays to investigate the effects of genetic selection for fat content on gene expression. A similar study was conducted using chickens divergently selected for high and low abdominal fat content (3). While these studies have provided important information about obesity, they have not provided information specific to abdominal obesity. A more complex model is needed in order to fully understand this disease.

Selection experiments have produced obesity models with more complex phenotypes than simple fat and lean lines. The mouse high epididymal (HE) and low fat (LF) lines have similar body weights (BW) but have divergent amounts of epididymal adipose tissue (Figure 2.1) (12, 17). Murine epididymal fat pad (EF) tissue, the adipose depot around the epididymis of males, is best correlated to human visceral adipose tissue, the adipose depot around internal organs. Visceral adipose tissue deposition is closely linked to abdominal obesity (51). The HE and LF lines were selected for EF weight because EF is easily dissected and is phenotypically highly correlated with total body fat

percentage in adult mice (18). The correlation between EF and total body fat in mice is similar to the correlation between visceral adipose tissue and total body fat in humans (18, 45). These mice may serve as models for understanding the role of visceral adipose tissue in human abdominal obesity because, while HE and LF mice do not represent extremes in obesity or leanness, respectively, there is a major difference in the mass of EF tissue and total fat content and the lines are similar in BW.

Here, we report results comparing gene expression in EF and liver between the HE and LF lines of mice. We chose to examine changes in the gene expression profile in the liver in addition to white adipose tissue because the liver is a major metabolic organ that has a significant impact on gluconeogenesis, lipid metabolism, and cholesterol biosynthesis (29). By comparing these lines, we identified genes that are differentially expressed due to dissimilar EF content without confounding the effects of BW. This is the first gene expression study, to our knowledge, to use a polygenic model that has different EF and total body fat content and similar body size.

Materials & Methods

Mice

Mice were maintained according to North Carolina State University's Institutional Animal Care and Use Committee protocol. The LF line was begun from 15 pairs of F_3 M16/L_6 cross mice. The HE line was begun from the random control lines generated from the M16/L_6 cross mice when the LF line was formed. For both lines, an average of four mating pairs per family, i.e. sixty pairs of mice, was made from the previous generation. Following the mating period, males were killed at 12 weeks of age to obtain carcass

measurements. One male was selected from each of the 15 full sib families. Selection was based upon right EF weight. There was no selection on the females, as these were mated randomly to the males. Litters from the selected sire were standardized to ten pups at 1 day of age. The LF line was selected using single-trait divergent selection for low 12-week EF content (16) while the HE line was selected using restricted index selection for high 12-week EF weight while holding 12-week BW constant (13).

Eleven male mice from the HE and twelve male mice from the LF lines of mice were euthanized at 5 months of age by CO_2 narcosis. Mice were weighed to obtain BW measurements. Livers and right EF pads were dissected, weighed, and snap frozen in liquid nitrogen for RNA extraction. Statistical analyses of weight data were performed to determine the line difference using ANOVA.

Microarrays

Total RNA was isolated from frozen adipose and liver using Tri-Reagent (Molecular Research Inc., Cincinnati, OH) following the manufacturer's protocol. RNA concentration was determined using the NanoDrop® ND-1000 spectrophotometer (Wilmington, DE) and integrity was verified using agarose gel electrophoresis. Equal amounts of total RNA from adipose and liver were pooled with 5 animals per pool per tissue (Figure 2.2). Each pool of RNA was labeled with both Cy3 and Cy5 using Pronto!™ Plus Indirect Systems (Promega, Madison, WI). Labeled cDNA at a concentration of 0.75 pmol dye/µl was hybridized to microarrays for 14-16 hours at 42°C. Post hybridization washes were also performed using Pronto!™ Plus Indirect Systems (Promega, Madison, WI). Arrays were printed at the Duke Microarray Facility using Operon's Mouse Oligo set

(version 4.0) which contains 35,852 70-mer probes representing 25,000 genes and 38,000 transcripts (**https://www.operon.com/arrays/oligosets_mouse.php?**). The location of probes on the microarray may be found at **http://data.genome.duke.edu/facility-website-files/spotted/available-arrays/mouse_V4.0.1_genelist_s-.xls**. Probe information can be found at **https://www.operon.com/arrays/omad.php**. A total of eight spotted arrays were used; four were used in a loop design while the other four arrays were used in a simple dye swap (Figure 2.3).

Microarray Data Collection

Following hybridizations, the arrays were scanned with a PE Scanarray 3000 (General Scanning, Watertown, MA). The data from the scanned images were extracted using GenePix Pro 6.0 (Axon Instruments, Inc., Union City, CA). Data were transformed to a $\log_2$ scale and Loess normalized to remove between and within array variation. The 95% confidence interval for each probe (4 replicates, Figure 2.2) was estimated for each line × tissue combination. Replicates with normalized signal intensity that were not within the boundaries of the 95% confidence interval were excluded. Data were analyzed for line differences using ANOVA with a false discovery rate (FDR) (2) correction using JMP Genomics software (SAS Institute, Cary, NC). Spots having an FDR p-value < 0.05 were considered to be statistically significant.

Real-Time RT-PCR

A total of 1μg RNA from each individual was reverse transcribed using Applied Biosystems High Capacity cDNA Reverse Transcription Kit (Foster City, CA). Real-time PCR reactions were performed using Applied Biosystems Power SYBR® Green PCR

Master Mix (Foster City, CA) in a BioRad iCycler (Hercules, CA) with minor modifications. Fluoresein was added to the SYBR Green master mix to a final concentration of 10 nM because fluoresein is the reference dye used by the BioRad iCycler and it is not present in the Applied Biosystems Power SYBR® Green PCR Master Mix. Cycling conditions were as follows: 95°C for 7 min, 60 cycles of (95°C for 30 sec, appropriate annealing temperature [Table 2.1] for 30 sec, 72.0°C for 30 sec), 72°C for 5 min, 95°C for 1 min, 55.0°C for 1 min, followed by a melt curve of 80 cycles of 10 seconds at 55°C with a 0.5°C increase every cycle. Fluorescence data were collected at the 72°C step. Mouse *ribosomal protein S18* and *β-actin* were used as housekeeping genes for normalization. All real-time PCR primers were designed using Beacon Designer 7 (PREMIER Biosoft International, Palo Alto, CA), except *β-actin* which was previously described (39). All PCR products were sequenced to confirm identity. Samples were run in triplicate, averaged, and imported into the relative expression software tool (REST©) for calculation of fold changes and determination of statistical significance (37). The standard curve was amplified in triplicate and imported directly into REST©.

Results

Mice

BW between the two lines of mice were different, with the HE line being on average 4.93 g heavier than the LF line ($p<0.05$) (Table 2.2). The EF weight was lower in the LF line when compared to the HE line as expected, with an average difference of 1005 mg ($p<0.0001$). The ratio between EF weight and BW was 2.4% higher in the HE line than the LF line ($p<0.0001$).

Microarrays

Using Operon's Mouse Oligo set (version 4.0) microarrays, we identified six up regulated genes in EF (Tables 2.3) and four up regulated genes in liver (Table 2.4) of the HE mice compared to LF mice (FDR $p<0.05$). Of these genes, *sortilin 1* was the only gene up regulated in both tissues. In addition, six genes in the EF and eight genes in the liver of the HE mice were down regulated compared to the LF mice. *Solute carrier family 25 member 16* (*SLC25A16*) and *PREDICTED: similar to vigilin* were the only genes down regulated in both tissues. Two genes (*5330423I11Rik*, and *BTB (POZ) domain containing 7*) exhibited differential expression across tissues, where they were up regulated in EF and down regulated in liver.

All differentially expressed genes in EF, except *sortilin 1*, had a fold change less than ±1.5. Seven genes (*sortilin 1*, *PREDICTED: similar to immunoglobulin light chain variable region*, *unc-13 homolog B* [*unc13b*], *SLC25A16*, *Mus musculus adult male spinal cord cDNA*, *Beta adducin*, and *selenium-binding protein 2* [*SBP2*]) differentially expressed in liver had fold changes greater than ±1.5. *SBP2* was the only gene found which had a greater than ±2 fold change in either tissue.

Three of the differentially expressed genes are linked on *Mus musculus* chromosome 3 (MMU3) (*Sortilin 1*, *guanine nucleotide binding protein, alpha inhibiting 3* [$G\alpha_{i3}$], and *SBP2*). *SBP2* is positioned at 43.26 cM, between 94.78 and 94.79 Mb on the plus strand. $G\alpha_{i3}$ is positioned at 48.8 cM between 108.24 and 108.27 Mb on the minus strand. *Sortilin 1* is located between 108.41 and108.49 Mb on the plus strand. The total

physical distance of these genes is 13.7 Mb, perhaps representing a genomic "hot spot" for genes associated with EF mass.

Real-Time RT-PCR

Five genes ($G\alpha_{i3}$, *solute carrier family 22 member 4* (*SLC22A4*), *SLC25A16*, *Sortilin 1*, and *SBP2*) were selected for real-time RT-PCR verification based upon the magnitude of their microarray fold-change and their physiological function. Of these five genes, two (*sortilin 1* and *SLC25A16*) were significantly differentially expressed in both EF and liver. The remaining three genes were evaluated in only the tissue in which they appeared to be differentially expressed. Only *SBP2* in liver and *sortilin 1* in EF were differentially expressed ($p<0.05$) by real-time RT-PCR (Table 2.5), with both genes down regulated in the HE line as compared to the LF. These expression patterns were concordant with microarray results for *SBP2* and discordant for *sortilin 1*. *SLC22A4* and *SLC25A16* had suggestive ($p<0.1$) down regulation in the EF of the HE line compared to the LF. Real-time RT-PCR results for *SLC25A16* were in agreement with microarray data, while *SLC22A4* results were not. Of the genes corroborated, *SBP2* had the highest expression according to the microarrays. Real-time RT-PCR consistently demonstrated a greater fold change than was observed in the microarrays for *SLC22A4*, *SLC25A16*, *sortilin 1*, in EF and *SBP2* in liver. These real-time RT-PCR fold changes range from -3.47 to -9.35, all of which were significant or suggestive according to real-time RT-PCR (Table 2.5). For all genes except *SBP2* and *SLC25A16*, the direction of change was different between microarray and real-time data.

Discussion

Genetic selection from crosses between the M16 and L_6 lines have resulted in HE and LF mice having similar BW and differing amounts of EF at three months of age. This selection has resulted in lines that have altered fat distribution (38). HE mice have a non-significant increase in subcutaneous fat (14) while LF mice have a lesser amount of subcutaneous fat (15). Though this study found a difference in the average BW of these mice, the HE line still had a much higher percentage of body fat as compared to the LF line ($p<0.0001$). The difference in BW of the HE mice may be explained by their age. These mice were 5 months old at sacrifice while genetic selection was based on 12 week old mice (Table 2.2). Comparing 5 month old mice to the 3 months old mice from the previous study, the LF line maintained a similar BW with means of 35.7 and 36.5 g, respectively. The HE line had mean BW of 40.7 g at 5 months of age and 35.9 g at 3 months of age. The BW gain by the HE line cannot be entirely explained by an increase in EF weight, because EF increased an average of 738 mg while the BW increased 4.8 g. Furthermore, the percent EF per BW in both lines approximately doubled between the studies (HE fold change = 2.02, LF fold change = 1.93). These results indicate that the increase in BW of HE mice from 3 to 5 months of age was not entirely caused by an increase in EF. This suggests that the HE mice continued to grow after 3 months accounting for most of the difference in BW. Another possibility is that genetic drift has occurred as it has been over a decade because these lines were evaluated for BW (12, 17).

Though these mice have slightly different BW, we continued our experiment to compare gene expression because EF comprised a highly significant different percentage of BW between the HE and LF lines. We identified a total of 19 genes with differential

expression between these two lines of mice (Tables 2.3 and 2.4) using Operon's Mouse Oligo set (version 4.0) microarrays. Unfortunately, real-time RT-PCR was unable to validate six out of seven of these genes (Table 2.5), likely due to reduced fold changes. Reduced correlation between microarray and real-time RT-PCR results for genes with a fold change of less than 1.5 has been observed previously in a study focused on the correlations between microarray and real-time RT-PCR results (9). This outcome agrees with our data, because only *SBP2*, the only gene with more than a 2-fold change, was validated by real-time RT-PCR. Our microarrays did not find many genes with a large fold change. We believe this is because the polygenic genetic selection which has resulted in the HE and LF lines has caused small changes in the expression of many genes, which was not observable with the limited number of arrays used. The small number of arrays and lack of probe repetition on the arrays also limited the ability to use a more stringent correction. For example, when the Bonferroni correction was used, no genes were found to be statistically significant (data not shown). When comparing microarray and real-time RT-PCR results, we also found a significant number of our genes showing expression in the opposite direction. One explanation for these discrepancies is that the primers used for real-time RT-PCR did not overlap the sequences used as the probe in the microarrays (data not shown). For most genes, these sequences were about 1000 bp apart, except *sortilin 1*. For *sortilin 1*, there was a distance of 3,829 bp between the 3' real-time RT-PCR primer and the 5' end of the microarray probe. Because our microarray data were unable to be validated by real-time RT-PCR, our microarray experiment can only be used as a tool to identify candidate genes that may play a role in the differential phenotypes associated with the HE and LF lines.

When these microarray results were compared to a quantitative trait loci (QTL) study using a cross between M16 and L_6 lines of mice, which are the parental strains for the HE and LF, one differentially expressed gene was found to be within the confidence interval of a QTL associated with EF weight (41). This gene, *SLC22A4*, is located at 28.0 cM on chromosome 11 and the QTL, *Epfq4*, peak is located at 17.4 cM. Further support for this gene as a positional candidate gene for *Epfq4* comes from a study in humans which found single nucleotide polymorphisms in *SLC22A4* associated with type 1 diabetes (42). *SLC22A4* encodes an organic cation transporter (OCTN1), an ergothioneine transporter most commonly associated with rheumatoid arthritis and Crohn's disease (24). Ergothioneine is an antioxidant that mimics carnitine in its ability to transport activated fatty acids into the mitochondrial matrix for subsequent β-oxidation (26, 46). OCTN1 plays a role in lipid metabolism by increasing ergothioneine concentrations in cells which leads to increased fatty acid oxidation and metabolism. Though microarray and real-time RT-PCR data presented conflicting results for this gene, this does not detract from the fact that *SLC22A4* is located near the *Epfq4* QTL and is differentially expressed between the lines.

In addition to comparing our microarray results to QTL studies, we also looked for genomic co-localization of differentially expressed genes. We found differential expression of three genes within a 13.7 Mb region of MMU3. In a cross between M16 and L_6 mice, growth QTL in this region have been associated with several genotypes including 3, 6, and 10 week BW, growth between 3 and 6 weeks, growth between 3 and 6 weeks adjusted for 3 week BW, heart weight adjusted for 10 week BW, and kidney weight (40, 41). No QTL

were observed for EF weight in this region of MMU3. This chromosomal area needs further study as an allelic difference may exist.

In addition to being linked, *sortilin 1*, $G\alpha_{i3}$, and *SBP2* have biological evidence for a role in the HE/LF phenotype. *SBP2*, the gene which was most differentially down regulated in the liver according to our microarrays, may be associated with increased hepatic lipid metabolism. SBP2 is dramatically down regulated in the liver upon peroxisome proliferator-activated receptor (PPAR) activation (6, 21, 22). PPARs, a class of nuclear hormone transcription factors, play a major role in lipid metabolism in the liver (10). SBP2 is also dramatically down regulated in the liver of an atherosclerosis-susceptible strain of mice when fed a high-fat enriched atherogenic diet (36). Large negative fold changes in SBP2 (as high as 25-fold) were found in these studies, which is much greater than the change in transcript level we observed (Table 2.5). In addition to a correlation between decreased SBP2 levels and PPAR activation, studies have shown reduced selenium levels in obese subjects (23, 27, 49). These studies show that SBP2 down regulation in the liver is characteristic of increased cholesterol and lipid metabolism, suggesting that these activities are increased in HE or decreased in LF mice.

Though microarray and real-time data presented conflicting results in regards to the change in expression of *sortilin 1*, there is some physiological evidence for sortilin's role in regulating adipose mass. Sortilin is a type-1 receptor, also known as neurotensin receptor-3, which functions as a sorting receptor in the Golgi compartment and as a clearance receptor on the cell surface (30). Sortilin is both necessary and sufficient for the formation of glucose storage vesicles (GSVs) (44). In 3T3-L1 pre-adipocytes, glucose transporter

isoform 4 (Glut4), the mediator of insulin-stimulated glucose uptake, is located primarily in endosomes and is rapidly degraded. In adipocytes, however, Glut4 is localized in GSVs (44). The transfer of Glut4 from GSVs to the plasma membrane is the mechanism by which insulin regulates glucose transport into adipocytes. By regulating the availability of GSVs, sortilin can limit the availability of Glut4 and hence the amount of glucose transported into adipocytes. Furthermore, in adipocytes, insulin causes a portion of sortilin to be translocated to the plasma membrane (31). At the cell surface, sortilin binds to lipoprotein lipase, the rate-limiting enzyme in hydrolysis of triglycerides, and targets lipoprotein lipase for endocytosis and degradation, which can lead to increased plasma triglyceride levels (32). Our microarray data indicate that *sortilin 1* is differentially expressed in the HE and LF mice, perhaps affecting the number of GSVs, and subsequently glucose uptake.

Gα$_{i3}$, which was up regulated in EF of HE mice compared to LF according to our microarrays, has also been associated with obesity. Gα$_{i3}$ has been shown to be increased in the livers of obese humans and mice (4, 8), and, in obese mice, the concentration Gα$_{i3}$ per mg of protein was reduced while the total amount of Gα$_{i3}$ per EF was unchanged (8). Gα$_{i3}$ is involved in regulating signal transduction from G-protein coupled receptors. The Gα$_{i}$ family inhibits adenylyl cyclase, which synthesizes cyclic AMP (11). Some antilipolytic factors use this pathway to exert their effects. For instance, TNF-α stimulates lipolysis in adipocytes by reducing Gα$_{i3}$ protein levels (20). Our results indicate that *Gα$_{i3}$* is up regulated in the HE line when compared to LF mice. This outcome agrees with other mouse and human studies because the breakdown of fat is expected to be decreased in HE mice; hence *Gα$_{i3}$* expression is increased.

Another gene which may play a role in fatty acid metabolism is *SLC35A16*. *SLC25A16*, which encodes Graves' Disease Carrier (GDC) protein, has a potential role in the synthesis and oxidation of fatty acids. GDC does not appear to have a direct role in Grave's disease; instead its predominant substrate appears to be coenzyme A or a coenzyme A precursor (35). This is notable because coenzyme A is well known for its role in the synthesis and oxidation of fatty acids. Our microarrays indicate *SLC25A16* is down regulated in both liver and EF tissue in HE mice compared to LF, which suggests that fatty acid oxidation is either decreased in HE or increased in LF mice.

In addition to these genes which have an explainable role in the HE/LF phenotype, we have also found differential expression of several genes whose effects are more ambiguous. Our microarrays indicate that *Unc13b*, which may be involved in insulin secretion, is up regulated in liver of HE mice when compared to LF. Unc13-1 is a diacylglycerol receptor that is essential for secretory vesicle priming and is associated with protein exocytosis. In pancreatic islets, Unc13-1 is necessary for insulin secretion (25, 28, 43). Mutating a similar gene in mice, *Unc5h3*, results in animals with reduced fat deposits and unchanged organ size (5). Another gene identified which has a less defined role in the HE/LF phenotype is *ubiquitin specific protease 19* (*Usp19*). *Usp19* is decreased in the skeletal muscle of starved rats and its expression is inversely proportional to muscle mass (7). The specific role of Usp19 is unclear, but it is known that this protein is involved with ubiquitination and degradation of proteins. Other genes which are not discussed have no known role in lipid metabolism, adiposity, or obesity. To our knowledge, this is the first study to report an association between these genes and adipose deposition.

In conclusion, we have identified several genes not previously associated with adipose deposition. This study was the first to look at gene expression in the HE and LF lines of mice in which we found differential regulation of genes known to play a role in glucose uptake and lipid metabolism. These data suggest that lipolysis and oxidation of fatty acids are decreased in EF when HE mice are compared to the LF line. In liver, our data suggest that lipid metabolism is increased in the HE line when compared to the LF. This can be inferred from the down regulation of SBP2, which is characteristic of PPAR activation and, therefore, increased fatty acid metabolism. This finding is contrary to expectations, as one would expect decreased metabolism in liver and increased storage of lipids in EF of the HE line. However, increased sortilin levels may cause an increase in the amount of plasma triglyceride; hence the liver may be compensating for this by metabolizing more lipids. In addition to having a physiological role in obesity, three genes (*sortilin 1*, *SBP2*, and $G\alpha_{i3}$) showed genomic co-localization. This cluster of genes on MMU3 may represent a genomic "hot spot" for genes associated with adiposity. We also identified *SLC22A4* as a positional candidate for the *Epfq4* QTL. Additional studies are needed to determine if polymorphisms in *SLC22A4* are associated with EF mass and to ascertain if the linked genes on MMU3 represents a *bona fide* "hot spot" for genes associated with adipose deposition.

References:

1. **Baranova A, Collantes R, Gowder SJ, Elariny H, Schlauch K, Younoszai A, King S, Randhawa M, Pusulury S, Alsheddi T, Ong JP, Martin LM, Chandhoke V, and Younossi ZM**. Obesity-related differential gene expression in the visceral adipose tissue. *Obesity Surgery* 15: 758-765, 2005.

2. **Benjamini Y, and Hochberg Y**. Controlling the false discovery rate - a practical and powerful approach to multiple testing. *Journal of the Royal Statistical Society Series B-Methodological* 57: 289-300, 1995.

3. **Bourneuf E, Hérault F, Chicault C, Carré W, Assaf S, Monnier A, Mottier S, Lagarrigue S, Douaire M, Mosser J, and Diot C**. Microarray analysis of differential gene expression in the liver of lean and fat chickens. *Gene* 372: 162-170, 2006.

4. **Caro JF, Raju MS, Caro M, Lynch CJ, Poulos J, Exton JH, and Thakkar JK**. Guanine nucleotide binding regulatory proteins in liver from obese humans with and without type II diabetes: Evidence for altered "cross-talk" between the insulin receptor and G_i-proteins. *Journal of Cellular Biochemistry* 54: 309-319, 1994.

5. **Choi YS, Hong S-B, Jeon HK, Kim EJ, Oh W-J, Joe S-Y, Han JS, Lee M-J, and Lee H-W**. Insertional mutation in the intron 1 of Unc5h3 gene induces ataxic, lean and hyperactive phenotype in mice. *Experimental Animals* 52: 273-283, 2003.

6. **Chu RY, Lim H, Brumfield L, Liu H, Herring C, Ulintz P, Reddy JK, and Davison M**. Protein profiling of mouse livers with peroxisome proliferator-activated receptor α activation. *Molecular and Cellular Biology* 24: 6288-6297, 2004.

7. **Combaret L, Adegoke OAJ, Bedard N, Baracos V, Attaix D, and Wing SS**. USP19 is a ubiquitin-specific protease regulated in rat skeletal muscle during catabolic states. *American Journal of Physiology - Endocrinology and Metabolism* 288: E693-E700, 2005.

8. **Cormont M, Tanti J-F, Van Obberghen E, and Le Marchand-Brustel Y**. Expression of guanine-nucleotide-binding proteins in lean and obese insulin-resistant mice. *Molecular and Cellular Endocrinology* 99: 169-176, 1994.

9. **Dallas PB, Gottardo NG, Firth MJ, Beesley AH, Hoffmann K, Terry PA, Freitas JR, Boag JM, Cummings AJ, and Kees UR**. Gene expression levels assessed by oligonucleotide microarray analysis and quantitative real-time RT-PCR – how well do they correlate? *BMC Genomics* 6: 59, 2005.

10. **Desvergne B, and Wahli W**. Peroxisome proliferator-activated receptors: Nuclear control of metabolism. *Endocrine Reviews* 20: 649-688, 1999.

11. **Dorsam RT, and Gutkind JS**. G-protein-coupled receptors and cancer. *Nature Reviews Cancer* 7: 79-94, 2007.

12. **Eisen EJ**. Genetics of body composition in mice. In: *Forty-Third Annual National Breeders Roundtable Proceedings*. St. Louis, MO: 1994, p. 67-89.

13. **Eisen EJ**. Restricted index selection in mice designed to change body fat without changing body weight: direct responses. *Theoretical and Applied Genetics* 83: 973-980, 1992.

14. **Eisen EJ**. Restricted selection index in mice designed to change body fat without changing body weight: correlated responses. *Theoretical and Applied Genetics* 84: 307-312, 1992.

15. **Eisen EJ**. Selection for components related to body-composition in mice: correlated responses. *Theoretical and Applied Genetics* 75: 177-188, 1987.

16. **Eisen EJ**. Selection for components related to body-composition in mice: direct responses. *Theoretical and Applied Genetics* 74: 793-801, 1987.

17. **Eisen EJ, Benyon LS, and Douglas JA**. Long-term restricted index selection in mice designed to change fat-content without changing body-size. *Theoretical and Applied Genetics* 91: 340-345, 1995.

18. **Eisen EJ, and Leatherwood JM**. Predicting percent fat in mice. *Growth* 45: 100-107, 1981.

19. **Flegal KA, Graubard BI, Williamson DF, and Gail MHH**. Excess deaths associated with underweight, overweight, and obesity. *Journal of the American Medical Association* 293: 1861-1867, 2005.

20. **Gasic S, Tian B, and Green A**. Tumor necrosis factor α stimulates lipolysis in adipocytes by decreasing G_i protein concentrations. *Journal of Biological Chemistry* 274: 6770-6775, 1999.

21. **Giometti CS, Liang XL, Tollaksen SL, Wall DB, Lubman DM, Subbarao V, and Rao MS**. Mouse liver selenium-binding protein decreased in abundance by peroxisome proliferators. *Electrophoresis* 21: 2162-2169, 2000.

22. **Giometti CS, Tollaksen SL, Liang XL, and Cunningham ML**. A comparison of lives protein changes in mice and hamsters treated with the peroxisome proliferator Wy-14,643. *Electrophoresis* 19: 2498-2505, 1998.

23. **Gjørup I, Gjørup T, and Andersen B**. Serum selenium and zinc concentrations in morbid obesity. Comparison of controls and patients with jejunoileal bypass. *Scandinavian Journal of Gastroenterology* 23: 1250-1252, 1988.

24. **Gründemann D, Harlfinger S, Golz S, Geerts A, Lazar A, Berkels R, Jung N, Rubbert A, and Schömig E**. Discovery of the ergothioneine transporter. *Proceedings of the National Academy of Sciences of the United States of America* 102: 5256-5261, 2005.

25. **Kang LJ, He ZX, Xu PY, Fan JM, Betz A, Brose N, and Xu T**. Munc13-1 is required for the sustained release of insulin from pancreatic beta cells. *Cell Metabolism* 3: 463-468, 2006.

26. **Kerby GP, and Taylor SM**. Effect of carnitine and ergothioneine on human platelet metabolism. *Proceedings of the Society for Experimental Biology and Medicine* 132: 435-439, 1969.

27. **Kimmons JE, Blanck HM, Tohill BC, Zhang J, and Khan LK**. Associations between body mass index and the prevalence of low micronutrient levels among US adults. *Medscape General Medicine* 8: 59, 2006.

28. **Kwan EP, Xie L, Sheu L, Nolan CJ, Prentki M, Betz A, Brose N, and Gaisano HY**. Munc13-1 deficiency reduces insulin secretion and causes abnormal glucose tolerance. *Diabetes* 55: 1421-1429, 2006.

29. **Lewis GF, Carpentier A, Adeli K, and Giacca A**. Disordered fat storage and mobilization in the pathogenesis of insulin resistance and type 2 diabetes. *Endocrine Reviews* 23: 201-229, 2002.

30. **Mazella J**. Sortilin/neurotensin receptor-3: a new tool to investigate neurotensin signaling and cellular trafficking? *Cellular Signalling* 13: 1-6, 2001.

31. **Morris NJ, Ross SA, Lane WS, Moestrup SK, Petersen CM, Keller SR, and Lienhard GE**. Sortilin is the major 110-kDa protein in GLUT4 vesicles from adipocytes. *Journal of Biological Chemistry* 273: 3582-3587, 1998.

32. **Nielsen MS, Jacobsen C, Olivecrona G, Gliemann J, and Petersen CM**. Sortilin/neurotensin receptor-3 binds and mediates degradation of lipoprotein lipase. *Journal of Biological Chemistry* 274: 8832-8836, 1999.

33. **Ogden CL, Carroll MD, Curtin LR, McDowell MA, Tabak CJ, and Flegal KM**. Prevalence of overweight and obesity in the United States, 1999-2004. *Journal of the American Medical Association* 295: 1549-1555, 2006.

34. **Okosun IS, Chandra KMD, Boev A, Boltri JM, Choi ST, Parish DC, and Dever GEA**. Abdominal adiposity in US adults: prevalence and trends, 1960-2000. *Preventive Medicine* 39: 197-206, 2004.

35. **Palmieri F**. The mitochondrial transporter family (SLC25): physiological and pathological implications. *Pflugers Archiv-European Journal of Physiology* 447: 689-709, 2004.

36. **Park JY, Seong JK, and Paik Y-K**. Proteomic analysis of diet-induced hypercholesterolemic mice. *Proteomics* 4: 514-523, 2004.

37. **Pfaffl MW, Horgan GW, and Dempfle L**. Relative expression software tool (REST©) for group-wise comparison and statistical analysis of relative expression results in real-time PCR. *Nucleic Acids Research* 30: e36, 2002.

38. **Prasetyo H, and Eisen EJ**. Correlated responses in development and distribution of fat depots in mice selected for body composition traits. *Theoretical and Applied Genetics* 78: 217-223, 1989.

39. **Rasooly R, Kelley DS, Greg J, and Mackey BE**. Dietary *trans* 10, *cis* 12-conjugated linoleic acid reduces the expression of fatty acid oxidation and drug detoxification enzymes in mouse liver. *British Journal of Nutrition* 97: 58-66, 2007.

40. **Rocha JL, Eisen EJ, Van Vleck LD, and Pomp D**. A large-sample QTL study in mice: I. Growth. *Mammalian Genome* 15: 83-99, 2004.

41. **Rocha JL, Eisen EJ, Van Vleck LD, and Pomp D**. A large-sample QTL study in mice: II. Body composition. *Mammalian Genome* 15: 100-113, 2004.

42. **Santiago JL, Martínez A, de la Calle H, Fernández-Arquero M, Figueredo MÁ, de la Concha EG, and Urcelay E**. Evidence for the association of the SLC22A4 and SLC22A5 genes with Type I diabetes: a case control study. *BMC Medical Genetics* 7: 54, 2006.

43. **Sheu L, Pasyk EA, Ji JZ, Haung XH, Gao XD, Varoqueaux F, Brose N, and Gaisano HY**. Regulation of insulin exocytosis by Munc13-1. *Journal of Biological Chemistry* 278: 27556-27563, 2003.

44. **Shi J, and Kandror KV**. Sortilin is essential and sufficient for the formation of Glut4 storage vesicles in 3T3-L1 adipocytes. *Developmental Cell* 9: 99-108, 2005.

45. **Smith SR, Lovejoy JC, Greenway F, Ryan D, deJonge L, de la Bretonne J, Volafova J, and Bray GA**. Contributions of total body fat, abdominal subcutaneous

adipose tissue compartments, and visceral adipose tissue to the metabolic complications of obesity. *Metabolism* 50: 425-435, 2001.

46. **Steiber A, Kerner J, and Hoppel CL**. Carnitine: a nutritional, biosynthetic, and functional perspective. *Molecular Aspects of Medicine* 25: 455-473, 2004.

47. **Stein CJ, and Colditz GA**. The epidemic of obesity. *Journal of Clinical Endocrinology and Metabolism* 89: 2522-2525, 2004.

48. **Stevens J**. Obesity, fat patterning and cardiovascular risk. In: *Nutrition and biotechnology in heart disease and cancer* edited by Longenecker JB, Kritchevsky D, and Drezner MK. New York, NY: Plenum Publishing Corporation, 1995, p. 21-27.

49. **Stockdale T**. Obesity, diabetes and other problems. *Nutrition and Health* 17: 205-210, 2003.

50. **Stylianou IM, Clinton M, Keightley PD, Pritchard C, Tymowska-Lalanne Z, Bünger L, and Horvat S**. Microarray gene expression analysis of the Fob3b obesity QTL identifies positional candidate gene Sqle and perturbed cholesterol and glycolysis. *Physiological Genomics* 20: 224-232, 2005.

51. **Wajchenberg BL**. Subcutaneous and visceral adipose tissue: their relation to the metabolic syndrome. *Endocrine Reviews* 21: 697-738, 2000.

Table 2.1 Real-Time RT-PCR Primers and Conditions

Gene	Primer Sequence Forward	Primer Sequence Reverse	Product Length (bp)	Annealing Temperature (°C)	Efficiency*
S18	5'-CGCCATCACTGCCATTAAGG-3'	5'-CACTCGCTCCACCTCATCC-3'	118	59.4	80.9%
β-actin	5'-TCATGAAGTGTGACGTTGACATCCGT-3'	5'-CCTAGAAGCACTTGCGGTGCACGATG-3'	285	56.0	76.3%
$G\alpha_{i3}$	5'-GCTTTATTGAGAGGATGGC-3'	5'-TAATAGAGAAGACTGCTGGAG-3'	161	57.2	88.1%
SBP2	5'-CGGCAGTATGACATCTCTAAC-3'	5'-TTGGTCCTCCAGCACTTG-3'	105	61.8	101.7%
SLC22A4	5'-ATCCAGAAAGCCGCAAAG-3'	5'-CCACTGAGGTTAGCATCC-3'	181	57.2	118.9%
SLC25A16	5'-TCCTACCCATTTGATGTGAC-3'	5'-CAGCGGATGTAGTTCAGAG-3'	169	53.6	104.6%
Sortilin 1	5'-GACCAACAATACGCACCAG-3'	5'-TCTTTCCATAATCCTCACTTCG-3'	170	55.3	94.7%

All real-time PCR primers were designed using Beacon Designer 7, except β-actin which was previously described (39).
Annealing temperatures were empirically determined.
*Efficiencies of reactions performed in both epididymal fat pads and liver were averaged.

Table 2.2 HE & LF Mouse Weights – A Comparison of Two Studies

Line	Study	Number of Animals	Age	Body Weight (g)	Epididymal Fat Pad (mg)	Epididymal Fat Pad %
HE	Current	11	5 months	40.7 ± 5.0†	1328 ± 618*	3.30 ± 1.11%*
LF	Current	12	5 months	35.7 ± 4.0†	323 ± 152*	0.89 ± 0.36%*
HE	(12, 17)	40-50	3 months	35.9 ± 0.4	590 ± 19†	1.63 ± 0.04%†
LF	(12, 17)	40-50	3 months	36.5 ± 0.5	171 ± 19†	0.46 ± 0.04%†

All comparisons are between lines and within a study and a column
Statistically significant changes are indicated by: * $p<0.0001$ or † $p<0.05$

Table 2.3 Epididymal Fat Microarray Results

Accession No.	Probe*	Gene	Name	Difference (HE - LF)†	-log$_{10}$ p-value	Chromosome
NM_019972	M400011349	Sort1	sortilin 1	1.51	4.073	3
AK019905	M400015027	5330423I11Rik	RIKEN cDNA 5330423I11 gene	1.44	4.346	9
NM_019687	M200013911	SLC22A4	solute carrier family 22 (organic cation transporter), member 4	1.39	4.131	11
NM_010306	M200004485	$G\alpha_{i3}$	guanine nucleotide binding protein, alpha inhibiting 3	1.29	3.728	3
NM_172806	M400015611	Btbd7	BTB (POZ) domain containing 7	1.22	4.323	12
XM_485555	M400005531	LOC433839	similar to Tubulin beta-2 chain	1.19	3.640	5
NM_026473	M200012034	Tubb6	tubulin, beta 6	-1.20	3.860	18
NM_001033393	M300016900	Tmem104	transmembrane protein 104	-1.20	3.974	11
NM_027804	M200004058	Usp19	ubiquitin specific protease 19	-1.28	3.801	9
XM_142112	M400007989		PREDICTED: similar to Vigilin (High density lipoprotein-binding protein)	-1.42	3.853	X
AK009987	M400013686	2310058N22Rik	RIKEN cDNA 2310058N22 gene	-1.46	3.888	12
NM_175194	M300010589	SLC25A16	solute carrier family 25 (mitochondrial carrier, Graves disease autoantigen), member 16	-1.49	4.289	10

*Probe name in Operon's Mouse Oligo (version 4.0) dataset

†Results are reported as fold changes

Table 2.4 Liver Microarray Results

Accession No.	Probe*	Gene	Name	Difference (HE - LF)†	-log$_{10}$ p-value	Chromosome
NM_019972	M400011349	Sort1	sortilin 1	1.75	4.257	3
XM_135462	M400006575	Q811C3	PREDICTED: similar to immunoglobulin light chain variable region	1.61	3.587	6
NM_021468	M300006093	Unc13b	unc-13 homolog B	1.53	3.602	4
XM_489636	M400000610	Lrch3	PREDICTED: similar to leucine-rich repeats and calponin homology domain containing 3	1.37	3.607	16
XM_142112	M400007989		PREDICTED: similar to Vigilin (High density lipoprotein-binding protein)	-1.24	3.845	X
AK019905	M400015027	5330423I11Rik	RIKEN cDNA 5330423I11 gene	-1.34	4.021	9
NM_146218	M300014038	Rfwd3	ring finger and WD repeat domain 3	-1.40	4.387	8
AK040021	M400015611	Btbd7	BTB (POZ) domain containing 7	-1.47	5.172	12
NM_175194	M300010589	SLC25A16	solute carrier family 25 (mitochondrial carrier, Graves disease autoantigen), member 16	-1.53	4.360	10
AK039690	M400015409	BB195284	*Mus musculus* adult male spinal cord cDNA, RIKEN full-length enriched library	-1.62	3.833	6
NM_013458	M400010442	Add2	Beta adducin	-1.69	3.903	6
NM_019414	M400000117	SBP2	Selenium-binding protein 2	-2.63	3.850	3

*Probe name in Operon's Mouse Oligo (version 4.0) dataset

†Results are reported as fold changes

Table 2.5 Real-Time RT-PCR Results

Gene	Tissue	Microarray Fold Change	Microarray $-\log_{10}$ p-value	Real-Time Fold Change	Real-Time Standard Error	Real-Time p-value
$G\alpha_{i3}$	EF	1.29	3.728	-1.59	0.225 - 1.701	0.670
SLC22A4	EF	1.39	4.131	-9.35	0.021 - 1.612	0.071
SLC25A16	EF	-1.49	4.289	-3.42	0.084 - 1.067	0.069
Sortilin 1	EF	1.51	4.073	-6.45	0.036 - 0.731	0.012
SBP2	Liver	-2.63	3.850	-3.47	0.097 - 0.978	0.004
SLC25A16	Liver	-1.53	4.360	1.09	0.759 - 1.679	0.674
Sortilin 1	Liver	1.75	4.257	-1.11	0.542 - 1.696	0.643

Microarray fold change and –log10(p-value) calculated in JMP Genomics
Real-time RT-PCR fold change, standard error, and p-value calculated in REST© (37).

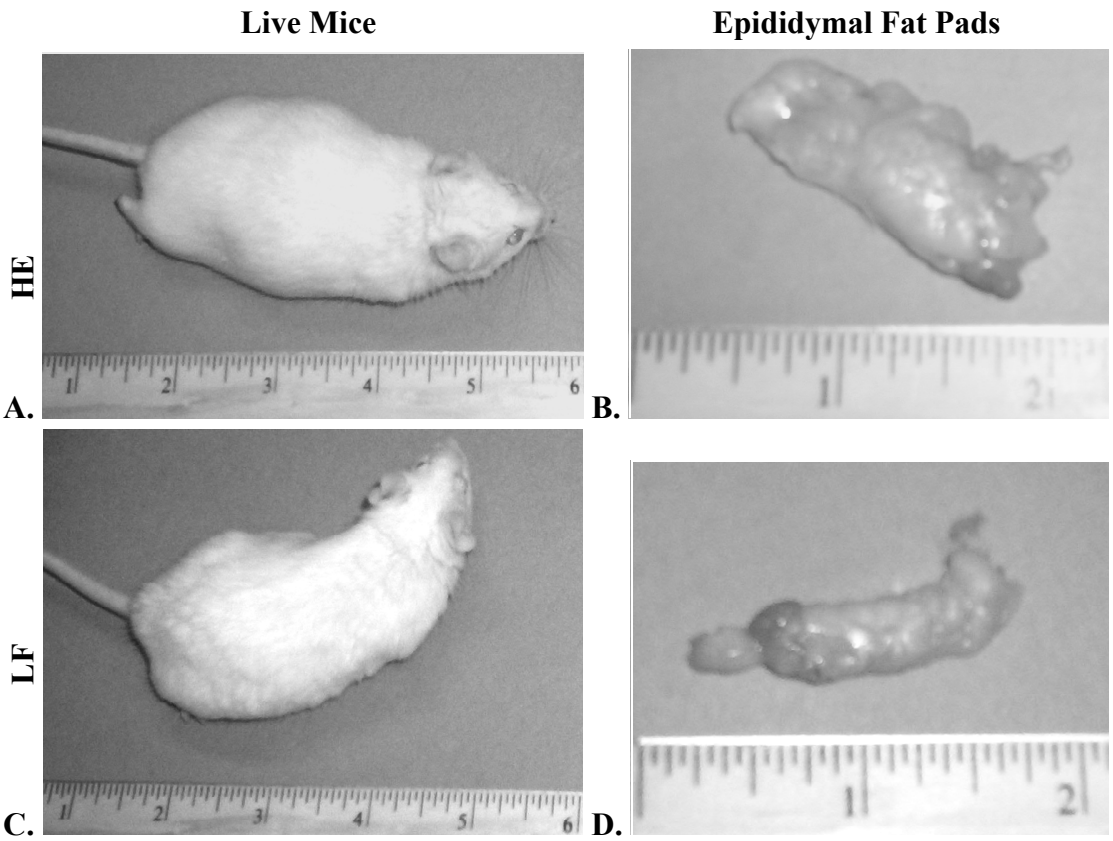

Figure 2.1 High Epididymal and Low Fat Mice
Pictures of an **A.** HE and **C.** LF mouse. **B.** and **D.** are epididymal fat pads from HE and LF mice, respectively. Ruler is shown to demonstrate scale.

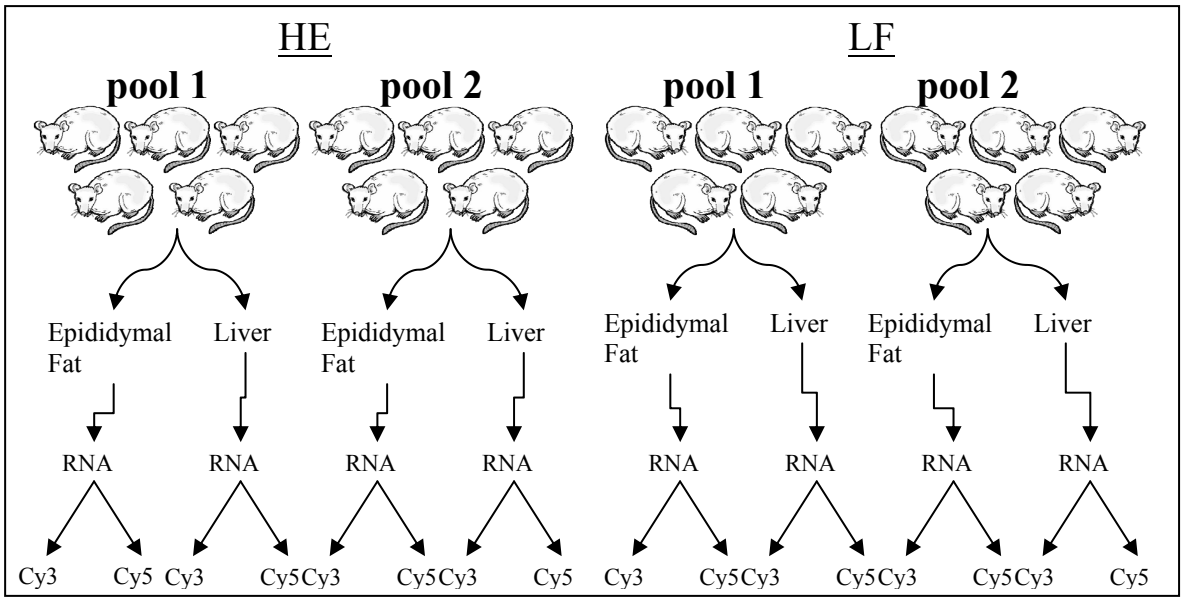

Figure 2.2 Biological and Technical Replicates
Ten mice per line were used in the microarray study. After tissue dissection and RNA extraction, RNA from five mice were pooled making two biological replicates per tissue within each mouse line. Two technical replicates per biological replicate were made by labeling each RNA with both Cy3 and Cy5.

Array	Cy3	Cy5
1	HE_EF_1	HE_L_1
2	HE_L_1	LF_EF_1
3	LF_EF_1	LF_L_1
4	LF_L_1	HE_EF_1
5	HE_EF_2	LF_EF_2
6	LF_EF_2	HE_EF_2
7	LF_L_2	HE_L_2
8	HE_L_2	LF_L_2

Figure 2.3 Experimental Design
Mice were divided into two replicates as indicated in Figure 2. Labelings from the first group were hybridized to the arrays in a loop design (arrays 1 – 4). In this design, each array was hybridized with a liver (L) or epididymal fat (EF) labeling. Labelings from the second group were hybridized using a dye swap design (arrays 5 – 8); arrays were hybridized with labelings from the same tissue type but different lines (HE or LF).

trans-10, *cis*-12-Conjugated Linoleic Acid Regulation of Gene Expression in the Liver of a Polygenic Obese Line of Mice

Ryan P. Ceddia[1], Ralph L. House[1], Joseph P. Cassady[1], Eugene J. Eisen[1],

Thomas E. Eling[3], Jennifer B. Collins[4], Sherry F. Grissom[4], Melissa S. Ashwell[1],

and Jack Odle[1]

[1]Department of Animal Science, North Carolina State University at Raleigh

Raleigh, NC 27695

[3]Laboratory of Molecular Carcinogenesis, National Institute of Environmental Health Sciences

Research Triangle Park, NC 27709

[4] National Institute of Environmental Health Sciences Microarray Group

Research Triangle Park, NC 27709

Corresponding author: Dr. Melissa S. Ashwell, Department of Animal Science, Raleigh, NC 27695, USA

melissa_ashwell@ncsu.edu; 919-513-7488; 919-515-6884 (fax)

Number of Tables: 4

Number of Figures: 2

Keywords: gene expression, genomics, mice, liver, conjugated linoleic acid, obesity

Acknowledgements: We thank Dr. Ben Corl for conducting the fatty acid analysis and Peggy Overton for coordinating the phenotypic data collection. BASF kindly donated the *trans*-10, *cis*-12-CLA used in this experiment. The authors gratefully acknowledge Shelly Nolin and Audrey O'Nan for technical assistance and Dr. Michael G. Gonda for his critical review of the manuscript.

Abstract

trans-10, *cis*-12-Conjugated Linoleic Acid (CLA) causes a rapid reduction of body and adipose mass in mice. CLA causes these changes by decreasing the size and number of adipocytes. In addition to changes in adipose tissue of CLA fed mice, numerous studies have reported an increase in mass, cytoplasmic vacuolization, and fatty acid synthesis and oxidation in liver of CLA fed mice. The livers of CLA fed mice gain mass due to lipid accumulation; however, the precise molecular mechanisms are unknown. In order to elucidate these mechanisms, we examined the fatty acid composition, histology, and gene expression profile of liver from a polygenic obese line of mice fed CLA. Using a Periodic acid-Schiff (PAS) stain, histological evidence suggests that glycogen content is unchanged in the liver of the CLA fed mouse, implying that hepatic cytoplasmic vacuolization is due to increased lipid, but not glycogen, content. Examination of the fatty acid profile suggests that stearoyl CoA desaturase (SCD) activity is unaffected by CLA. Analysis of gene expression data identified 1393 genes differentially expressed in the liver of CLA fed mice at a nominal P-value of 0.01. Following Bonferroni correction and excluding lowly expressed transcripts, 198 genes were identified as being differentially expressed with 17 genes having ≥ 2 fold change. Real-time RT-PCR showed up regulation of *acylglycerol-3-phosphate O-acyltransferase 2* (*Agpat2*) and *diacylglycerol O-acyltransferase 2* (*Dgat2*), two genes necessary for triglyceride biosynthesis, in CLA fed mice. Furthermore, microarray and real-time RT-PCR data demonstrated greater expression of *B-cell leukemia/lymphoma 6* (*Bcl6*), a nuclear transcriptional repressor, and *signal transducer and activator of transcription 5B* (*Stat5b*), a transcription factor, in the liver of CLA fed mice.

Both genes are associated with immunoregulation. Comparing real-time RT-PCR to microarray gene expression data suggest a Bonferroni correction to microarray data are necessary in order to eliminate false positive results. Further verification of microarray results is needed to validate microarray data after a Bonferroni correction.

Abbreviations

Acetyl CoA oxidase (ACOX), acylglycerol-3-phosphate O-acyltransferase 2 (Agpat2), conjugated linoleic acid (CLA), cytochrome P450 family 2, subfamily e, polypeptide 1 (Cyp2e1), diacylglycerol O-acyltransferase 2 (Dgat2), epidermal growth factor receptor (EGFR), false discovery rate (FDR), Fatty acid synthase (FAS), glyceraldehyde-3-phosphate dehydrogenase (GAPDH), hypoxanthine guanine phosphoribosyl transferase 1 (Hprt), insulin-like growth factor binding protein 2 (Igfbp-2), Institute for Cancer Research (ICR), Janus kinase (Jak), linoleic acid (LA), malic enzyme (ME), minimum information about microarray experiments (MIAME), National Center for Biotechnology Information (NCBI), National Institute of Environmental Health Sciences (NIEHS), Periodic acid-Schiff (PAS), phosphatidylinositol 3-kinase, regulatory subunit (p85 alpha) (Pik3r1), ribosomal protein S18 (S18), signal transducer and activator of transcription (Stat), stearoyl CoA desaturase (SCD), suppressor of cytokine signaling 6 (Socs6), tyrosine kinase 2 (Tyk2).

Introduction

Conjugated linoleic acid (CLA) is a term that refers to positional and geometrical isomers of linoleic acid (LA) (48). CLA is a naturally occurring *trans*-fatty acid produced in the rumen as an intermediate during biohydrogenation of unsaturated fatty acids (17, 47).

Not surprisingly, the main source of natural CLA in the diet comes from ruminant products such as milk, cheese, beef, and lamb (16, 48). Until recently, it has been very difficult to purify specific isomers of CLA; hence, most studies have focused on feeding a mixture of CLA isomers. Using purified isomers, the *trans*-10, *cis*-12 isomer was found to have delipidative effects (15, 20, 41, 42) while the *cis*-9, *trans*-11 isomer was found to have anti-carcinogenic effects (41).

The *trans*-10, *cis*-12-CLA isomer has been shown to have delipidative effects in mice, rats, chicks, pigs, and humans (2, 22, 23). The effects of CLA on obesity vary between and within species; in mice, CLA reduces fat-body mass by 50 to 70% (23). Numerous studies report that the feeding of CLA decreases adipose mass in mice, which may be caused by reduced size and number of adipocytes (4, 29, 53, 58). Most studies indicate that energy expenditure is increased in CLA fed mice (11, 36, 51, 56) while studies on feed intake produce mixed results (50). In addition to changes in adipose tissue of CLA fed mice, numerous studies have reported an increase in size, cytoplasmic vacuolization, and fatty acid synthesis and oxidation in liver of CLA fed mice (11, 21-23, 41, 59). Much of the increased mass of the liver may be explained by accumulation of lipids (21, 25, 26). Increased fatty acid synthesis may, in part, be responsible for the rise in liver lipids (11, 37). Alternatively, accumulation of fatty acids in the liver of CLA fed animals may be derived from delipidated adipose tissue instead of fatty acid synthesis (8, 9).

Numerous studies have attempted to elucidate the molecular mechanisms of the actions of CLA. To date, four microarray studies have used gene expression profiling to examine the effects of CLA (12, 21, 29, 46). These studies have found regulatory pathways

involved in development, signal transduction, and fatty acid metabolism affected by CLA. In a previous study by House and colleagues (21), we reported microarray data from adipose tissue of the polygenic obese line of mice, M16, fed 1% *trans*-10, *cis*-12-CLA with 92% purity. These data suggest that the delipidative effects of CLA occur through a pleiotropic reduction in fatty acid and triglyceride translocation and storage, decreased glucose availability, and increased fatty acid oxidation. In addition to adipose tissue, CLA influences metabolism of the liver. We previously reported (21) that CLA caused the liver to accumulate 61% more fat and 33% more weight after 14 days of feeding CLA. Here we report gene expression and fatty acid composition data from livers of the M16 mice that were fed *trans*-10, *cis*-12-CLA for 14 days (21). These data show that CLA causes differential regulation of many genes in the murine liver. Furthermore, we also report histology results which suggest that the increase in liver weight was due primarily to an increase in lipid content.

Materials & Methods

Mice

Mice were maintained according to North Carolina State University's Institutional Animal Care and Use Committee protocol. The M16 line of mice, used in this study, was selected from an ICR (Institute for Cancer Research) base population. The M16 line is a moderately obese line that was selected for 3-6 week post-weaning gain (13, 14, 19).

Diet Composition

Mice were fed purified AIN93G pellets (Harlan Teklad, Madison, WI) formulated with either 1% *trans*-10, *cis*-12-CLA or 1% LA as a treatment control. The *trans*-10, *cis*-

12-CLA was kindly donated by BASF (Ludwigshafen, Germany), and LA was purchased from Nu-Chek-Prep (Elysian, MN). Dietary CLA and LA content were analyzed, confirming 92% and 99% purity, respectively. Pellets were stained with inert red and blue dyes to ensure the appropriate diet was fed.

Histology

Liver tissues from three mice from each treatment were snap frozen in liquid nitrogen and stored at -80°C. Histology was performed at the North Carolina State University College of Veterinary Medicine Histology Laboratory. Samples were thawed in 10% v/v neutral buffered formalin, embedded in 100% OCT embedding medium in PBS (Sakura Finetek, Torrence, CA), snap frozen in liquid nitrogen, and sectioned. Glycogen content was visualized using Periodic Acid-Schiff (PAS) staining as previously described (34). In this reaction, periodic acid oxidizes polysaccharides, such as glycogen, forming aldehydes which react with Schiff's reagent to form an insoluble magenta compound. Two sister 5µm sections were cut on a Leica 2135 Microtome (Leica Microsystems, Wetzlar, Germany); one section was digested with amylase to remove glycogen prior to PAS staining. The presence of glycogen was demonstrated by the loss of staining after amylase digestion when compared to the untreated sister section. Slides were visually inspected for changes in glycogen content.

Fatty Acid Composition of Tissues

Lipids were extracted from liver tissue and fatty acids were quantified by gas-liquid chromatography as previously described (1).

RNA Extractions

Total RNA was isolated from liver using TriReagent (Sigma, St. Louis, MO) and further purified with Qiagen RNeasy Mini kit (Qiagen, Valencia, CA) following the manufacturer's protocol with modifications previously described (54).

Microarrays

Microarrays were hybridized as previously described (21). Four Agilent (Palo Alto, CA) mouse oligo microarray slides containing 20,000 probes were designed in collaboration with the NIEHS Toxicogenomics Research Consortium and Paradigm Genetics (Research Triangle Park, NC). Total RNA was labeled with cyanine 3 (Cy3)- and cyanine 5 (Cy5)-labeled dCTP using the Agilent Fluorescent Direct Label kit (Palo Alto, CA) following the manufacturer's protocol. Hybridization of slides was for 16 hours in a rotating hybridization oven using the Agilent 60-mer-oligo microarray processing protocol. Subsequently, slides were washed with a 6× SSC-0.005% Triton X-102 wash solution for 10 min at room temperature, followed by a second wash with a solution of 0.1× SSC-0.005% Triton X-102 for 5 minutes and dried under a nitrogen stream. Slides were scanned with an Agilent G2565BA microarray scanner (Palo Alto, CA).

Microarray Data Collection and Analysis

Microarray data were collected and analyzed as previously described (21). Briefly, microarray data extraction was performed using Agilent G2567AA Feature Extraction software, following Agilent's direct labeling protocol. Rosetta Resolver version 3.2, build 3.2.2.0.33 (Rosetta Biosoftware, Kirkland, WA) was used to analyze data. Intensity plots were produced and genes were identified as candidate genes if $P < 0.01$ using Rosetta Resolver error model (49). Raw data been deposited in the National Center for

Biotechnology Information (NCBI) Gene Expression Omnibus in accordance with "minimum information about microarray experiments" (MIAME) (5). P-values from Rosetta Resolver were converted to false discovery rate (FDR) P-values. FDR P-values were calculated by arranging samples in order of their P-values. The P-value was then multiplied by the total number of genes and divided by their rank based upon their P-value resulting in the FDR P-value (3). Alternatively, nominal P-values from Rosetta Resolver were corrected using a Bonferroni correction. The Bonferroni correction identified an uncorrected P-value ($P < 4.79203 \times 10^{-05}$) as the threshold for statistical significance. These were further reduced by only considering the genes which had an average intensity greater than 200 for both treatments or 300 for one treatment group. This cutoff was chosen because the gene with the lowest intensity that PCR was able to amplify had an intensity of 220 (data not shown).

Real-Time RT-PCR

Genes targeted for quantitative real-time RT-PCR verification were selected based on their involvement in signal transduction pathways. Other genes, which were not statistically significant based on microarray results, were selected based on their role in lipid metabolism or have been previously shown to be differentially expressed in the liver of other mice fed CLA (46). Real-time RT-PCR primers were designed using Beacon Designer 7 (PREMIER Biosoft International, Palo Alto, CA) or selected from primers previously designed by Rasooly and colleagues (Table 3.1) (46). PCR products were sequenced to confirm their identity.

Total RNA was quantitated using a NanoDrop® ND-1000 spectrophotometer (Wilmington, DE). A total of 1µg RNA was reverse transcribed using Applied Biosystems High Capacity cDNA Reverse Transcription Kit (Foster City, CA). Real-time RT-PCR reactions were performed using Applied Biosystems Power SYBR® Green PCR Master Mix (Foster City, CA) in a BioRad iCycler (Hercules, CA) with minor modifications. Fluorescein was added at a final concentration of 10 nM because fluorescein is needed as the reference dye in the BioRad iCycler and is absent in the Applied Biosystems Power SYBR® Green PCR Master Mix. Cycling conditions were as follows: 95°C for 7 min, 60 cycles of (95°C for 30 sec, appropriate annealing temperature [Table 3.1] for 30 sec, 72.0°C for 30 sec), 72°C for 5 min, 95°C for 1 min, 55.0°C for 1 min, followed by a melt curve of 80 cycles of 10 seconds at 55°C with a 0.5°C increase every cycle. Mouse *glyceraldehyde-3-phosphate dehydrogenase* (*GAPDH*), *hypoxanthine guanine phosphoribosyl transferase 1* (*Hprt*), and *cytochrome P450 family 2, subfamily e, polypeptide 1* (*Cyp2e1*) were used as housekeeping genes for normalization. Gene expression data were collected from two replicates of each sample and three replicates of each standard curve point. Duplicate samples were averaged and imported into the Relative Expression Software Tool (REST©) for calculation of fold changes and determination of statistical significance (45). Each replicate was imported directly into REST©. Outlier samples and samples with a heterogeneous dissociation curve, as determined by melt curve analyses, were excluded.

Results

Histology

It has been previously hypothesized that cytoplasmic vacuolization in murine liver is caused by intracellular glycogen (10, 11). PAS staining and digestion of slides showed no observable difference between treatments (Figure 3.1), suggesting that CLA does not alter glycogen content.

Fatty Acid Composition of Liver

The *trans*-10, *cis*-12-CLA isomer (18:2) was only present in the livers of mice fed the *trans*-10, *cis*-12-CLA supplemented diet (Table 3.2). The ratio of 16:0/16:1 was unchanged while the ratio of 18:0/18:1 was decreased in liver tissue from mice fed *trans*-10, *cis*-12-CLA. The 20:2 isomer was increased in the liver of *trans*-10, *cis*-12-CLA fed mice. A decrease in the 20:3 and 20:4 isomers were also observed.

Microarray and Real-Time RT-PCR Validation

Analysis of gene expression data identified 1393 genes differentially expressed in the liver of CLA vs. LA treated mice at a nominal P-value of 0.01. Seventy-nine of these genes had a ≥ 2 fold change. After FDR correction, 775 genes were differentially expressed ($P < 0.05$), with 63 genes differentially expressed with ≥ 2 fold change. Following Bonferroni correction and excluding lowly expressed transcripts, 198 genes were identified as being differentially expressed with 17 genes having ≥ 2 fold change (Supplementary Table 3.S1). Quantitative real-time RT-PCR was used to validate the microarray results for 15 genes (Table 3.3) (Figure 3.2). Real-time RT-PCR confirmed differential expression of *B-cell leukemia/lymphoma 6* (*Bcl6*) and *signal transducer and activator of transcription 5B* (*Stat5b*) and in the correct direction. Furthermore, according to real-time RT-PCR *ribosomal protein S18*, *1-acylglycerol-3-phosphate O-acyltransferase 2* (*Agpat2*) and

diacylglycerol O-acyltransferase 2 (*Dgat2*) were differentially expressed even though these genes were not identified using microarrays. We were not able to verify differential expression of the *epidermal growth factor receptor* (*EGFR*), *phosphatidylinositol 3-kinase, regulatory subunit (p85 alpha)* (*Pik3r1*), *stearoyl CoA desaturase-1* (*SCD-1*), *suppressor of cytokine signaling 6* (*Socs6*), or *tyrosine kinase 2* (*Tyk2*) genes. Of the genes tested by real-time RT-PCR, only *Bcl6* was statistically significant based on microarrays after the Bonferroni correction.

Discussion

Feeding CLA to mice causes many physiological changes, including increased mass and cytoplasmic vacuolization in the livers of CLA fed animals. Previously, we demonstrated that our CLA fed mice had 61% more lipid present in the liver (21). Lipid accumulation causes an increase in cytoplasmic vacuolization, but increased cytoplasmic vacuolization also may be caused by the presence of intracellular glycogen. The possibility of increased intracellular glycogen in the CLA fed murine liver has been reported, but not confirmed (10, 11). In these previous studies, liver sections from CLA fed mice were histologically analyzed in two pathology laboratories in each study. All labs observed an increase in cytoplasmic vacuolization (10, 11). In both studies, one lab determined that the vacuoles were characteristic of increased lipid content while the other lab concluded that glycogen content also may be increased. Here, our visual inspection of the histological results suggests there is no change in the amount of glycogen present in the liver in CLA and LA fed mice (Figure 3.1). Therefore, cytoplasmic vacuolization in the liver may be caused by lipid accumulation.

Because feeding CLA increased the amount of hepatic lipids (21), we examined the fatty acid profile. Conversion of the saturated fatty acids to their corresponding monounsaturated fatty acids is regulated by SCD, also known as Δ^9 desaturase, hence comparing the ratios of unsaturated to monounsaturated fatty acids provides an indication of the level of SCD activity (38). Our fatty acid profile indicated that there was a decrease in the ratios of 18:0/18:1 and no change in the ratios of 16:0/16:1 in the livers of our mice (Table 3.2). These results suggest that SCD activity is increased, based upon the decreased ratio of 18:0/18:1, or unchanged, based upon the unvarying 16:0/16:1 ratio. The results for 18:0/18:1 ratios are concordant with our microarray data (FDR, $P \leq 0.05$) because these data show increased *SCD-1* expression while the ratios of 16:0/16:1 are in agreement with our real-time RT-PCR data because these results demonstrate no change in expression (Table 3.3). Previous studies also present conflicting results as the level or activity of SCD-1 has been shown to be either reduced (30, 43), unaffected (33, 46, 55), or increased (44, 52) in murine liver when fed CLA. While our results suggest that 18:0/18:1 ratio is decreased and 16:0/16:1 ratios are unchanged, we previously demonstrated different results, with 16:0/16:1 increased and 18:0/18:1 unchanged, in adipose tissue of mice fed *trans*-10, *cis*-12-CLA (21). It is possible that hepatic steatosis may be caused by accretion of lipoprotein originating from delipidated adipose tissue (8, 9). This transport of lipid from adipose to liver tissues may mask changes in the ratios of saturated to unsaturated fatty acids. Given the number of studies that have been unable to produce concordant results for *SCD-1* expression in the liver of CLA fed mice, it is not surprising that we show disparate results between liver and adipose.

As was the case for *SCD-1*, real-time RT-PCR and microarray data produced discrepant results for multiple genes. We were not able to validate five of our genes. It is likely that we were not able to verify some of these because a reduced correlation between microarray and real-time RT-PCR results for genes with a fold change of less than 1.5 has been observed in a study focused on the correlations between microarray and real-time RT-PCR results (7). The Bonferroni correction may have been necessary for our data to reduce our false positive rate. *Bcl6*, the only gene statistically significant after the Bonferroni correction, was validated by real-time RT-PCR. Several of the genes which were not confirmed by real-time RT-PCR (*SCD-1*, *Pik3r1*, and *Tyk2*) were statistically significant at a FDR P-value ≤ 0.05 (data not shown). For this reason, the Bonferroni correction appears to be most appropriate for our microarray data.

Genes associated with immunoregulation were found to have differential regulation according to both microarray and real-time RT-PCR data. *Bcl6* and *Stat5b* appear to be up regulated in the livers of CLA fed mice. Both of these genes encode transcription factors. Bcl6 is a zinc finger transcription factor that acts as a sequence-specific repressor of transcription (24). High levels of *Bcl6* expression are associated with a favorable prognosis for non-Hodgkin's lymphomas (24). Given the fact that CLA has beneficial effects against cancer, it is not remarkable that *Bcl6* is up regulated in CLA fed mice (2, 23, 35). Bcl6 has the highest affinity for Stat (signal transducer and activator of transcription) DNA binding sites, hence it acts to repress transcription from Stats (24). Stats, such as Stat5b, are transcription factors involved in the Janus kinase (Jak)/Stat pathway. The Jak/Stat pathway mediates signal transduction from cytokines, many of which are associated with immune

response (18, 27, 32, 39). CLA is known to have a beneficial effect on immunoregulation (2, 23, 35, 40, 47); hence it is not unexpected that we see up regulated of genes in the liver associated with an immune response.

We also detected differential expression of several genes by real-time RT-PCR, which were not detected by the microarrays. We suspected these genes would be differentially expressed due to their role in lipid biosynthesis. We found up regulation of *Agpat2* and *Dgat2* according to real-time RT-PCR. Agpat2 converts lysophosphatidic acid to phosphatidic acid, which represents the second step in triglyceride biosynthesis (31, 57). Dgat2 is also involved in triglyceride biosynthesis, catalyzing the reaction that joins diacylglycerol to long chain fatty acyl-CoAs, which represents the last step in triglyceride biosynthesis (6, 28). These results suggest that lipid biosynthesis is up regulated in the liver of CLA fed mice. This agrees with the conclusion made by a previous microarray study which found increased fatty acid synthesis in the liver of CLA fed mice (46). This also conforms with our finding that lipid content is increased in the liver of CLA fed mice (21).

Recently, a similar gene expression study was conducted feeding 0.5% *trans* 10, *cis* 12-CLA with 88.1% purity to two mice per treatment group for a microarray experiment and six mice per treatment group for a quantitative real-time RT-PCR experiment (46). Therefore, we wanted to compare our results with those reported by Rasooly and coworkers (46). Several of the primers were used in this study to directly compare our real-time RT-PCR results with those of Rasooly and coworkers (46) (Table 3.3). Neither study found a difference in expression of *acetyl CoA oxidase* (*ACOX*) in either microarray or real-time RT-PCR data. In addition, *malic enzyme* (*ME*), which was found to be differentially

expressed according to their microarray data but not according to real-time RT-PCR data, was not differentially expressed in either our microarray or real-time RT-PCR data. Similarly, *SCD-1* was found to be differentially expressed in our microarray data but not differentially expressed according to either their microarray or real-time RT-PCR data. *Fatty acid synthase* (*FAS*) was not shown to be differentially expressed according to both groups' microarray data and our real-time RT-PCR data, but was differentially expressed according to their real-time RT-PCR data. We also attempted to verify the expression of *EGFR* which was differentially expressed according to both microarray experiments. While real-time RT-PCR and microarray data showed that *EGFR* was down regulated, our real-time RT-PCR data were not statistically significant ($p=0.27$).

In this study we have begun to elucidate some of the molecular mechanisms of CLA's effects on the murine liver. As expected, livers from CLA fed mice contained more lipid (21). Our histological analysis of these livers suggest that glycogen is unchanged, indicating that increased mass and cytoplasmic vacuolization are primarily caused by lipid. Analysis of the fatty acid profile indicated that SCD activity was most likely unchanged. Additionally, gene expression studies indicate that triglyceride biosynthesis is increased in the liver of the CLA fed mouse. This result agrees with previous reports that indicate increased fatty acid synthesis may be responsible for the rise in hepatic lipid mass (11, 37). We also observed up regulation of genes associated with immunoregulation which highlights the beneficial role of CLA in health. While we were not able to validate our microarray data with a nominal P-value < 0.01, comparing real-time RT-PCR to microarray

gene expression data suggests a Bonferroni correction is necessary to eliminate false positive results. Further verification of microarray results is needed to validate this data.

References:

1. **Averette Gatlin L, See MT, Hansen JA, Sutton D, and Odle J**. The effects of dietary fat sources, levels, and feeding intervals on pork fatty acid composition. *Journal of Animal Science* 80: 1606-1615, 2002.

2. **Belury MA**. Dietary conjugated linoleic acid in health: Physiological effects and mechanisms of action. *Annual Review of Nutrition* 22: 505-531, 2002.

3. **Benjamini Y, and Hochberg Y**. Controlling the false discovery rate - a practical and powerful approach to multiple testing. *Journal of the Royal Statistical Society Series B-Methodological* 57: 289-300, 1995.

4. **Bouthegourd JC, Martin JC, Gripois D, Roseau S, Blouquit MF, Even PC, Tome D, and Quignard-Boulange A**. Efficaciy of dietary CLA and CLA plus Guarana (ADI pill) on body adiposity, and adipocytes cell number and size. *The FASEB Journal* 16: A370-A370, 2002.

5. **Brazma A, Hingamp P, Quackenbush J, Sherlock G, Spellman P, Stoeckert C, Aach J, Ansorge W, Ball CA, Causton HC, Gaasterland T, Glenisson P, Holstege FCP, Kim IF, Markowitz V, Matese JC, Parkinson H, Robinson A, Sarkans U, Schulze-Kremer S, Stewart J, Taylor R, Vilo J, and Vingron M**. Minimum information about a microarray experiment (MIAME) – toward standards for microarray data. *Nature Genetics* 29: 365-371, 2001.

6. **Cases S, Stone SJ, Zhou P, Yen E, Tow B, Lardizabal KD, Voelker T, and Farese RV**. Cloning of DGAT2, a second mammalian diacylglycerol acyltransferase, and related family members. *Journal of Biological Chemistry* 276: 38870-38876, 2001.

7. **Dallas PB, Gottardo NG, Firth MJ, Beesley AH, Hoffmann K, Terry PA, Freitas JR, Boag JM, Cummings AJ, and Kees UR**. Gene expression levels assessed by oligonucleotide microarray analysis and quantitative real-time RT-PCR – how well do they correlate? *BMC Genomics* 6: 59, 2005.

8. **Degrace P, Demizieux L, Gresti J, Chardigny J-M, Sébédio J-L, and Clouet P**. Association of liver steatosis with lipid oversecretion and hypotriglyceridaemia in C57BL/6J mice fed *trans*-10,*cis*-12-linoleic acid. *FEBS Letters* 546: 335-339, 2003.

9. **Degrace P, Demizieux L, Gresti J, Chardigny J-M, Sébédio J-L, and Clouet P**. Hepatic steatosis is not due to impaired fatty acid oxidation capacities in C57BL/6J mice fed the conjugated *trans*-10,*cis*-12-isomer of linoleic acid. *Journal of Nutrition* 134: 861-867, 2004.

10. **DeLany JP, Blohm F, Truett AA, Scimeca JA, and West DB**. Conjugated linoleic acid rapidly reduces body fat content in mice without affecting energy intake. *American Journal of Physiology - Regulatory Integrative and Comparative Physiology* 276: R1172-R1179, 1999.

11. **DeLany JP, and West DB**. Changes in body composition with conjugated linoleic acid. *Journal of the American College of Nutrition* 19: 487S-493S, 2000.

12. **Ecker J, Langmann T, Moehle C, and Schmitz G**. Isomer specific effects of Conjugated Linoleic Acid on macrophage ABCG1 transcription by a SREBP-1c dependent mechanism. *Biochemical and Biophysical Research Communications* 352: 805-811, 2007.

13. **Eisen EJ**. Population size and selection intensity effects on long-term selection response in mice. *Genetics* 79: 305-323, 1975.

14. **Eisen EJ, Bakker H, and Nagai J**. Body-composition and energetic efficiency in two lines of mice selected for rapid growth-rate and their F_1 crosses. *Theoretical and Applied Genetics* 49: 21-34, 1977.

15. **Evans M, Lin X, Odle J, and McIntosh M**. *Trans*-10, *cis*-12 conjugated linoleic acid increases fatty acid oxidation in 3T3-L1 preadipocytes. *Journal of Nutrition* 132: 450-455, 2002.

16. **Evans ME, Brown JM, and McIntosh MK**. Isomer-specific effects of conjugated linoleic acid (CLA) on adiposity and lipid metabolism. *Journal of Nutritional Biochemistry* 13: 508-516, 2002.

17. **Fritsche J, and Steinhart H**. Analysis, occurrence, and physiological properties of trans fatty acids (TFA) with particular emphasis on conjugated linoleic acid isomers (CLA) - a review. *Fett/Lipid* 100: 190-210, 1998.

18. **Haan C, Kreis S, Margue C, and Behrmann I**. Jaks and cytokine receptors - An intimate relationship. *Biochemical Pharmacology* 72: 1538-1546, 2006.

19. **Hanrahan JP, Eisen EJ, and Legates JE**. Effects of population size and selection intensity of short-term response to selection for postweaning gain in mice. *Genetics* 73: 513-530, 1973.

20. **Hargrave KM, Li CL, Meyer BJ, Kachman SD, Hartzell DL, Della-Fera MA, Miner JL, and Baile CA**. Adipose depletion and apoptosis induced by *trans*-10, *cis*-12 conjugated linoleic acid in mice. *Obesity Research* 10: 1284-1290, 2002.

21. **House RL, Cassady JP, Eisen EJ, Eling TE, Collins JB, Grissom SF, and Odle J**. Functional genomic characterization of delipidation elicited by *trans*-10, *cis*-12-

conjugated linoleic acid (t10c12-CLA) in a polygenic obese line of mice. *Physiological Genomics* 21: 351-361, 2005.

22. **House RL, Cassady JP, Eisen EJ, McIntosh MK, and Odle J**. Conjugated linoleic acid evokes de-lipidation through the regulation of genes controlling lipid metabolism in adipose and liver tissue. *Obesity Reviews* 6: 247-258, 2005.

23. **Jahreis G, Kraft J, Tischendorf F, Schöne F, and von Loeffelholz C**. Conjugated linoleic acids: Physiological effects in animal and man with special regard to body composition. *European Journal of Lipid Science and Technology* 102: 695-703, 2000.

24. **Jardin F, Ruminy P, Bastard C, and Tilly H**. The *BCL6* proto-oncogene: a leading role during germinal center development and lymphomagenesis. *Pathologie Biologie* 55: 73-83, 2007.

25. **Kelley DS, Bartolini GL, Newman JW, Vemuri M, and Mackey BE**. Fatty acid composition of liver, adipose tissue, spleen, and heart of mice fed diets containing *t*10, *c*12-, and *c*9, *t*11-conjugated linoleic acid. *Prostaglandins Leukotrienes and Essential Fatty Acids* 74: 331-338, 2006.

26. **Kelley DS, Bartolini GL, Warren JM, Simon VA, Mackey BE, and Erickson KL**. Contrasting effects of *t*10,*c*12-and *c*9,*t*11-conjugated linoleic acid isomers on the fatty acid profiles of mouse liver lipids. *Lipids* 39: 135-141, 2004.

27. **Kisseleva T, Bhattacharya S, Braunstein J, and Schindler CW**. Signaling through the JAK/STAT pathway, recent advances and future challenges. *Gene* 285: 1-24, 2002.

28. **Lardizabal KD, Mai JT, Wagner NW, Wyrick A, Voelker T, and Hawkins DJ**. DGAT2 is a new diacylglycerol acyltransferase gene family - Purification, cloning, and expression in insect cells of two polypeptides from *Mortierella ramanniana* with diacylglycerol acyltransferase activity. *Journal of Biological Chemistry* 276: 38862-38869, 2001.

29. **LaRosa PC, Miner J, Xia YN, Zhou Y, Kachman S, and Fromm ME**. *Trans*-10, *cis*-12 conjugated linoleic acid causes inflammation and delipidation of white adipose tissue in mice: a microarray and histological analysis. *Physiological Genomics* 27: 282-294, 2006.

30. **Lee KN, Pariza MW, and Ntambi JM**. Conjugated linoleic acid decreases hepatic stearoyl-CoA desaturase mRNA expression. *Biochemical and Biophysical Research Communications* 248: 817-821, 1998.

31. **Leung DW**. The structure and functions of human lysophosphatidic acid acyltransferases. *Frontiers in Bioscience* 6: D944-D953, 2001.

32. **Levy DE, and Darnell JE**. STATs: Transcriptional control and biological impact. *Nature Reviews Molecular Cell Biology* 3: 651-662, 2002.

33. **Lin XB, Loor JJ, and Herbein JH**. *Trans*10,*cis*12-18:2 is a more potent inhibitor of de novo fatty acid synthesis and desaturation than *cis*9,*trans*11-18:2 in the mammary gland of lactating mice. *Journal of Nutrition* 134: 1362-1368, 2004.

34. **Luna LG, and Armed Forces Institute of Pathology**. *Manual of histologic staining methods of the Armed Forces Institute of Pathology*. New York: Blakiston Division, McGraw-Hill, 1968.

35. **MacDonald HB**. Conjugated linoleic acid and disease prevention: A review of current knowledge. *Journal of the American College of Nutrition* 19: 111S-118S, 2000.

36. **Miner JL, Cederberg CA, Nielsen MK, Chen XL, and Baile CA**. Conjugated linoleic acid (CLA), body fat, and apoptosis. *Obesity Research* 9: 129-134, 2001.

37. **Moya-Camarena SY, Vanden Heuvel JP, Blanchard SG, Leesnitzer LA, and Belury MA**. Conjugated linoleic acid is a potent naturally occurring ligand and activator of PPAR alpha. *Journal of Lipid Research* 40: 1426-1433, 1999.

38. **Ntambi JM**. Regulation of stearoyl-CoA desaturase by polyunsaturated fatty acids and cholesterol. *Journal of Lipid Research* 40: 1549-1558, 1999.

39. **O'Shea JJ, Gadina M, and Schreiber RD**. Cytokine signaling in 2002: New surprises in the Jak/Stat pathway. *Cell* 109: S121-S131, 2002.

40. **O'Shea M, Bassaganya-Riera J, and Mohede ICM**. Immunomodulatory properties of conjugated linoleic acid. *American Journal of Clinical Nutrition* 79: 1199S-1206S, 2004.

41. **Pariza MW, Park Y, and Cook ME**. The biologically active isomers of conjugated linoleic acid. *Progress in Lipid Research* 40: 283-298, 2001.

42. **Park Y, Storkson JM, Albright KJ, Liu W, and Pariza MW**. Evidence that the *trans*-10,*cis*-12 isomer of conjugated linoleic acid induces body composition changes in mice. *Lipids* 34: 235-241, 1999.

43. **Park Y, Storkson JM, Ntambi JM, Cook ME, Sih CJ, and Pariza MW**. Inhibition of hepatic stearoyl-CoA desaturase activity by *trans*-10,*cis*-12 conjugated

linoleic acid and its derivatives. *Biochimica et Biophysica Acta - Molecular and Cell Biology of Lipids* 1486: 285-292, 2000.

44. **Peters JM, Park Y, Gonzalez FJ, and Pariza MW**. Influence of conjugated linoleic acid on body composition and target gene expression in peroxisome proliferator-activated receptor α-null mice. *Biochimica et Biophysica Acta - Molecular and Cell Biology of Lipids* 1533: 233-242, 2001.

45. **Pfaffl MW, Horgan GW, and Dempfle L**. Relative expression software tool (REST©) for group-wise comparison and statistical analysis of relative expression results in real-time PCR. *Nucleic Acids Research* 30: e36, 2002.

46. **Rasooly R, Kelley DS, Greg J, and Mackey BE**. Dietary *trans* 10, *cis* 12-conjugated linoleic acid reduces the expression of fatty acid oxidation and drug detoxification enzymes in mouse liver. *British Journal of Nutrition* 97: 58-66, 2007.

47. **Roche HM, Noone E, Nugent A, and Gibney MJ**. Conjugated linoleic acid: A novel therapeutic nutrient? *Nutrition Research Reviews* 14: 173-187, 2001.

48. **Sébédio J-L, Gnaedig S, and Chardigny J-M**. Recent advances in conjugated linoleic acid research. *Current Opinion in Clinical Nutrition and Metabolic Care* 2: 499-506, 1999.

49. **Stoughton R, and Dai H**. Statistical Combining of Cell Expression Profiles. US: Rosetta Inpharmatics, Inc., 2002.

50. **Takahashi Y, Kushiro M, Shinohara K, and Ide T**. Dietary conjugated linoleic acid reduces body fat mass and affects gene expression of proteins regulating energy metabolism in mice. *Comparative Biochemistry and Physiology Part B: Biochemistry and Molecular Biology* 133: 395-404, 2002.

51. **Terpstra AHM, Beynen AC, Everts H, Kocsis S, Katan MB, and Zock PL**. The decrease in body fat in mice fed conjugated linoleic acid is due to increases in energy expenditure and energy loss in the excreta. *Journal of Nutrition* 132: 940-945, 2002.

52. **Tsuboyama-Kasaoka N, Miyazaki H, Kasaoka S, and Ezaki O**. Increasing the amount of fat in a conjugated linoleic acid-supplemented diet reduces lipodystrophy in mice. *Journal of Nutrition* 133: 1793-1799, 2003.

53. **Tsuboyama-Kasaoka N, Takahashi M, Tanemura K, Kim H-J, Tange T, Okuyama H, Kasai M, Ikemoto S, and Ezaki O**. Conjugated linoleic acid supplementation reduces adipose tissue by apoptosis and develops lipodystrophy in mice. *Diabetes* 49: 1534-1542, 2000.

54. **Vidal H**. Quantification of lipid-related mRNAs by reverse transcription competitive polymerase chain reaction in human white adipose tissue biopsies. *Methods in Molecular Biology* 155: 83–88, 2001.

55. **Viswanadha S, McGilliard ML, and Herbein JH**. Desaturation indices in liver, muscle, and bone of growing male and female mice fed *trans*-10,*cis*-12 conjugated linoleic acid. *Lipids* 41: 763-770, 2006.

56. **West DB, Blohm FY, Truettt AA, and DeLany JP**. Conjugated linoleic acid persistently increases total energy expenditure in AKR/J mice without increasing uncoupling protein gene expression. *Journal of Nutrition* 130: 2471-2477, 2000.

57. **West J, Tompkins CK, Balantac N, Nudelman E, Meengs B, White T, Bursten S, Coleman J, Kumar A, Singer JW, and Leung DW**. Cloning and expression of two human lysophosphatidic acid acyltransferase cDNAs that enhance cytokine-induced signaling responses in cells. *DNA and Cell Biology* 16: 691-701, 1997.

58. **Xu XF, and Pariza MW**. Dietary conjugated linoleic acid reduces mouse adipocyte size and number. *The FASEB Journal* 16: A370-A370, 2002.

59. **Yamasaki M, Kitagawa T, Chujo H, Koyanagi N, Nishida E, Nakaya M, Yoshimi K, Maeda H, Nou S, Iwata T, Ogita K, Tachibana H, and Yamada K**. Physiological difference between free and triglyceride-type conjugated linoleic acid on the immune function of C57BL/6N mice. *Journal of Agricultural and Food Chemistry* 52: 3644-3648, 2004.

Table 3.1 Real-time RT-PCR Primers

Primer	Accession Number	Primer Sequence Forward	Primer Sequence Reverse	Product Length (bp)	Annealing Temperature (°C)	Efficiency
ACOX*	NM_015729	5'-GGTGGGTGGTATGGTGTCGTAC-3'	5'-CAAAGACCTTAACGGTCACGTAGTG-3'	278	56.0	79.8%
Agpat2	NM_026212	5'-TTCGTTCGGTCCTTC-3'	5'-CGCTTAGGGAGTATTTC-3'	146	54.0	89.7%
Bcl6	NM_009744	5'-CAACCTGAAGACCCACAC-3'	5'-TACGGCTTCTCTCCAGTG-3'	129	57.2	151.7%
β-actin*	NM_007393	5'-TCATGAAGTGTGACGTTGACATCCGT-3'	5'-CCTAGAAGCACTTGCGGTGCACGATG-3'	285	56.0	80.6%
Cyp2e1	NM_021282	5'-CATCCAAAGAGAGGCACAC-3'	5'-CACTTCTTGTCATCGTAATCG-3'	150	57.2	79.1%
Dgat2	NM_026384	5'-CGTTGGCTGGTAACTTCC-3'	5'-CCACGATGATGATAGCATTG-3'	132	59.9	93.8%
EGFR	NM_007912	5'-AATGTCTGCCACCTATGC-3'	5'-ATTTGGAAGAAACTGGAAGG-3'	176	56.0	85.1%
FAS*	NM_007988	5'-CTGAAGAGCCTGGAAGATCGG-3'	5'-CCCTCCCGTACACTCACTCGT-3'	365	56.0	83.1%
GAPDH	NM_008084	5'-GGAGAAACCTGCCAAGTATG-3'	5'-GGAGTTGCTGTTGAAGTCG-3'	124	59.9	91.8%
Hprt*	NM_013556	5'-GTTGGATACAGGCCAGACTTTGTTG-3'	5'-GAGGGTAGGCTGGCCTATAGGCT-3'	352	56.0	81.2%
Igfbp-2	NM_008342	5'-AGACGCTACGCTGCTATC-3'	5'-CTGCTACCACCTCCCAAC-3'	196	59.6	79.9%
ME*	NM_008615	5'-ACGAGTGCTACAAGGTGACCAA-3'	5'-CTCCAGGGAACACGTAGGAATT-3'	129	56.0	81.5%
Pik3r1	U50413	5'-AATCCTGTCATTCCTGTAGC-3'	5'-ACTGAAGCGTAAGCCAAC-3'	142	55.7	90.8%
S18	NM_011296	5'-CGCCATCACTGCCATTAAGG-3'	5'-CACTCGCTCCACCTCATCC-3'	118	59.4	105.0%
SCD-1*	NM_009127	5'-TGTAAACAGCCTGTTCGTTAGCA-3'	5'-CCTTAGAAACTTTCTTCCGGTCGTAA-3'	299	56.0	76.1%
Socs6	NM_018821	5'-AATGGTAGTATGCTGGTCAG-3'	5'-TTTCTACAGGCAAATCTTATGG-3'	108	56.3	118.7%
Stat5b	NM_011489	5'-TGATGGCGTGATGGAAGTATTG-3'	5'-CCGTCTGGCTTGTTGATGAG-3'	117	59.9	110.2%
Tyk2	NM_018793	5'-CTGTCTAGCGAGGAGGAG-3'	5'-GGAAGGAATGAGGGATGC-3'	151	59.5	120.8%

Primers used for Real-Time RT-PCR. All primers were designed using Beacon Designer 7 (PREMIER Biosoft International, Palo Alto, CA) unless otherwise stated. Annealing temperatures were empirically determined.
*Designed by (43).

Table 3.2 Fatty Acid Composition of Liver Tissue from Mice Fed LA or CLA[a]

Parameter	LA	CLA	SEM	P-Value
		g/100 g fatty acids		
C14:0	0.52	0.68	0.05	0.061
C16:0	22.67	24.77	0.70	0.051
C18:0	6.37	5.19	0.38	0.046
C16:1(n9)	1.75	1.71	0.23	0.899
C18:1(n9)	23.72	31.97	2.56	0.039
C18:2(n6)	23.01	20.40	1.45	0.224
C18:2 (CLA)	nd	0.66	0.02	<0.0001
C18:3(n6)	0.39	0.23	0.04	0.014
C18:3(n3)	0.86	1.02	0.06	0.089
C20:1(n9)	0.50	0.63	0.06	0.178
C20:2(n6)	0.37	0.63	0.02	<0.0001
C20:3(n3)	1.19	0.60	0.06	<0.0001
C20:4(n6)	10.73	5.79	0.64	<0.0001
C22:6(n3)	4.77	3.30	0.35	0.009
		ratio		
C16:0/C16:1	8.99	10.51	1.17	0.372
C18:0/C18:1	0.31	0.18	0.04	0.045
Sat/Unsat[b]	0.43	0.45	0.02	0.465

[a] Values are least square means of n = 8 mice per treatment.
[b] (C14:0+C16:0+C18:0)/(C16:1+C18:1+C18:2+C18:3+C20:1+C20:2+C20:3+C20:4+C22:6)

Table 3.3 Microarray and Real-time RT-PCR Comparison

	Present Study				Rasooly *et al.*, 2007			
	Microarray		**Real-Time**		**Microarray**		**Real-Time**	
Gene	**P-value**	**Fold Change**	**P-value**	**Fold Change**	**P-value**	**Fold Change**	**P-value**	**Fold Change**
GAPDH	0.3604	0.12	0.793	-0.07	N/A	N/A	N/A	N/A
Hprt	0.3995	-0.13	0.732	0.08	N/A	N/A	N/A	N/A
Cyp2e1	0.9958	0.00	0.951	-0.01	N/A	N/A	N/A	N/A
S18	0.1444	0.36	<0.001	0.98	N/A	N/A	N/A	N/A
β-actin	0.1444	0.22	0.126	0.32	N/A	N/A	N/A	N/A
ACOX	0.3748	-0.20	0.965	-0.01	0.47	0.01	0.08	-1.00
Agpat2	0.2869	0.34	<0.001	1.18	N/A	N/A	N/A	N/A
Bcl6	<0.0001	1.12	0.036	0.99	N/A	N/A	N/A	N/A
Dgat2	0.3744	0.20	0.006	0.64	N/A	N/A	N/A	N/A
EGFR	0.0019	-0.40	0.269	-0.46	<0.05	-2.69	N/A	N/A
FAS	0.2588	0.18	0.642	-0.14	0.17	1.64	0.03	2.48
Igfbp-2	0.1252	-0.34	0.453	-0.30	<0.05	-2.56	N/A	N/A
ME	0.1040	0.26	0.620	0.14	0.01	5.30	0.24	1.60
Pik3r1	0.0012	0.33	0.314	-0.37	N/A	N/A	N/A	N/A
SCD-1	0.0011	0.82	0.888	-0.04	0.13	0.88	0.28	2.37
Socs6	0.0044	-0.27	0.905	0.03	N/A	N/A	N/A	N/A
Stat5b	0.0020	0.24	0.046	0.60	N/A	N/A	N/A	N/A
Tyk2	0.0001	0.41	0.282	-0.35	N/A	N/A	N/A	N/A

All fold changes are reported as partial fold changes.
All P-values from this study are nominal P-values.
N/A indicate values not reported.

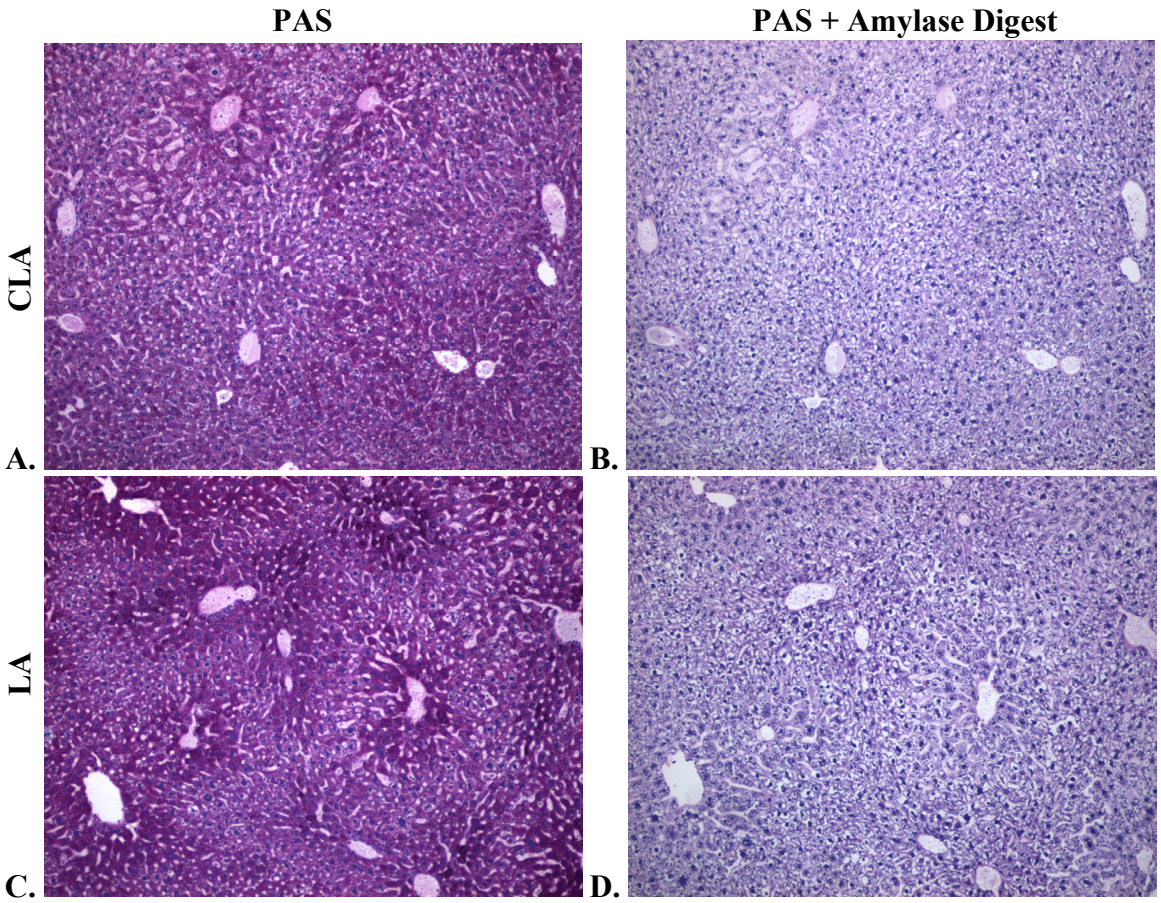

Figure 3.1 Detection of Glycogen Content in Livers
Nuclei are stained blue while carbohydrates are stained magenta. Amylase is an enzyme which breaks down polysaccharides, including glycogen. B and D are digested with amylase while A and C are undigested. Visual inspection suggests no difference between livers from CLA fed (A and B) and LA fed (C and D) livers.

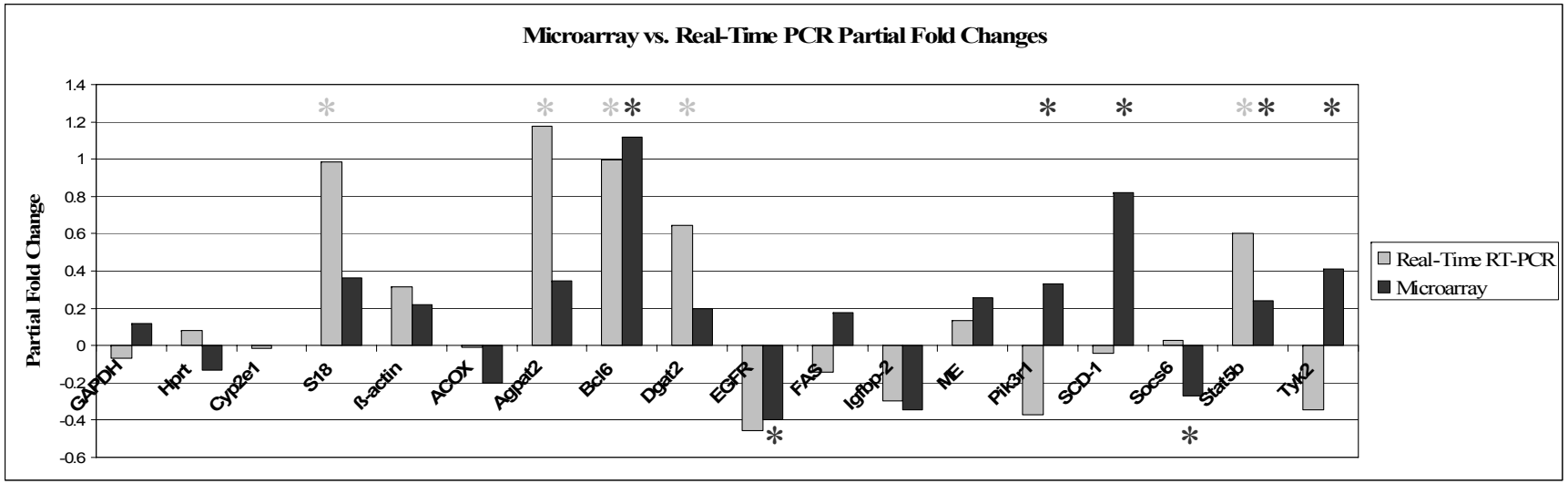

Figure 3.2 Microarray vs. Real-time RT-PCR Partial Fold Changes
Microarray and real-time RT-PCR partial fold changes based upon *GAPDH*, *Hprt*, and *Cyp2e1*.
* indicate statistically significant with microarray (black) (nominal $P < 0.01$) and real-time RT-PCR (gray) (REST© calculations, $P < 0.05$).
Abbreviations: *GAPDH* (*glyceraldehyde-3-phosphate dehydrogenase*), *Hprt* (*hypoxanthine guanine phosphoribosyl transferase 1*), *Cyp2e1* (*cytochrome P450 family 2, subfamily e, polypeptide 1*), *S18* (*ribosomal protein S18*), *β-actin*, *ACOX* (*acetyl CoA oxidase*), *Agpat2* (*acylglycerol-3-phosphate O-acyltransferase 2*), *Dgat2* (*diacylglycerol O-acyltransferase 2*), *EGFR* (*epidermal growth factor receptor*), *FAS* (*Fatty acid synthase*), *Igfbp-2* (*insulin-like growth factor binding protein 2*), *ME* (*malic enzyme*), *Pik3r1* (*phosphatidylinositol 3-kinase, regulatory subunit [p85 alpha]*), *SCD-1* (*stearoyl CoA desaturase-1*), *Socs6* (*suppressor of cytokine signaling 6*), *Stat5b* (*signal transducer and activator of transcription 5b*), *Tyk2* (*tyrosine kinase 2*)

Supplementary Table 3.S1 Microarray Results after Bonferroni Correction

Gene Name	Accession Number	Description	Fold Change	P-Value
BC024537	NM_146237	Mus musculus cDNA clone IMAGE:4988615.	2.36	3.05E-14
Ramp2	AK090111	RIKEN cDNA 2210401K01 gene	2.30	1.96E-11
TC1073196		Mus musculus olfactory receptor MOR256-47 (MOR256-47) pseudogene	2.24	4.07E-08
Pdcd8	NM_012019	programmed cell death 8	2.19	4.64E-16
4930564N15Rik	AK016222	Testis expressed gene 261	2.14	8.33E-11
Bcl6	NM_009744	B-cell leukemia/lymphoma 6	2.12	2.06E-08
Olfr50	NM_146946	olfactory receptor 50	2.12	3.16E-08
Hoxd4	NM_010469	homeo box D4	2.08	1.04E-08
Rnpc1	NM_019547	RNA-binding region (RNP1, RRM) containing 1	2.07	4.68E-09
Myh2	NM_144961	Mus musculus myosin, heavy polypeptide 2, skeletal muscle, adult (Myh2), mRNA	2.02	3.92E-06
AI849053	AK079063	Expressed sequence AI849053	2.01	5.53E-17
Iqwd1	AK004618	IQ motif and WD repeats 1	1.98	1.47E-07
Noc3l	NM_021315	nucleolar complex associated 3 homolog (S. cerevisiae)	1.96	3.00E-05
Sprr1a	NM_009264	small proline-rich protein 1A	1.95	2.01E-08
H2-Oa	NM_008206	histocompatibility 2, O region alpha locus	1.95	7.34E-08
MGC79224	L36434	hypothetical LOC432486	1.93	5.49E-09
A630026L20	AK041647	Hypothetical protein A630026L20	1.93	2.00E-15
Havcr1	NM_134248	hepatitis A virus cellular receptor 1	1.91	3.40E-06
Atrnl1	AK050882	Attractin like 1	1.91	5.10E-06
Tsfm	NM_025537	Ts translation elongation factor, mitochondrial	1.89	4.25E-08
Atp2a1	NM_007504	ATPase, Ca++ transporting, cardiac muscle, fast twitch 1	1.86	1.93E-07
Rad51l1	NM_009014	RAD51-like 1 (S. cerevisiae)	1.85	2.00E-05
Adam1a	NM_172126	a disintegrin and metallopeptidase domain 1a	1.85	1.25E-13

Supplementary Table 3.S1 Microarray Results after Bonferroni Correction

Gene Name	Accession Number	Description	Fold Change	P-Value
1700013L23Rik	BC019967	RIKEN cDNA 1700013L23 gene	1.83	5.49E-06
Alg2	AB041604	Mus musculus RIKEN cDNA 1300013N08 gene (1300013N08Rik), mRNA	1.80	8.17E-07
Higd1b	NM_080846	HIG1 domain family, member 1B	1.79	2.96E-06
Adrm1	AK010919	adhesion regulating molecule 1	1.75	1.00E-05
Ptprn	NM_008985	protein tyrosine phosphatase, receptor type, N	1.74	4.48E-07
Mybph	NM_016749	myosin binding protein H	1.73	2.62E-08
1700018O18Rik	AK006096	major facilitator superfamily domain containing 2	1.73	2.81E-08
6330530A05Rik	NM_172383	RIKEN cDNA 6330530A05 gene	1.72	1.53E-06
Aire	NM_009646	autoimmune regulator (autoimmune polyendocrinopathy candidiasis ectodermal dystrophy)	1.72	8.35E-13
Cdh13	NM_019707	cadherin 13	1.71	5.87E-07
D3Ertd194e	AK044865	Mus musculus 9.5 days embryo parthenogenote cDNA, RIKEN full-length enriched library, clone:B130008O17 product:CDNA FLJ14450 FIS, CLONE HEMBB1001736, WEAKLY SIMILAR TO EUKARYOTIC TRANSLATION INITIATION FACTOR 3 SUBUNIT 9 homolog [Homo sapiens], full inser	1.70	1.00E-05
Gna11	NM_010301	guanine nucleotide binding protein, alpha 11	1.70	8.65E-07
Pdrg1	NM_178939	p53 and DNA damage regulated 1	1.68	2.00E-05
2010107H07Rik	BC011230	RIKEN cDNA 2510015F01 gene	1.68	2.00E-05
Serpina7	NM_177920	serine (or cysteine) peptidase inhibitor, clade A (alpha-1 antiproteinase, antitrypsin), member 7	1.68	4.33E-07
Wfdc2	NM_026323	WAP four-disulfide core domain 2	1.67	4.00E-05
Olfr1123	NM_146350	Mus musculus olfactory receptor MOR264-17 (MOR264-17), mRNA	1.67	6.69E-06
Ccdc70	NM_026459	RIKEN cDNA 1700112P19 gene	1.67	4.63E-06
Grina	NM_023168	glutamate receptor, ionotropic, N-methyl D-asparate-associated protein 1	1.66	4.71E-08

Supplementary Table 3.S1 Microarray Results after Bonferroni Correction

Gene Name	Accession Number	Description	Fold Change	P-Value
		(glutamate binding)		
Snca	NM_009221	synuclein, alpha	1.65	1.36E-07
Hipk3	NM_010434	homeodomain interacting protein kinase 3	1.63	5.22E-07
Dpp3	AK015959	dipeptidylpeptidase 3	1.62	2.43E-06
Cenpp	NM_025495	RIKEN cDNA 1700022C02 gene	1.61	2.00E-05
Homer2	AB017136	homer homolog 2 (Drosophila)	1.61	4.26E-06
Arfgef1	AK085726	ADP-ribosylation factor guanine nucleotide-exchange factor 1(brefeldin A-inhibited)	1.61	6.63E-07
C330002D13Rik	AK049111	RIKEN cDNA 4921515G04 gene	1.60	5.03E-11
Rnu11	AF357361	Mus musculus clone MBII-407 C/D box snoRNA, partial sequence.	1.60	5.08E-06
C130076O07Rik	AK048567	RIKEN cDNA C130076O07 gene	1.60	5.64E-08
Pdap1	XM_132501	Actin related protein 2/3 complex, subunit 1B	1.60	1.87E-06
Rhof	NM_175092	ras homolog gene family, member f	1.60	2.73E-06
Psmb8	NM_010724	proteosome (prosome, macropain) subunit, beta type 8 (large multifunctional peptidase 7)	1.60	4.25E-06
Zfp369	NM_178364	zinc finger protein 369	1.60	1.80E-06
Slc35d1	NM_177732	solute carrier family 35 (UDP-glucuronic acid/UDP-N-acetylgalactosamine dual transporter), member D1	1.59	1.69E-08
Vnn1	NM_011704	vanin 1	1.58	3.33E-06
Klk12	AK009217	Kallikrein 12	1.58	4.66E-10
Epb4.2	NM_013513	erythrocyte protein band 4.2	1.57	4.29E-06
Clecsf8	NM_010819	C-type lectin domain family 4, member d	1.57	3.77E-06
H13	NM_010376	histocompatibility 13	1.56	7.32E-07
Kcnq4	AF249747	Potassium voltage-gated channel, subfamily Q, member 4	1.55	2.59E-08
Tmem153	NM_178919	expressed sequence AI451006	1.55	1.61E-06
2310002L09Rik	AK009124	RIKEN cDNA 2310002L09 gene	1.54	3.24E-08

Supplementary Table 3.S1 Microarray Results after Bonferroni Correction

Gene Name	Accession Number	Description	Fold Change	P-Value
Cgn	AK018143	Cingulin	1.54	5.68E-06
Spata9	NM_029343	spermatogenesis associated 9	1.53	1.05E-06
Apeg1	BC062643	aortic preferentially expressed gene 1	1.52	1.00E-05
Rxrb	NM_011306	retinoid X receptor beta	1.51	1.57E-06
Senp6	AK053904	SUMO/sentrin specific peptidase 6	1.51	4.99E-08
2010315L10Rik	NM_025917	RIKEN cDNA 2010315L10 gene	1.49	5.28E-06
Bgn	NM_007542	biglycan	1.48	9.07E-08
9430079M16Rik	BC038619	tetraspanin 9	1.48	2.00E-05
Stat1	NM_009283	signal transducer and activator of transcription 1	1.48	2.00E-05
Aytl2	NM_145376	acyltransferase like 2	1.47	4.00E-05
Tsnaxip1	NM_024445	translin-associated factor X (Tsnax) interacting protein 1	1.47	3.00E-05
A2bp1	NM_183188	ataxin 2 binding protein 1	1.46	4.00E-05
Tmem2	NM_031997	transmembrane protein 2	1.45	3.20E-06
Hif1an	AK009856	hypoxia-inducible factor 1, alpha subunit inhibitor	1.45	6.15E-06
AI840782	AI840782	UI-M-AM0-adn-h-01-0-UI.s1 NIH_BMAP_MAM Mus musculus cDNA clone UI-M-AM0-adn-h-01-0-UI 3', mRNA sequence.	1.45	2.70E-06
Ndufa13	NM_023312	NADH dehydrogenase (ubiquinone) 1 alpha subcomplex, 13	1.45	3.00E-05
Dnajb10	NM_020266	DnaJ (Hsp40) homolog, subfamily B, member 10	1.44	1.00E-05
Olfr1132	NM_146836	Mus musculus olfactory receptor MOR177-1 (MOR177-1), mRNA	1.43	1.00E-05
Mbd3	NM_013595	methyl-CpG binding domain protein 3	1.43	2.00E-05
4930552N02Rik	AK016098	Olfactory receptor 275	1.43	1.00E-05
Zfp312	NM_080433	zinc finger protein 312	1.42	6.80E-06
Cda	AB041806	Mus musculus hypothetical protein, MNCb-2457 (AB041806), mRNA	1.41	6.91E-06
Pmvk	NM_026784	phosphomevalonate kinase	1.41	2.00E-05
Lrp2	XM_130308	Mus musculus cDNA clone IMAGE:4972734 5	1.40	5.74E-06

Supplementary Table 3.S1 Microarray Results after Bonferroni Correction

Gene Name	Accession Number	Description	Fold Change	P-Value
Slc27a3	AF072758	Solute carrier family 27 (fatty acid transporter), member 3	1.40	8.54E-07
Dhx33	NM_178367	DEAH (Asp-Glu-Ala-His) box polypeptide 33	1.40	3.98E-07
Dci	NM_010023	dodecenoyl-Coenzyme A delta isomerase (3,2 trans-enoyl-Coenyme A isomerase)	1.40	2.00E-05
4930433N12Rik	NM_053265	RIKEN cDNA 4930433N12 gene	1.39	4.00E-05
Aldob	NM_144903	aldolase 2, B isoform	1.39	2.00E-05
Pou5f1	NM_013633	POU domain, class 5, transcription factor 1	1.37	4.00E-05
Grm3	NM_181850	glutamate receptor, metabotropic 3	1.35	2.00E-05
Ltb4r2	NM_020490	leukotriene B4 receptor 2	1.35	1.00E-05
St18	NM_173868	suppression of tumorigenicity 18	1.33	3.00E-05
Olfr860	NM_146528	Mus musculus olfactory receptor MOR146-7P (MOR146-7P) pseudogene	-1.25	3.00E-05
Ppih	NM_028677	peptidyl prolyl isomerase H	-1.25	2.00E-05
Gzmn	NM_153052	granzyme N	-1.25	9.82E-06
Vtn	NM_011707	vitronectin	-1.26	8.43E-06
Nudt7	NM_024437	nudix (nucleoside diphosphate linked moiety X)-type motif 7	-1.28	2.24E-07
Ifi47	NM_008330	interferon gamma inducible protein 47	-1.30	3.90E-06
Pqlc2	NM_145384	PQ loop repeat containing 2	-1.30	3.00E-05
Zfp533	NM_178723	zinc finger protein 533	-1.31	4.40E-06
Brf1	NM_028193	BRF1 homolog, subunit of RNA polymerase III transcription initiation factor IIIB (S. cerevisiae)	-1.33	7.30E-06
C6	NM_016704	complement component 6	-1.34	5.19E-06
Agxt	NM_016702	alanine-glyoxylate aminotransferase	-1.36	3.00E-05
Ear5	NM_019398	eosinophil-associated, ribonuclease A family, member 5	-1.40	5.04E-06
Qdpr	NM_024236	quininoid dihydropteridine reductase	-1.40	4.00E-05
Dusp1	NM_013642	dual specificity phosphatase 1	-1.41	4.00E-05

Supplementary Table 3.S1 Microarray Results after Bonferroni Correction

Gene Name	Accession Number	Description	Fold Change	P-Value
Psma8	AK010717	Proteasome (prosome, macropain) subunit, alpha type, 8	-1.41	2.00E-05
4933405L10Rik	AK016673	RIKEN cDNA 4933405L10 gene	-1.42	3.00E-05
Tcfap2b	NM_009334	transcription factor AP-2 beta	-1.43	2.00E-05
Fbxw14	NM_015793	F-box and WD-40 domain protein 14	-1.43	7.11E-06
V1rc25	NM_134180	Mus musculus vomeronasal 1 receptor, C25 (V1rc25), mRNA	-1.43	3.00E-05
Prokr2	NM_144944	G protein-coupled receptor 73-like 1	-1.44	1.00E-05
Wdr19	AK052303	WD repeat domain 19	-1.45	2.29E-06
1700023B02Rik	NM_025854	RIKEN cDNA 1700023B02 gene	-1.45	1.76E-07
NAP108760-1		Mus musculus olfactory receptor MOR256-46P (MOR256-46P) pseudogene	-1.46	4.99E-06
Pou2af1	NM_011136	POU domain, class 2, associating factor 1	-1.46	9.92E-07
Pkd2l1	NM_181422	polycystic kidney disease 2-like 1	-1.47	5.79E-06
Pnrc1	XM_131355	Proline-rich nuclear receptor coactivator 1	-1.48	2.00E-05
Tesp2	NM_009356	testicular serine protease 2	-1.49	1.00E-05
Arnt	NM_009709	aryl hydrocarbon receptor nuclear translocator	-1.49	2.43E-06
Olfr801	NM_146285	Mus musculus olfactory receptor MOR110-10 (MOR110-10), mRNA	-1.49	6.84E-07
C8b	NM_133882	complement component 8, beta subunit	-1.49	4.00E-05
4930481B07Rik	AK015605	RIKEN cDNA 4930481B07 gene	-1.50	3.00E-06
Ptprk	NM_008983	protein tyrosine phosphatase, receptor type, K	-1.50	6.56E-06
Usp54	NM_030180	ubiquitin specific peptidase 54	-1.50	8.35E-06
Rdh11	AK077207	Retinol dehydrogenase 11	-1.50	2.00E-05
D830007B15Rik	AK077061	RIKEN cDNA D830007B15 gene	-1.51	2.00E-05
Atf7	AK047901	activating transcription factor 7	-1.51	7.18E-08
Tnni3k	AK084817	TNNI3 interacting kinase	-1.51	2.00E-05
Adamts7	BC058991	a disintegrin-like and metallopeptidase (reprolysin type) with	-1.52	4.88E-08

Supplementary Table 3.S1 Microarray Results after Bonferroni Correction

Gene Name	Accession Number	Description	Fold Change	P-Value
		thrombospondin type 1 motif, 7		
Ucn3	NM_031250	Mus musculus urocortin 3 (Ucn3), mRNA	-1.52	3.59E-06
Olfr242	NM_010974	olfactory receptor 242	-1.52	1.18E-06
Gal	NM_010253	galanin	-1.52	3.91E-09
Slco1a1	NM_013797	solute carrier organic anion transporter family, member 1a1	-1.52	2.00E-05
Robo2	AK129396	roundabout homolog 2 (Drosophila)	-1.52	2.95E-06
Olfr716	NM_146604	Mus musculus olfactory receptor MOR260-2 (MOR260-2), mRNA	-1.53	1.29E-06
1110007C02Rik	NM_027923	RIKEN cDNA 1110007C02 gene	-1.54	7.38E-08
Slc10a1	NM_011387	solute carrier family 10 (sodium/bile acid cotransporter family), member 1	-1.54	2.97E-06
Pigf	NM_008838	phosphatidylinositol glycan, class F	-1.54	1.00E-07
Stam2	NM_019667	signal transducing adaptor molecule (SH3 domain and ITAM motif) 2	-1.55	5.09E-07
Ube2a	NM_019668	ubiquitin-conjugating enzyme E2A, RAD6 homolog (S. cerevisiae)	-1.56	6.76E-06
Hcrtr1	NM_198959	hypocretin (orexin) receptor 1	-1.56	3.00E-05
Arl15	NM_172595	ADP-ribosylation factor related protein 2	-1.56	4.32E-07
2010106G01Rik	BC016267	RIKEN cDNA 2010106G01 gene	-1.57	5.81E-06
9330140K16Rik	AK122448	RIKEN cDNA 9330140K16 gene	-1.58	1.00E-05
2610206B13Rik	AK020974	RIKEN cDNA 2610206B13 gene	-1.58	6.70E-07
Pou2f1	NM_011137	POU domain, class 2, transcription factor 1	-1.59	5.02E-08
6530401C20Rik	NM_173405	RIKEN cDNA 6530401C20 gene	-1.60	4.72E-06
BC022654	BC022654	Mus musculus, clone IMAGE:4219318, mRNA	-1.60	4.00E-05
Anubl1	XM_132758	AN1, ubiquitin-like, homolog (Xenopus laevis)	-1.60	4.02E-06
Jub	NM_010590	ajuba	-1.61	2.00E-05
Prdm1	NM_007548	PR domain containing 1, with ZNF domain	-1.61	8.07E-06
Nical	NM_138315	microtubule associated monoxygenase, calponin and LIM domain	-1.62	2.00E-05

Supplementary Table 3.S1 Microarray Results after Bonferroni Correction

Gene Name	Accession Number	Description	Fold Change	P-Value
		containing 1		
A_51_P340763		H3053A11-3 NIA Mouse 15K cDNA Clone Set Mus musculus cDNA clone H3053A11 3', mRNA sequence.	-1.63	4.41E-09
Nmbr	NM_008703	neuromedin B receptor	-1.65	3.00E-05
Flcn	NM_146018	folliculin	-1.65	6.61E-10
Syt17	NM_138649	synaptotagmin XVII	-1.66	1.36E-08
BU962533	BU962533	AGENCOURT_10616779 NIH_MGC_169 Mus musculus cDNA clone IMAGE:6743287 5', mRNA sequence.	-1.67	7.75E-07
Aldoa-ps2	AK016845	unnamed protein product; FRUCTOSE-BISPHOSPHATE ALDOLASE A (EC 4.1.2.13) (MUSCLE-TYPE ALDOLASE) homolog [Rattus norvegicus] (SWISSPROT|P05065, evidence: FASTY, 95.3%ID, 100%length, match=1089) putative; Mus musculus adult male testis cDNA, RIKEN full-lengt	-1.67	2.73E-07
Acvr2b	NM_007397	activin receptor IIB	-1.67	4.85E-06
2610044O15Rik	NM_153780	RIKEN cDNA 2610044O15 gene	-1.68	1.66E-09
Slc25a28	AK034173	solute carrier family 25, member 28	-1.68	3.85E-09
Nodal	NM_013611	nodal	-1.69	3.87E-08
A_51_P254731		RIKEN cDNA 4930544G21 gene	-1.69	8.00E-08
Irf6	NM_016851	interferon regulatory factor 6	-1.73	4.52E-08
Olfr1095	NM_146730	Mus musculus olfactory receptor MOR179-1 (MOR179-1), mRNA	-1.73	2.18E-09
2310046A06Rik	AK009836	RIKEN cDNA 2310046A06 gene	-1.74	1.28E-08
Atp5b	AK079828	ATP synthase, H+ transporting mitochondrial F1 complex, beta subunit	-1.75	1.30E-07
Mecp2	NM_010788	methyl CpG binding protein 2	-1.76	1.20E-10
Zic1	NM_009573	zinc finger protein of the cerebellum 1	-1.79	9.17E-06
Brd8	AK014475	bromodomain containing 8	-1.79	1.00E-05
1700007K09Rik	AK005730	RIKEN cDNA 1700007K09 gene	-1.80	4.00E-05

Supplementary Table 3.S1 Microarray Results after Bonferroni Correction

Gene Name	Accession Number	Description	Fold Change	P-Value
Rtp3	NM_153100	transmembrane protein 7	-1.80	5.61E-07
Kcnd2	NM_019697	potassium voltage-gated channel, Shal-related family, member 2	-1.82	3.59E-09
NAP057079-1		Mus musculus olfactory receptor GA_x5J8B7W6KF8-5425983-5425664 (GA_x5J8B7W6KF8-5425983-5425664) pseudogene	-1.82	2.33E-10
Lin9	AK089989	lin-9 homolog (C. elegans)	-1.83	7.93E-06
4930503E15Rik	AK015687	RIKEN cDNA 4930503E15 gene	-1.84	4.62E-09
BB085087	AK051383	Expressed sequence BB085087	-1.85	7.24E-10
Xist	X59289	X (inactive)-specific transcript, antisense	-1.87	6.73E-06
Aass	NM_013930	aminoadipate-semialdehyde synthase	-1.87	1.32E-11
Hsd3b4	NM_008294	hydroxysteroid dehydrogenase-4, delta<5>-3-beta	-1.89	1.38E-06
Nol5	NM_018868	nucleolar protein 5	-1.90	3.00E-05
Cyp7b1	NM_007825	cytochrome P450, family 7, subfamily b, polypeptide 1	-1.90	1.00E-05
Olfr846	NM_146282	Mus musculus olfactory receptor MOR149-3 (MOR149-3), mRNA	-1.94	2.00E-05
Tes	NM_207176	testis derived transcript	-1.96	4.97E-10
NAP002111-001		ZINC FINGER	-1.96	1.00E-05
Cul2	NM_029402	cullin 2	-1.97	3.50E-06
Slc9a4	NM_177084	solute carrier family 9 (sodium/hydrogen exchanger), member 4	-2.06	2.27E-07
Atrx	NM_009530	alpha thalassemia/mental retardation syndrome X-linked homolog (human)	-2.07	1.00E-05
AK079230	AK079230	Mus musculus adult male urinary bladder cDNA, RIKEN full-length enriched library, clone:9530044O11 product:unknown EST, full insert sequence.	-2.07	2.64E-07
TC958426		Dachshund 1 (Drosophila)	-2.09	4.78E-15
Rg9mtd2	NM_175389	RNA (guanine-9-) methyltransferase domain containing 2	-2.11	2.00E-05
Tspyl4	NM_133745	TSPY-like 4	-2.40	7.90E-13

List of genes statistically significant after Bonferroni correction. P-values are nominal.